Automating the Initialisation of Relay Autotuning using Control Performance Monitoring

by

Grant John Albertus

Thesis presented in partial fulfilment
of the requirements for the Degree

of

MASTER OF ENGINEERING

EXTRACTIVE METALLURGICAL ENGINEERING

in the Faculty of Engineering
at Stellenbosch University

Supervisors

Dr. Auret
Prof. Dorfling

March 2020

DECLARATION

By submitting this thesis electronically, I declare that the entirety of the work contained therein is my own, original work, that I am the sole author thereof (save to the extent explicitly otherwise stated), that reproduction and publication thereof by Stellenbosch University will not infringe any third party rights and that I have not previously in its entirety or in part submitted it for obtaining any qualification.

Date: March 2020

PLAGIARISM DECLARATION

1. Plagiarism is the use of ideas, material and other intellectual property of another's work and to present is as my own.

2. I agree that plagiarism is a punishable offence because it constitutes theft.

3. I also understand that direct translations are plagiarism.

4. Accordingly all quotations and contributions from any source whatsoever (including the internet) have been cited fully. I understand that the reproduction of text without quotation marks (even when the source is cited) is plagiarism.

5. I declare that the work contained in this assignment, except where otherwise stated, is my original work and that I have not previously (in its entirety or in part) submitted it for grading in this module/assignment or another module/assignment.

Initials and surname: GJ Albertus

Date: 15 November 2019

ABSTRACT

Relay autotuning is an automated procedure that obtains accurate tuning parameters for the process controller when required. An automated controller tuning procedure would be desirable within industry due to the poor controller response resultant from incorrect manual tuning of control loops. However, it is not known in industry how relay autotuning should be implemented and present literature studies do not extensively address this problem. Therefore, the aim of the research was to determine a control performance monitoring (CPM) technique that initiates relay autotuning due to incorrect tuning parameters. Furthermore, key parameters and factors associated with relay autotuning were evaluated such that a robust procedure can be proposed. To simulate realistic process conditions a milling circuit simulation model with disturbances and sensor noise was used as a case study.

Historical benchmarking was identified as a technique suitable to initiate the relay autotuning procedure. The product particle size's (PSE) variance was selected as a benchmark to which the current control performance was assessed. Defined as the PSE's variance at a period of good controller performance without the presence of faults, the 90th percentile of the PSE ($\sigma^2_{threshold}$) at normal operating conditions (NOC) was utilised as the historical benchmark. Using the benchmark, the current controller performance was assessed as poor if the variance of the PSE (σ^2_{PSE}) was persistently larger than the $\sigma^2_{threshold}$. As a result, the relay start time was defined as the allowable time σ^2_{PSE} is above $\sigma^2_{threshold}$ before relay autotuning is initiated.

In addition to $\sigma^2_{threshold}$, the historical benchmarking method required selection of a moving variance length. For the project, the choice of a 1 hour sliding window was assessed as suitable, as it was able to detect the oscillations that occur. The poor controller performance was detected as an increase in the moving variance over time. To simulate conditions of poor controller performance and incorrect tuning parameters, valve degradation was implemented on the PSE control loop. The valve was changed from linear to quick opening characteristics. Without retuning the controller, there was a persistent increase in variance due to the current tuning parameters being too aggressive. Therefore, oscillations within the milling circuit was produced.

The relay autotuning procedure was evaluated as beneficial in the reduction of variance when valve degradation was implemented. Therefore, relay autotuning can attenuate faults which introduce oscillations into the process if the original tuning parameters are too aggressive. In addition, key parameters were assessed for industrial application. The relay amplitude is suggested to be the smallest value possible to overcome the hysteresis band. Furthermore, a smaller relay amplitude reduces the inflated tuning parameters observed at lower sensor noise levels. With respect to the historical benchmarking technique, earlier initialisation of the relay autotuner resulted in better controller performance. Lastly, varying the extent of valve wear showed that retuning is not necessary for small degrees of valve wear. Despite the improved controller performance, economic performance assessment of relay autotuning and key parameters were inconclusive.

OPSOMMING

Relê outo instemming is ’n geoutomatiseerde prosedure wat akkurate instemmingsparameters vir die proseskontroleerder verkry wanneer nodig. ’n Geoutomatiseerde prosedure vir beheerderinstemming sal verkieslik wees in industrie as gevolg van die swak beheerderrespons wat volg uit verkeerde handinstemming van beheerlusse. Dit is egter nie bekend in industrie hoe relê outo instemming geïmplimenteer moet word nie en huidige literatuurstudies adresseer nie hierdie probleem breedvoerig nie. Daarom is die doel van hierdie navorsing om ’n beheer doeltreffendheid monitering (CPM) -tegniek wat relê outo instemming inisieer as gevolg van verkeerde instemmingsparameters, te bepaal. Verder, sleutelparameters en faktore geassosieer met relê outo insteming is geëvalueer op so ’n manier dat ’n robuuste prosedure voorgestel kan word. Om realistiese proseskondisies te simuleer, is ’n meulstroomsimulasiemodel met steuringe en sensorgeraas gebruik as ’n gevallestudie.

Historiese normstelling is geïdentifiseer as ’n gepaste tegniek om die relê outo instemming prosedure te inisieer. Die produkpartikelgroote (PSE) se variansie is geselekteer as ’n norm waarvolgens die stroombeheerderdoeltreffendheid geassesseer is. Gedefinieer as die PSE se variansie by ’n periode van goeie beheerdoeltreffendheid sonder die teenwoordigheid van foute, is die 90ste persentiel van die PSE ($\sigma^2_{threshold}$) by normale bedryfskondisies (NOC) gebruik as die historiese norm. Deur die norm te gebruik, is die stroombeheerder se doeltreffendheid geassesseer as swak as die variansie van die PSE (σ^2_{PSE}) aanhoudend groter as die $\sigma^2_{threshold}$ was. As ’n gevolg is die relê begintyd gedefinieer as die toelaatbare tyd σ^2_{PSE} oor $\sigma^2_{threshold}$ voor relê outo instemming geïnisieer is.

Meer as $\sigma^2_{threshold}$, het die historiese normstellingtegniek ’n seleksie van beweging variansie lengte nodig gehad. Vir die projek is die keuse van ’n een uur skuifvenster geassesseer as gepas, omdat dit die ossillasies wat voorkom kon waarneem. Die swak beheerderdoeltreffendheid is waargeneem as ’n verhoging in die bewegende variansie oor tyd. Om die kondisies van die swak beheerderdoeltreffendheid en verkeerde intemmingsparameters te simuleer, is klepdegradasie op die PSE beheerlus geïmplementeer. Die klep is verander van liniêr na vinnige openingskarakteristieke. Sonder om die beheerder oor in te stem, was daar ’n aanhoundende verhoging in variansie as gevolg van die stroom instemmingsparameters wat te aggressief was. Daarom is ossillasie binne die meulstroom geproduseer.

Die relê outo instemming prosedure is geëvalueer as voordelig in die verlaging van variansie as klepdegradasie geïmplementeer word. Daarom kan relê outo instemming foute verminder wat ossillasies in die proses veroorsaak as die oorspronklike instemmingparameters te aggressief is. Daarby is sleutelparameters geassesseer vir industriële toepassing. Die relê-amplitude is voorgestel om die kleinste waarde moontlik te wees om die histerese band te oorkom. Verder, ’n kleiner relê-amplitude verminder die uitgesitte instemmingsparameters waargeneem by laer sensorgeraasvlakke. Met respek tot die historiese normstellingtegniek het die vroeër inisiëring van die relê outo instemmer beter beheerderdoeltreffendheid tot gevolg gehad. Laastens, deur die omvang van klepverwering te varieer, is dit gewys dat herinstemming nie noodsaaklik is vir klein grade van klepverweer nie. Ten spyte van die verbeterde beheerderdoeltreffendheid, is die ekonomiese doeltreffendheidassesseering van relê outo instemming en sleutelparameters onbeslis.

ACKNOWLEDGEMENTS

I would like to thank everyone who has helped me during my time as a master's student, specifically I would like to thank:

- My parents and sister for the patience, love and constant support throughout.
- Dr. Lidia Auret for giving me this opportunity as well as pushing me to do my best. You have taught me a lot of valuable skills and I appreciate your guidance.
- Prof. Christie Dorfling for your guidance and taking up the mantle as my supervisor.
- Ryan Pottinger and Marno Basson for helping me throughout and being supportive friends. You have made this experience enjoyable.
- To my friend Michael Page for your support.

Contents

List of Figures

List of Tables

Nomenclature

Acronyms:

Acronyms	Description
ANOVA	Analysis of variance
BP	Basket price
C	Costs
CFF	Cyclone feed flow rate
CGP	Critical gain and period
CPI	Control performance indicator
CPM	Control performance monitoring
DRF	Decentralised relay feedback
EPA	Economic performance assessment
EPF	Economic performance function
EPI	Economic performance indicator
FCOR	Filtering and correlation analysis
HG	Head grade
IAE	Integral of the absolute error
IRF	Independent single relay feedback
ISE	Integral of the squared error
ITAE	Integral of the time weighted absolute error
ITNAE	Integral of the multiplied error
LPM	Linear process model

Acronyms	Description
MFS	Mill feed solids
MIMO	Multiple input multiple output
MR	Minerals recovery
MV	Minimum variance
MVC	Minimum variance control
NOC	Normal operating conditions
P	Profit
PF	Performance function
PI	Proportional integral
PID	Proportional integral derivative
PSE	Product particle size
R	Revenue
SFW	Sump feed water
SISO	Single input single output
SRF	Sequential relay feedback
SVOL	Sump volume

Symbols:

Symbol	Description
α	Amplitude ratio (Ch. 2)/Extent of valve degradation (Ch. 5)
γ	Covariance
ε	Hysteresis band
η	Control performance indicator
ϑ	Economic performance function
λ	Parameter for IMC tuning relations
μ	Population mean
ν	Disturbance variable
π	Pi
ρ	Cross correlation coefficient
σ	Standard deviation
σ^2	Variance
σ_{MV}^2	Minimum variance
$\sigma_{threshold}^2$	90th percentile of the controlled variable's variance for a period of good control performance
τ	Time constant (Ch. 2)/Time delay (Ch. 3)
τ_d	Derivative mode of PID controller
τ_I	Integral time of PID controller
φ	Phase shift
Ψ	Overall economic performance indicator
ω	Frequency
ω_c	Critical frequency

Symbol	Description
A_0	Fourier coefficient
A_n	Fourier coefficient
a	Amplitude of oscillations for the controlled variable
ā	Threshold controlled variable value for saturation relay
B_n	Fourier coefficient
D	Time delay
d	Relay amplitude
e	Error between controlled variable and its set point
f_{RA}	Relay amplitude factor
G_p	Process transfer function
J	Performance criterion
K	Preload gain
K_c	Controller gain
K_p	Process gain
K_u	Critical gain
N	Describing function
n_L	Sensor noise level
n_O	Observed sensor noise level
P_u	Critical period
q	q operator
t_{RS}	Relay start time
u	Manipulated variable
y	Controlled variable

Chapter 1
Introduction

Chapter overview

Chapter 1 serves as the introduction to the thesis and provides a brief background into process control with respect to relay autotuning. Furthermore, a brief introduction into process control monitoring is discussed. Subsequently, the aim for the thesis is stated with relevant motivation as to the need for the research. Thereafter, the objectives are stated such that the aim is achieved. With consideration of the thesis aim, the scope of the research is discussed as well as the contributions made by the thesis. Lastly, the thesis layout is set out.

1.1. Background

Process engineering industries are designed to convert raw materials into a product at a specified quality or throughput. Process control systems have, therefore, been implemented in order to maintain process variables at design specifications whether it be for safety or product quality. The main benefit of implementing process control is the possibility of reducing process variable variance such that these variables can operate closer to optimal conditions.

Although process control systems have advanced and become complex, a large portion of these process controllers are proportional-plus-integral-plus-derivative (PID) control. From literature evaluated, there is an estimated 500 to 5000 control loops present on industrial plants, depending on the size and type of plant. In addition, most control loops use Proportional-plus-Integral control (PI) (Desborough and Miller, 2002; Gao *et al.*, 2016). Therefore, with a large number of processing plants utilizing PID control or PI control, it is essential that tuning of these control loops is satisfactory in the reduction of the product variability.

Despite the need to correctly tune process controllers, literature states that only 20% of these control loops perform satisfactorily. Of the poor performing control loops, 30% of these control loops performed poorly due to incorrect controller tuning parameters that have been determined manually (Ho *et al.*, 2003; Jelali, 2013). Additionally, Ender (1993) states that for several processing industries, incorrect manual controller tuning results in increased product variability. Manual tuning is the most common method used for controllers which can be a tedious and time consuming process (Berner, 2015). Therefore, with numerous control loops present on processing plants, the controller tuning and subsequent controller performance is dependent on the experience and availability of time of the individual tuning the controller (Berner, 2015).

The use of an automated procedure for determining process controller tuning parameters can be beneficial in reducing the number of poorly tuned controllers (Berner, 2015). Automated tuning procedures determine accurate tuning parameters while reducing the extensive

knowledge required for tuning of controllers. In addition, the automated procedure inherently reduces the manual labour required to retune several control loops. Relay autotuning has been identified as one of these automated procedures (Åström and Lee, 1995; Berner, 2015). The relay autotuning method involves generating sustained closed loop oscillations to obtain important process information, namely the critical gain and period (Yu, 2006). Once the critical gain and period are obtained, tuning relations such as the Ziegler-Nichols tuning rules can be used to obtain tuning parameters. Specifically the technique can be applied to PID or PI controllers (Åström and Lee, 1995).

The relay autotuning procedure is further beneficial because it is closed loop, in contrast to open loop procedures such as the Ziegler-Nichols methodology. Consequently, the controlled variable will not drift significantly from the process set point. Furthermore, the relay autotuning procedure is relatively faster as compared to alternative methods, such as step testing, for processes with large time constants. Research indicates the application of relay autotuning is two to four times the critical period of the process (Yu, 2006).

Although the benefits of relay autotuning can be observed, there remains a lack of utilisation within industry. Possible reasoning for the lack of utilisation is the requirement for parameters to be known beforehand. For example, the relay amplitude as well as convergence criteria of the limit cycle are required before the automated procedure can be used. Therefore, despite automated procedures reducing the knowledge required to tune controllers, relay autotuning is limited in this regard. In addition, the utilisation of relay autotuning is hampered by a shortage of literature studies evaluating these key parameters. As a result, there is no procedure presented that implements the relay autotuning specifically due to incorrect controller tuning parameters.

However, there is potential in using control performance monitoring (CPM) to provide a framework for using a robust relay autotuning procedure within industry. CPM is defined as observing and evaluating the performance of control loops using data from routine plant operation as well as using frameworks to diagnose control loops (Bauer *et al.*, 2016). CPM techniques involve defining a benchmark, such that the current control performance can be assessed against the required performance for the process (Jelali, 2013). Various CPM benchmarks have been defined, however, it is generally accepted that the benchmark incorporates the variance of the controlled variable. Variance is widely evaluated due to the direct implications on the economic performance of processing industry, specifically its representation of the product-quality consistency. Notably in CPM is the use of the Harris index, named after its publication by Harris in 1989. The Harris index is the comparison of the controlled variable's variance to a theoretically achievable minimum variance regardless of the controller used.

Following the use of a CPM benchmark to evaluate the current status of a control loop, if control performance is determined as poor, diagnosing the cause of poor controller performance is the proceeding step. Once the fault behind poor control performance is determined, corrective measures have to be implemented. In several cases the corrective measure required is retuning. Therefore, the combination of detecting poor controller performance, using CPM, and relay autotuning has potential to bear fruit in processing industries.

1.2. Aim

In processing industries, once process controllers have been commissioned, control performance is generally seen as acceptable or good. Additionally, the half-life of a good control loop is roughly six months (Ruel, 2002). Decay of control performance has been attributed to several possible issues, namely changes in the conditions of the raw materials being utilized, failures in plant hardware or software, or degradation in processing equipment such as valve wear due to abrasive environments. The problems are further cascaded with the lack of process controller retuning to accommodate for these process changes (Jelali, 2013). In addition, if the controllers are retuned, incorrect manual controller tuning is often observed. Manual retuning imposes challenges such as time constraints for operators, large number of control loops prevalent on processing plants with limited maintenance resources, lastly lack of process control knowledge or skilled operators.

Relay autotuning is an automated procedure that can obtain controller tuning parameters and reduce the inaccuracies produced from manual tuning of controllers. Over the years, several theoretical and small-scale studies have been applied on relay autotuning, specifically in improving the initial relay autotuner proposed by Åström and Hägglund in 1984. Although extensive studies have been applied to relay autotuning, there remains no comprehensive study on implementing relay autotuning within industry. More importantly there is a shortage of studies applied to processing systems that are experiencing faults with inadequate controller tuning settings to adapt to these faults. Furthermore, the key parameters associated with relay autotuning have not been investigated and, therefore, suitable parameter selection for industrial application is limited.

The bulk of relay autotuning literature has been applied on improving the accuracy of the obtained critical gain and period as well as the use of differing relay autotuning configurations for process model identification. Therefore, the benefits of relay autotuning can be observed theoretically in small-scale experiments. However, further knowledge is required such that implementation of relay autotuning is robust and achievable within industry. As a result, the aim of the project is to design a procedure that automates relay autotuning, using CPM to detect poor controller performance due to incorrect tuning parameters. Specifically, a milling circuit simulation model will be used for the project.

The milling circuit has been proposed as a case study for the thesis due to the benefits process control can provide. Reducing the energy costs required for comminution and the reduction of variance in product quality (specifically the particle size) can be observed with the addition of process control. The main focus, however, is to assess the benefits of retuning a process experiencing poor control due to incorrect tuning parameters. In addition, the economic benefit of relay autotuning can be observed using economic performance assessment of an industrial process such as the milling circuit.

1.3. Objectives

The following objectives were sequentially constructed and motivated to achieve the aim of the thesis:

Objective 1: Design and implement a suitable relay autotuning procedure that can be applied to the established milling circuit simulation model in Simulink and MATLAB. The milling circuit model incorporates variations that can occur within industry (i.e. process noise and disturbances) and would assist in bringing credibility in the assessment of relay autotuning results obtained.

Objective 2: Determine a robust CPM technique such that poor control performance can be detected. More importantly, the objective is to use a technique whereby the resultant poor controller performance due to incorrect tuning parameters can be used to initiate retuning with relay autotuning.

Objective 3: Implement a control performance degradation model. The degradation model is implemented such that interesting observable effects on the process can be assessed with CPM. Furthermore, the degradation model should be realistic for the milling circuit and induce conditions whereby retuning is necessary. Therefore, the effects of relay autotuning in counteracting the degradation model can be evaluated.

Objective 4: Analyse the CPM technique in the detection of a poorly performing control loop due to the fault implemented in the milling circuit simulation model. The technique needs to be robust for various conditions presented in industry, therefore, assessment of the CPM technique is necessary.

Objective 5: Implement relay autotuning, once a control loop is performing poorly, at various conditions applicable to the procedure. As will be discussed in the relay autotuning and methodology section, relay autotuning used with the CPM requires selection of various parameters. As a result, various conditions for relay autotuning can be assessed to produce a robust relay autotuning procedure for industry.

Objective 6: Evaluate relay autotuning and key parameters with respect to controller and economic performance. Economic performance assessment is important as it potentially grants viability and justification for implementing relay autotuning in an industrial setting. Furthermore, controller performance allows assessment of suitable parameters for implementing relay autotuning.

1.4. Research scope

The thesis presented discusses various literature associated with relay autotuning as well as control performance monitoring, however, the following list provides the boundaries to which the research is applied:

- The thesis will evaluate relay autotuning as an automated retuning method applied to a simulation of a milling circuit only.
- Evaluation of key parameters are applied to single input, single output (SISO) retuning.
- The specific type of relay autotuner used in the thesis is the relay with hysteresis due to its applicability to industrial use, as a result of sensor noise.
- A valve degradation model will be used as a fault. The fault simulates conditions such as incorrect tuning parameters as well as low maintenance of process controllers within industry.
- Control performance monitoring, specifically historical benchmarking will be utilized to determine poor performing control loops for simulated models. Furthermore, historical benchmarking will be used to initiate the relay autotuning procedure.
- Controller and economic performance indicators will be utilized to evaluate the effect relay autotuning had on poorly performing control loops.

1.5. Contributions

With consideration of the aim and objectives, the thesis presented provides the following contributions:

- Relay autotuning has been applied to a minerals processing context, specifically a milling circuit.
- Application of relay autotuning is applied to a complex non-linear simulation model which is scarce in the current research of relay autotuning.
- Provides a technique whereby suitable key parameters for relay autotuning can be selected. The key parameter such as relay amplitude, sensor noise level, extent of oscillations within the system due to incorrect tuning parameters and lastly the relay start time designed from the CPM technique.
- Evaluation of key parameters associated with relay autotuning particularly with respect to their effect on controller and economic performance
- Evaluation of relay autotuning with hysteresis for a realistic approach towards relay autotuning in industry
- Simulation and evaluation of valve degradation effects on a milling circuit simulation model
- Evaluation of relay autotuning specifically applied to a control loop experiencing valve degradation
- Controller and economic performance of sequential relay autotuning.

1.6. Thesis layout

The structuring of the thesis is as follows:

Chapter 1 presents the introduction. Key subjects such as relay autotuning as well as control performance monitoring are introduced. Subsequently, the aim of the thesis is provided and the relevant research objectives.

Chapter 2 provides a literature review on relay autotuning. The theoretical findings are presented which provide a background to the procedural application of relay autotuning. Subsequently, an evaluation of literature sources pertaining to relay autotuning is performed whereby key findings and critical parameters associated with relay autotuning in literature are discussed.

Chapter 3 discusses control performance monitoring. A background of control performance indicators is presented and control performance techniques are assessed.

Chapter 4 discusses the economic performance assessment criteria required for evaluation of process controllers. Thereafter, economic performance assessment applied to the milling circuit simulation model is discussed which is essential for the methodology.

Chapter 5 provides the methodology to implementing relay autotuning using control performance monitoring. The milling circuit model considered is presented as well as the fault degradation model which will be implemented in the Simulink case study.

Chapter 6 presents the results and discussion section. The methodology and subsequent results obtained will be discussed towards the objectives of the thesis.

Chapter 7 concludes the findings observed from the research and answers the objectives proposed. Thereafter recommendations are proposed for future research.

Chapter 2
Relay Autotuning

Chapter overview

Chapter 2 provides information on relay autotuning. Initially, the theoretical formulation of the relay autotuning procedure is discussed. Thereafter, the modifications applied towards the initial relay autotuning procedure is provided, with discussions on saturation, preload and hysteresis on relay autotuning. Chapter 2 further establishes knowledge required for the relay autotuning procedure with the tuning relationships. Lastly, literature sources pertaining to relay autotuning are assessed and key information discussed relevant for the methodology section.

2.1. Background

Adaptive techniques have been developed to obtain controller tuning parameters for changing process conditions which require retuning. Adaptive techniques such as relay autotuning, gain scheduling and adaptive control have been recognised in literature as the three main adaptive techniques (Åström *et al.*, 1993). Within an industrial context, most process controllers have relay autotuning, step test methods, and gain scheduling built into their software (Hang *et al.*, 1993).

Gain scheduling is a technique which entails altering the controller tuning parameters based on changing process operating conditions. As a result, gain scheduling requires knowledge of the changing dynamics as well as knowledge on the corresponding controller tuning parameters needed for the changing process dynamics (Åström *et al.*, 1993). In contrast to gain scheduling, whereby the controller tuning parameters are predetermined, the step test method entails introducing a step change in the manipulated variable. Thereafter the dynamic response of the controlled variable is used to determine a time domain model, which is used to obtain new controller tuning parameters.

The relay autotuning procedure differs from the step test and gain scheduling method. The relay autotuner is used to determine the controller tuning parameters for changing process dynamics and is distinct from gain scheduling whereby the tuning parameters are known beforehand. In contrast to the step test method, the relay autotuner is based on modifying the Ziegler-Nichols method. The Ziegler-Nichols method determines the critical gain and period using a proportional regulator (Åström and Hägglund, 2017). The controller gain is gradually increased until oscillations occur for the controlled variable. The gain and period at which oscillations occur is the critical gain and period respectively. Furthermore, the Ziegler-Nichols tuning rules, based on the critical gain and period, can be used to obtain tuning parameters for the controller. However, the Ziegler-Nichols method has difficulties in maintaining the amplitude of oscillations within a controlled limit, as it is an open loop procedure used to

introduce excitation within the process (Åström and Hägglund, 2017). The relay autotuning procedure addresses this shortcoming.

The ideal relay autotuner is an automatic procedure that creates sustained oscillations for the determination of the critical gain and period. However, the amplitude of oscillation is maintained within a controlled limit. In contrast to automatic tuning methods such as the Cohen-Coon, Bristol, Yuwana and Seborg method which require large step changes or open loop testing, relay autotuning enables for controlled oscillations at an acceptable amplitude (Hang, Åström and Wang, 2002). Furthermore, applications of relay autotuning have proven to be successful in obtaining frequency domain models (e.g. critical gain and period, gain margin and phase margin) for simulations and small-scale experiments, producing controlled oscillations (Li, Eskinat and Luyben, 1991; Ho *et al.*, 2003; Li *et al.*, 2014; Berner, 2015). Therefore, based on these factors, relay autotuning can be a beneficial procedure used in industry and should be further assessed. Consequently, the following section highlights the relay autotuning procedure and how it differs from alternative automatic tuning techniques.

2.2. Relay autotuning procedure

Consider the generic feedback loop described in figure 2-1, whereby y is the controlled variable, y_{SP} is the desired set point of the controlled variable, e is the error between the controlled variable and its set point, u is the manipulated variable and lastly G_P is the process transfer function. From figure 2-1, control is switched from PID control to the relay autotuner and once the new tuning parameters are obtained, control is switched back to PID control. The method emphasises the contrasts from step test methods such as the Cohen-Coon method which are open loop.

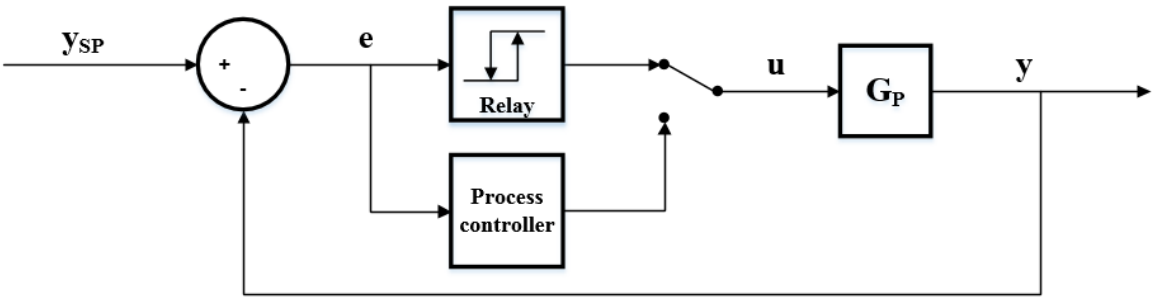

Figure 2-1: The relay autotuning feedback loop (adapted from Åström, Karl Johan (1995))

Figure 2-2 illustrates how the relay autotuning procedure is executed for an ideal relay if the controller gain is positive. The ideal relay autotuning procedure is defined by changing the manipulated variable with an amplitude d, known as the relay amplitude, and producing a square wave form. The ideal relay autotuning procedure is further defined by its symmetrical relay amplitude. From figure 2-2, as u is increased to the relay amplitude of d, y starts increasing after a certain dead time. As soon as y starts to increase from y_{SP}, u is switched to the opposite relay height, –d. Thereafter the relay amplitude is switched again when y crosses y_{SP}. A limit cycle is, therefore, produced with a critical period (P_u), where the critical gain (K_u) can be obtained.

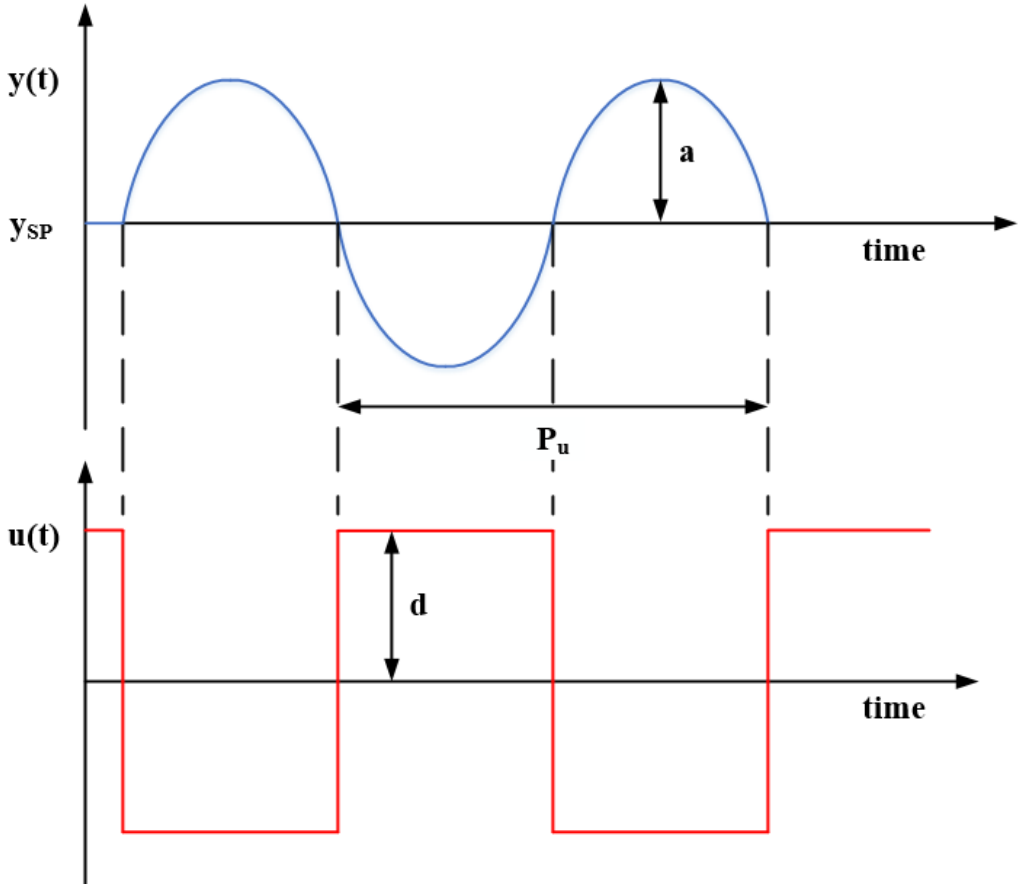

Figure 2-2: The ideal relay feedback procedure (adapted from Yu (2006))

2.3. Frequency domain models

The relay autotuning procedure generates frequency domain models inherently by obtaining the critical gain and period values. As previously stated, the relay procedure is modified from the Ziegler-Nichols method which originates from frequency response analysis (Åström, Karl Johan, 1995). Frequency response theory focuses on the idea that system dynamics can be determined using a sine wave, specifically the investigation of the propagation of the sine wave through the system.

Based on frequency response theory, if the input signal to a system is a sinusoidal wave, then the corresponding output signal will be a sinusoidal wave for a linear time invariant system (Åström, Karl Johan, 1995). The output signal will have the same frequency (ω) as the input signal, however, the output signal's amplitude and phase will be different. The amplitude ratio ($\alpha(\omega)$) as well as the phase shift ($\varphi(\omega)$) between the input and output signal are generally used to describe the relationship between the two signals (Åström, Karl Johan, 1995). Therefore, the amplitude ratio and phase shift are properties of frequency domain models and describe α and φ for all ω. Using these properties, the function $G(j\omega)$ is called the frequency response function of the system and is described by equation 2-1. Furthermore, the amplitude and phase functions are described by equation 2-2 and 2-3 respectively.

$$G(j\omega) = \alpha(\omega)e^{\varphi(\omega)j} \qquad \textbf{Equation 2-1}$$

$$\alpha(j\omega) = |G(j\omega)| \qquad \textbf{Equation 2-2}$$

$$\varphi(j\omega) = \arg(G(j\omega)) \qquad \textbf{Equation 2-3}$$

Consequently from the equations, the frequency response function $G(j\omega)$ can be described as a vector of length $\alpha(j\omega)$ that has an angle $\varphi(j\omega)$ from the real axis as shown in figure 2-3. Figure 2-3 is known as the Nyquist curve and fully describes the system's frequency response (Åström, Karl Johan, 1995). The Nyquist curve is a useful tool to graphically show the frequency response of a system, however, for controller tuning it is not necessary to determine all points on the Nyquist curve. The frequency point where φ is equal to -180° (where the function crosses the negative real axis) is known as the critical point, and is the point at which sustained oscillations will occur. Therefore, the Ziegler-Nichols method and relay autotuning procedure rely on obtaining sustained oscillations within the system at the critical point.

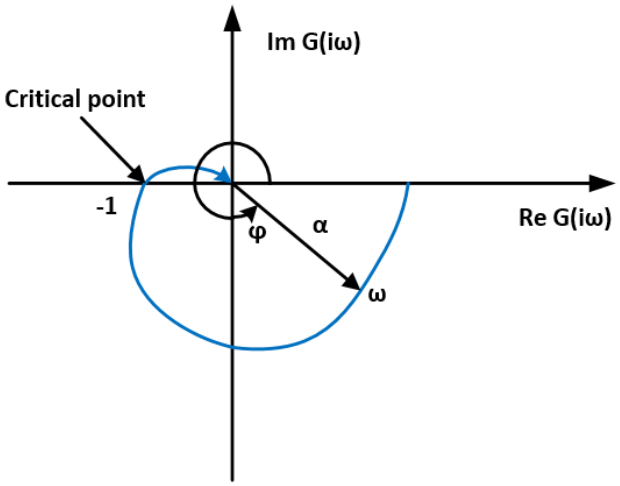

Figure 2-3: The Nyquist curve, a graphical interpretation for frequency response of process systems (adapted from Åström, Karl Johan (1995))

2.4. Describing functional analysis

As mentioned in the section on frequency domain models, if the input signal to a control system is a sinusoidal wave, the output signal will be a sinusoidal wave for a linear time invariant system. Relay autotuning uses the frequency response principle, however, the input signal is a square wave form. As compensation, the square wave form is approximated as a sinusoidal input using the Fourier transform. The procedure of approximating a non-linear signal such as a relay with a sinusoidal signal is known as describing functional analysis (Gelb and Vander Velde, 1968). Furthermore, for relay autotuning, the describing functional analysis is used to derive an expression for the K_u. Therefore, consider the system shown in figure 2-4, where $G_P(s)$ the process transfer function, e is the error between the controlled variable y and its desired set point y_{SP}, N is a non-linear element within the system, specifically a relay that outputs u.

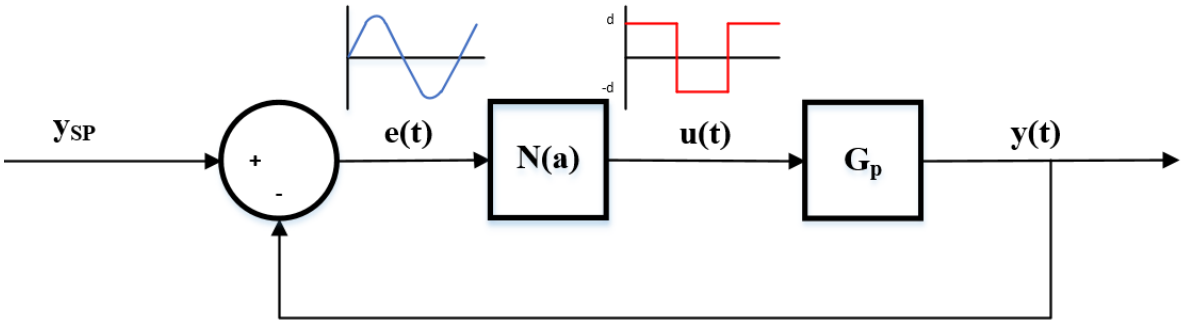

Figure 2-4: A feedback loop containing a non-linear element (N(a)) which can be described by its input's amplitude (adapted from Yu (2006))

From frequency response analysis, the relay outputs a square wave that introduces controlled oscillations in the system. Therefore, the input signal $e(t)$ to N is a sinusoidal wave propagating through the system:

$$e(t) = \mathrm{a}\sin\omega t \qquad \textbf{Equation 2-4}$$

Where a is the magnitude of $e(t)$. The Fourier transform is approximates the square wave form into a sinusoidal wave. Therefore the following equations approximate the output from N ($u(t)$) into a sinusoidal wave (Yu, 2006):

$$u(t) = A_0 + \sum_{n=1}^{\infty}(A_n\cos(\mathrm{n}\omega\mathrm{t}) + B_n\sin(\mathrm{n}\omega\mathrm{t})) \qquad \textbf{Equation 2-5}$$

Whereby A_0, A_n and B_n are evaluated as follows:

$$A_0 = \frac{1}{2\pi}\int_0^{2\pi} u(t)d(\omega t) \qquad \textbf{Equation 2-6}$$

$$A_n = \frac{1}{\pi}\int_0^{2\pi} u(t)\cos(n\omega t)\,d(\omega t) \qquad \textbf{Equation 2-7}$$

$$B_n = \frac{1}{\pi}\int_0^{2\pi} u(t)\sin(n\omega t)\,d(\omega t) \qquad \textbf{Equation 2-8}$$

Fundamentally, through integration, A_0 and A_n are equal to 0 because the relay output is symmetrical to the origin (an odd function) for the input-output relationship of $u(t)$ and $e(t)$. Consequently, the relay output can be described from partial integration of B_n.

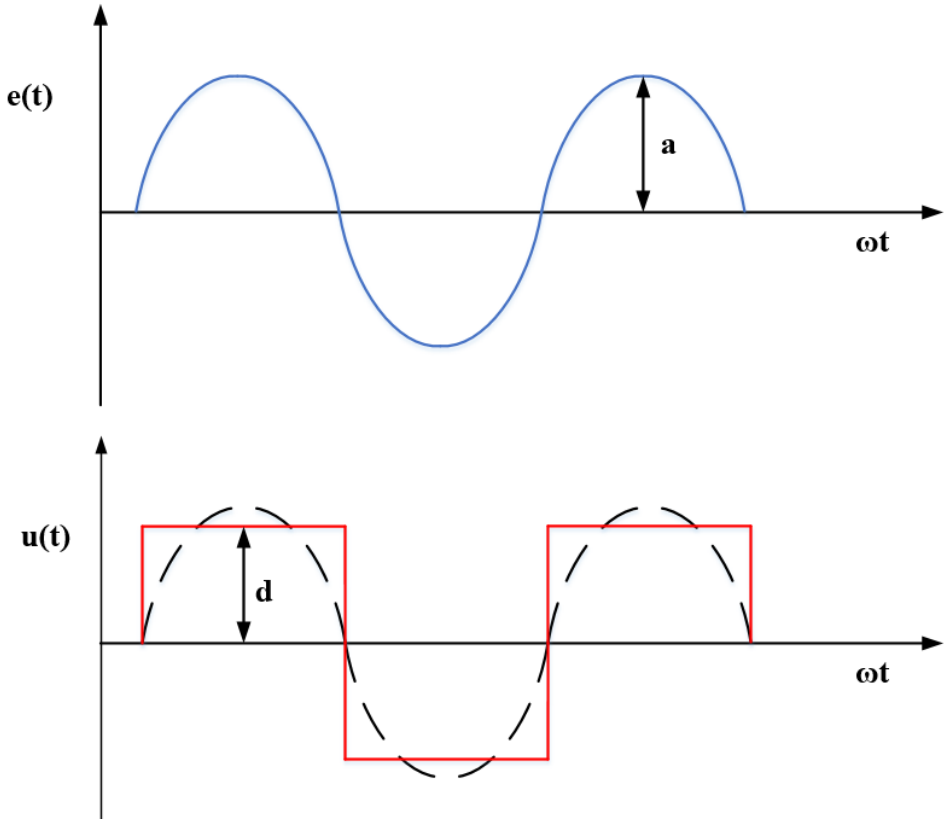

Figure 2-5: Input-output response for an ideal relay (adapted from Yu (2006))

Figure 2-5 illustrates the transformation of u into a sinusoidal wave and graphically aids in assessing the integration of B_n. Therefore, using integration by parts, B_n is evaluated as follows:

$$B_n = \frac{1}{\pi}\int_0^{\pi} d\sin(n\omega t)\, d(\omega t) + \int_{\pi}^{2\pi} -d\sin(n\omega t)\, d(\omega t) \qquad \textbf{Equation 2-9}$$

Subsequently, for odd and even harmonic terms:

$$B_n = \begin{cases} \frac{1}{n} \times \frac{4d}{\pi}, & n = 1, 3, 5 \ldots \\ 0, & n = 2, 4, 6 \ldots \end{cases} \qquad \textbf{Equation 2-10}$$

Resultantly, the square wave form is approximated into a sinusoidal wave using the following equation:

$$u(t) = \sum_{n=1}^{\infty} \frac{4d}{\pi n} \sin(n\omega t) \qquad \textbf{Equation 2-11}$$

For the ideal relay autotuner, only the principal harmonic (n = 1) is used to determine the approximated sinusoidal wave due to simplification (Yu, 2006). From the fundamental definition of $N(a)$ as the complex ratio of the output over the input, equation 2-12 is obtained. As a result, $N(a)$ is a function that describes its output with the amplitude (a) of its input and is a useful function, for relay autotuning, in determining K_u.

$$N(a) = \frac{B_1 + jA_1}{a} = \frac{4d}{\pi a} \qquad \textbf{Equation 2-12}$$

Using $N(a)$, if the process transfer function $G(j\omega)$ is known, then the condition for oscillations to occur within the process is described by equation 2-13. The equation follows theory from frequency response, whereby if the frequency response function crosses the negative real axis sustained oscillations will occur i.e. at the critical frequency (ω_u) where φ is equal to -180°. Therefore, the point where the negative inverse of the describing function crosses the process transfer function $G(j\omega_u)$ on the Nyquist curve will yield the critical point. K_u can be calculated from equation 2-14 and subsequently equation 2-15 (Li *et al.*, 2014). In addition, ω_u can be calculated from equation 2-15. From a graphical interpretation, K_u can be calculated as the amplitude ratio of $u(t)$ and $e(t)$ for a given frequency ω_u or period P_u (refer to figure 2-2 to calculate P_u).

$$1 + G(j\omega_u)N(a) = 0 \qquad \textbf{Equation 2-13}$$

$$K_u = \left|\frac{1}{G(j\omega_u)}\right| \qquad \textbf{Equation 2-14}$$

$$K_u = N(a) = \frac{4d}{\pi a} \qquad \textbf{Equation 2-15}$$

$$\omega_u = \frac{2\pi}{P_u} \qquad \textbf{Equation 2-16}$$

2.5. Improved relay autotuning

The use of describing functional analysis as a means for determining the critical gain and period leads to inaccuracies. Reportedly a 5-20% error in critical gain approximation from literature is observed (Yu, 2006). The source of the error is the approximation of a non-linear element (relay) with a linear approximation, namely describing functional analysis. Specifically the square wave form of the relay is approximated with the first harmonic from the Fourier transform, disregarding higher harmonics for simplicity. However, methodologies have been proposed to obtain accurate K_u and ω_u values by further building upon the ideal relay autotuner.

Methodologies such as the use of two relay tests to obtain accurate critical gain and period values have performed satisfactorily (Li, Eskinat and Luyben, 1991). Similarly, using discrete time systems for an accurate estimation of ω_u has been effective (Ren-Chiou, Shih-Haur and Cheng-Ching, 1992). These methodologies entail applying a relay test and then introducing adjustments. However, due to the source of the error originating from the approximation of a square wave using a sinusoidal wave, the intuitive solution is to modify the relay square wave form. Therefore, methodologies such as the saturation relay and preload relay procedures adjust the relay output to reflect a sinusoidal wave in order to obtain more accurate results (Yu, 2006). The saturation relay procedure entails the utilisation of a sinusoidal relay output before the controlled variable reaches a specific threshold value ā. The saturation relay input-output response is described by figure 2-6.

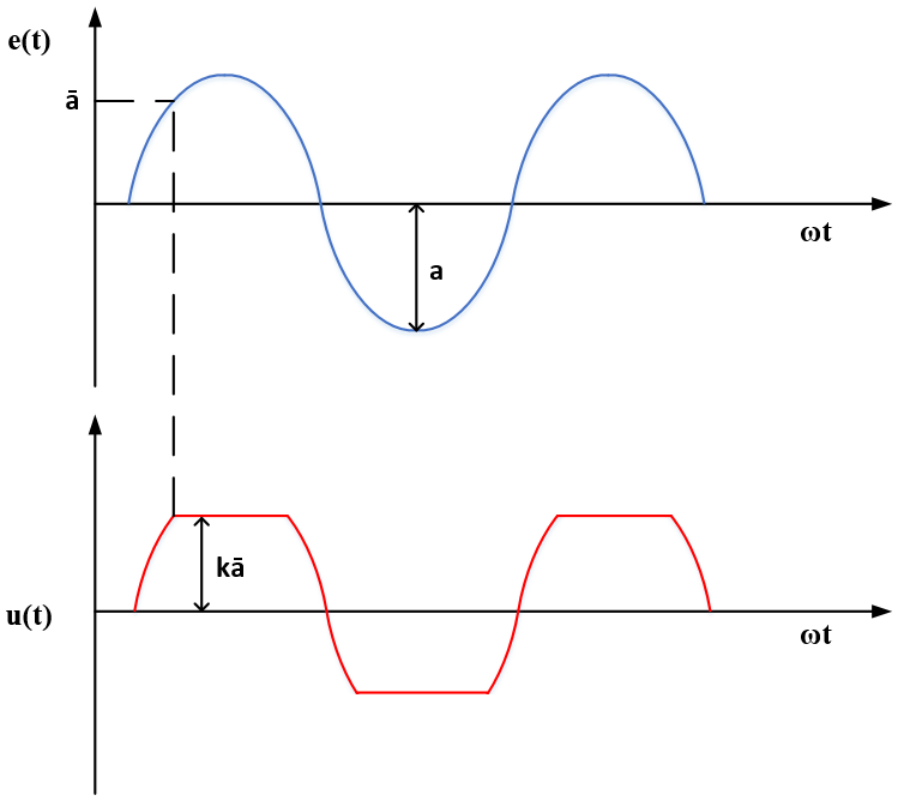

Figure 2-6: Input-output response for a saturation relay (adapted from Yu (2006)).

The relay output has a sinusoidal output proportionate to the error input signal (difference between the controlled variable and its set point) as is shown in equation 2-17, with the proportionality constant k. Therefore, if the input to the relay is less than ā, the relay output is:

$$u = ke \qquad \textbf{Equation 2-17}$$

However, if the error input is greater than ā, the relay output is the ideal square wave:

$$u = d \qquad \textbf{Equation 2-18}$$

Or

$$u = -d \qquad \textbf{Equation 2-19}$$

Similarly, the use of a preload relay procedure has yielded improved accuracy in determining the critical gain by up to 10% (Tan *et al.*, 2006). The proposed methodology is to increase the amplitude of the fundamental harmonic in comparison to the higher order harmonics with the use of an additional periodic output u_K as shown in equation 2-20 (Tan *et al.*, 2006).

$$u = u_R + u_K \qquad \textbf{Equation 2-20}$$

Therefore, the relay autotuning procedure is modified with a preload that amplifies the ideal relay autotuner such that a more accurate K_u and ω_u can be obtained. The preload schematic is depicted in figure 2-7:

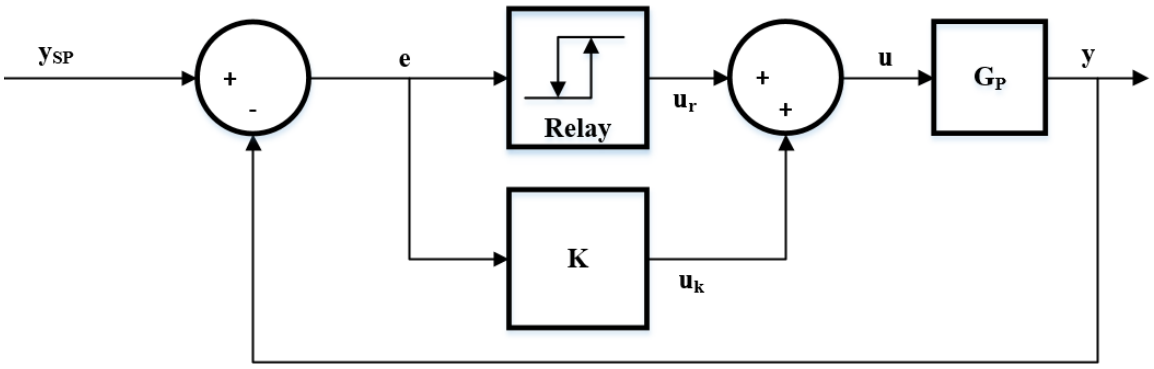

Figure 2-7: Preload relay autotuning feedback loop (adapted from Tan *et al* (2006))

The describing functional analysis and, subsequently, critical gain is modified to equation 2-21, with the addition of the preload gain K. The additional K term requires an extra design step in the process. However, extensive empirical studies have concluded that the recommended preload gain should be 20-30% of the relay amplitude (d) (Tan *et al.*, 2006).

$$N(a) = \left(\frac{4d}{\pi a} + K\right) = K_u \qquad \textbf{Equation 2-21}$$

2.6. Relay with hysteresis

As will be further discussed in the methodology section, in industry, noise is widely encountered within the process. The addition of noise in a process introduces random switching between the relay amplitudes. Resultantly, a relay with hysteresis is used to attenuate the random switching between relay amplitudes produced by noise within a process (Åström, Karl Johan, 1995). Figure 2-8 illustrates how a relay with hysteresis functions. The measured noise has to be larger than the hysteresis band (ε) before switching between relay amplitudes can occur.

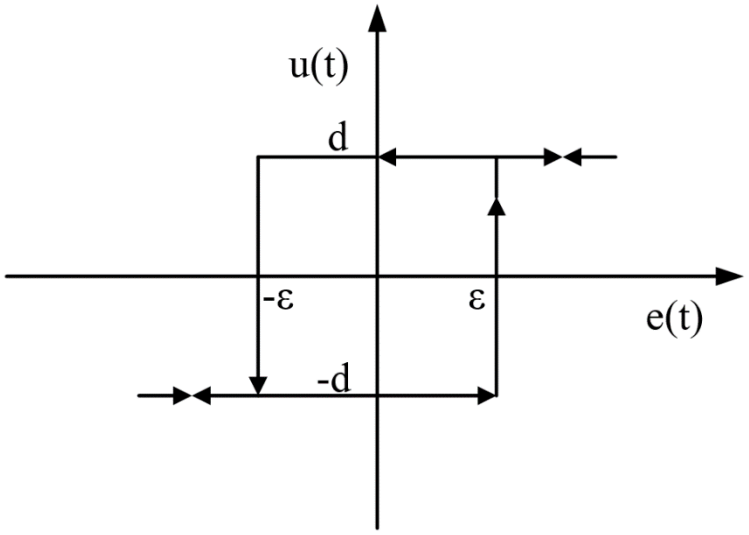

Figure 2-8: Input-output response for a relay system with a hysteresis band (adapted from Åström, Karl Johan (1995)).

Nonetheless, the addition of the hysteresis band requires an additional design specification for the relay autotuner. From literature studies, the expected ε should be 2 to 3 times the observed noise level (n_o) of the controlled variable (Berner, 2015; Soltesz, Mercader and Baños, 2017):

$$\varepsilon = (2,3)n_o \qquad \textbf{Equation 2-22}$$

Furthermore, for a relay autotuner with hysteresis, the experimental procedure is adapted in terms of switching of the relay amplitudes. The relay autotuner without hysteresis (ideal relay autotuner) would switch relay amplitudes when the process output crosses the set point value (refer to figure 2-2). However, as is shown in figure 2-9 for a positive gain, the relay output (u) has an amplitude change from d_1 to d_2 when the controlled variable (y) crosses ε. Thereafter the relay amplitude changes from d_2 to d_1 when y crosses $-\varepsilon$.

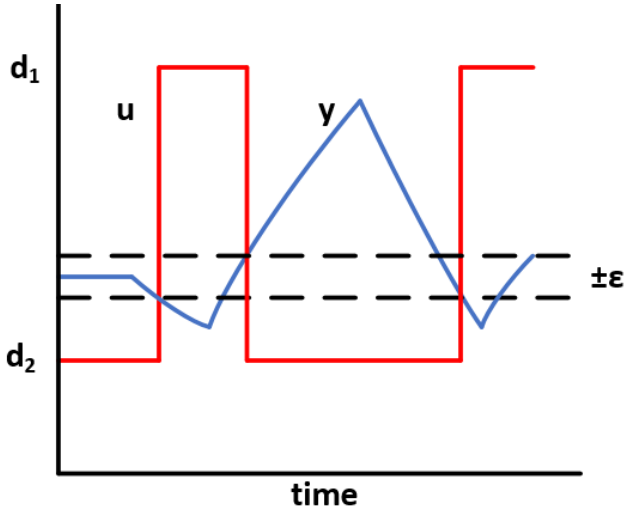

Figure 2-9: Relay autotuner with hysteresis procedure (adapted from Berner (2015))

Fundamentally, the describing function for a relay with hysteresis differs to the ideal relay and incorporates the hysteresis term. Despite the differing $N(a)$ described by equation 2-23 for a relay with hysteresis, the critical gain is determined with equation 2-15 (Åström and Hägglund, 2006). From frequency response analysis, the critical gain is obtained as a point intersecting the negative inverse of $N(a)$, which is a straight line parallel to the real axis for a relay with hysteresis. Therefore, the relay amplitude and hysteresis band can be altered to obtain differing points on this line, with each point relating to a different critical gain.

$$N(a) = \frac{4d}{\pi a^2}\sqrt{a^2 - \varepsilon^2} - \frac{4d\varepsilon}{\pi a^2}j \qquad \textbf{Equation 2-23}$$

2.7. Controller tuning

2.7.1. Ziegler-Nichols type tuning

The final procedure to relay autotuning is using the critical gain and period obtained to retune the process controller. For PID controllers there are two common methodologies used to obtaining tuning parameters namely, Ziegler-Nichols type tuning relations or model based tuning. The Zeigler-Nichols type of tuning relations express the PID tuning parameters as a relationship based on the critical gain and period. Table 2-1 shows the ratios for various tuning relationships based on the critical gain and period. The original Ziegler-Nichols tuning relationships worked well for a range of dead time (θ) to time constant ratios (τ), specifically ranging between 0.2 to 2 depending on the system (Yu, 2006). However, due to the poor controller performance outside of these bounds, the Tyreus-Luyben and Ciancone-Marlin tuning relationships are alternatives.

The Tyreus-Luyben is a more conservative tuning rule, derived from integrator plus dead time systems. The tuning relationship is recommended for systems that are time constant dominant. The conservative tuning rules have been recommended for interacting multivariable systems (Yu, 2006). The Ciancone-Marlin tuning rules were obtained from observing pure dead time processes and are recommended for dead time dominant processes (Yu, 2006).

Table 2-1: Ziegler-Nichols Type Tuning (adapted from (Yu, 2006))

Ziegler-Nichols	K_C	τ_I	τ_D
P	$K_u/2$	-	-
PI	$K_u/2.2$	$P_u/1.2$	-
PID	$K_u/1.7$	$P_u/2$	$P_u/8$
Tyreus-Luyben			
PI	$K_u/3.2$	$P_u/0.45$	-
PID	$K_u/2.2$	$P_u/0.45$	$P_u/6.3$
Ciancone-Marlin			
PI	$K_u/3.3$	$P_u/4$	-
PID	$K_u/3.3$	$P_u/4.4$	$P_u/8.1$

2.7.2. Model based tuning

In contrast to Ziegler-Nichols type tuning relations, whereby simple mathematical expressions can be used to tune the PI/PID controller, tuning parameters can be derived from an obtained process model. Commonly a first order plus dead time, integrator plus dead time and pure dead time process transfer functions are used to describe the system (Yu, 2006). An example of a model-based controller design method is the internal model control (IMC) method shown in table 2-2 (Rivera, Morarl and Skogestad, 1986). Several other model based tuning methods have been used for the relay approach, mostly utilizing first order with time delay, and integrator with time delay models. Model based tuning such as the λ-tuning (Berner, 2015), SIMC method (Skogestad, 2004) and AMIGO method (Åström and Hägglund, 2006; Berner, 2015) have been known to work successfully for obtained tuning parameters.

Table 2-2: IMC tuning relations (adapted from Yu (2006))

Models	K_C	τ_I	***Recommendations***
$\frac{K_p e^{-Ds}}{\tau s + 1}$	$\frac{\tau + {}^{D}/_{2}}{K_P \lambda}$	$\tau + {}^{D}/_{2}$	$\lambda > 1.7D$ $\lambda > 0.2\tau$
$\frac{K_p e^{-Ds}}{s}$	$\frac{2\lambda + {}^{D}/_{2}}{K_P(\lambda + D)^2}$	$2\lambda + D$	$\lambda > D$
$K_p e^{-Ds}$	$\frac{D}{K_p(2\lambda + D)}$	${}^{D}/_{2}$	$\lambda > D$

The model based tuning requires the critical gain and period to be known such that process model parameters can be obtained. Therefore, process model parameters such as K_p, τ and D can be obtained from the relay experiment. Friman and Waller suggested, for fitting an integrator plus dead time model, the following relationship be used (Yu, 2006):

$$K_p = \frac{\omega_u}{K_u} \qquad \textbf{Equation 2-24}$$

$$D = \frac{P_u}{4} \qquad \textbf{Equation 2-25}$$

In contrast, for a first order plus dead time model the following relationships can be utilized (Yu, 2006). For equation 2-26 and 2-27, either D or K_P is needed to solve τ, which can be obtained from the process data.

$$\tau = \frac{\tan(\tau - D\omega_u)}{\omega_u} \qquad \textbf{Equation 2-26}$$

$$\tau = \frac{\sqrt{(\mathrm{K_p}K_u) - 1}}{\omega_u} \qquad \textbf{Equation 2-27}$$

Further advances have been applied to the relay autotuning procedure for system identification. Methods such as asymmetrical relay autotuning whereby the relay amplitudes differ in height from the manipulated variable steady state value ($|h_1 \neq h_2|$), has been used with analytical equations to obtain process models (Berner, Åström and Hägglund, 2014). Furthermore, Luyben (2001) used the shape of the controlled variable to estimate process models. The process output can display differing shapes once a relay is applied to the process, subsequently, process information can be obtained from the shape factor which differ depending on the dead time to time constant ratio. Utilising the shape factor, as well as the critical gain and period, a process model can be determined.

2.8. Multivariable systems

The relay autotuning procedure has been evaluated for single-input-single-output (SISO) systems in the previous sections. However, the procedure for multiple-input-multiple-output (MIMO) is complex and requires different procedural configurations due to interacting control loops (Yu, 2006). When the relay technique is applied to MIMO systems there are three possible relay feedback schemes that can be used namely, independent single-relay feedback (IRF), sequential relay feedback (SRF) and decentralised relay feedback (DRF) (Wang *et al.*, 1997).

The independent single-relay feedback procedures involves subjecting only one control loop to the relay experiment while the rest manually controlled. Building upon IRF, sequential relay feedback involves treating a multivariable system as a sequence of SISO relay experiments. Initially the first control loop undergoes relay autotuning while the remaining control loops are under manual control. Once the relay autotuning procedure has been completed for one control loop, it becomes a closed loop with the new tuning parameters. The following step is to apply relay autotuning to another control loop, however, previously relay autotuned control loops remain under automatic control with their new control parameters. Generally the first control loop in the sequence is retuned, using the relay autotuner, for convergence of the controller tuning parameters (Wang *et al.*, 1997). In contrast, the decentralised relay feedback procedure involves simultaneously applying relay autotuning to all control loops. The DRF procedure is a complete closed loop test unlike the other techniques (Wang *et al.*, 1997).

2.9. Overview of relay autotuning literature

Following the establishment of theoretical information on relay autotuning, an evaluation of literature sources pertaining to relay autotuning has been summated in table 2-3. The table highlights the objectives of the proposed literature sources such as linear process models (LPM) as well as the critical gain and period (CGP). In addition, the experimental application of the relay autotuning is stated and the type of control system it was applied to i.e. SISO or MIMO. Lastly the success of the literature studies with regards to their objectives is evaluated.

Table 2-3: Overview of literature based on relay autotuning and its application in research

Reference	Objectives	Methodology	Type of relay	Application	System	Success
Ho *et al.*, 2003	Obtain accurate CGP	Iterative feedback tuning	Ideal relay	Lab scaled tests were performed on a coupled tank. Simulation studies were also performed on LPM	SISO	Yes
Cheng and Yu, 2000	Obtain accurate CGP for systems with hysteresis	Calculation of the hysteresis band and relay height adjustment	Ideal relay	Simulation case studies were performed on linear process models as well as a non-linear reactor/separator model.	SISO and MIMO	Yes
Luyben, 2001	Obtaining accurate LPM	Relay shape factor	Ideal relay	Simulation case studies on LPMs	SISO	Limited, method is not usable for all systems
Berner, Åström and Hägglund, 2014	Obtaining accurate LPM	Asymmetrical relay autotuning	Asymmetrical relay	Simulation case studies on LPMs	SISO	Yes
Thyagarajan and Yu, 2002	Obtaining accurate LPM	Relay shape factor	Ideal relay	Simulation case studies on LMPs	SISO	Yes
Li *et al.*, 2014	Obtaining accurate LPM	Relay with fractional order integrator (FOI)	Relay with FOI	Simulation case studies on LPMs	SISO	Limited, method performs worse against certain relay types
Levy *et al.*, 2012	Obtain accurate CGP	Relay feedback	Ideal relay	Simulation case studies on LPMs	SISO	Yes
Tan *et al.*, 2006	Obtain accurate CGP	Preload relay autotuning	Preload relay	Simulation case studies on linear process models as well as lab scaled tests on a coupled tank	SISO	Yes
Berner, 2015	Obtain accurate LPM	Asymmetrical relay autotuning	Asymmetrical relay	Simulation case studies on LPMs	SISO	Yes

Reference	Objectives	Methodology	Type of relay	Application	System	Success
Wang *et al.*, 1997	Obtaining CGP for MIMO system	Decentralized relay autotuning	Ideal and asymmetrical relay	Simulation case studies on LPMs	MIMO	Yes
Sommer and Kienle, 2012	CGP for MIMO system	Iterative feedback tuning	Ideal relay	Simulation case studies on LPMs	MIMO	Yes
Soltesz, Mercader and Baños, 2017	Obtain accurate LPM	Asymmetrical relay autotuning	Asymmetrical relay	Simulation case studies on LPMs	SISO	Yes
Loh *et al.*, 1993	Obtaining CGP for MIMO system	Sequential relay autotuning	Ideal	Simulation case studies on LPMs	MIMO	Yes
Hang, Åström and Ho, 1993	Obtain accurate CGP with the presence of static load disturbances	Biased relay output	Asymmetrical relay	Simulation case studies on LPMs	SISO	Yes
Shen, Wu and Yu, 1996	Obtain accurate CGP for asymmetrical oscillations	Biased relay output	Asymmetrical relay	Simulation case studies on LPMs	SISO	Yes
Vivek and Chidambaram, 2005	Obtaining accurate LPM	Symmetrical relay autotuning	Ideal relay	Simulation case studies on LPMs	SISO	Yes
Sung and Lee, 2006	Obtain accurate CGP	Iterative updating of integral time	Ideal relay	Simulation case studies on LPMs	SISO	Yes
Sung, Park and Lee, 1995	Obtain accurate CGP	Modified relay autotuner using 6 steps instead of 2	6 step relay	Simulation case studies on LPMs	SISO	Yes

2.9.1. Assessment of relay autotuning application

Table 2-3 describes various literature studies applied to relay autotuning. From literature, the bulk of research is directed at improving accuracy in relay autotuning. Few literature studies applied relay autotuning in a study where the current controller is performing poorly and retuning is required. As a result, there remains a void in linking relay autotuning and when relay autotuning should be applied, although the benefits of relay autotuning such as obtaining accurate tuning parameters have been exemplified in literature. For example, Cheng and Yu (2000) determined a method in improving the accuracy of obtaining tuning parameters using relay autotuning for valves that would experience hysteresis. However, there was no indication as to how unsatisfactory controller performance due to the hysteresis can be used to implement the modified relay autotuning procedure.

Furthermore, due to the majority of studies aimed at improving the accuracy in obtaining results from a relay autotuner, several case studies were simulations based on linear processes. Simulation case studies on a linear process are utilised because the critical gain and period values are known beforehand and, therefore, the values obtained through relay autotuning can be directly compared to the ground truth. Consequently, the shortage of small-scale practical experiments as well as industrially applied relay autotuning is a major shortcoming and limitation in building confidence for industrial application.

2.9.2. Relay methodology

The literature studies have highlighted certain aspects which are crucial in relay autotuning, namely how to obtain frequency domain models using differing relay autotuning procedures. From table 2-3, the ideal relay has been proven successful in determining adequate controller tuning parameters, despite the inaccuracies due to the approximation of a square wave with a sinusoidal wave. Nonetheless, for obtaining accurate process models and tuning parameters, the modified relay autotuning procedures have also been proven successful. However, there has not been an economic performance assessment comparing the ideal relay autotuner to the more accurate modified relay autotuners. Therefore, it cannot be stated which procedure would be best suited for industrial application.

Despite the shortage of economical assessment of relay autotuners, a subjective argument can be made for industry. As mentioned previously, an industrial process will have numerous control loops which are often manually tuned by operators. Furthermore, the tuning of controllers requires knowledge of the system such that the best possible parameters are selected. As a result, minimisation of parameter selection of the automated procedure would be beneficial for an inexperienced operator. Therefore, it is plausible to use the ideal relay autotuner due to the removal of various additional choices the operator would need for the modified relay autotuning procedures. For example the preload relay autotuner inherently produces accurate critical gain and period values, however, the user is required to select a preload gain.

2.9.3. Critical parameters and limitations

Despite the reduction in user choices with the ideal relay autotuner, there are two factors which need to be taken into consideration: how long the relay autotuning procedure should be applied as well as the relay amplitude. Selection of the relay amplitude as well as period convergence is a shortcoming of relay autotuning as an automatic procedure due to the reliance of process knowledge required. The user is required to determine the suitable duration of the relay autotuning procedure as well as the relay amplitude which would produce sustained oscillations of the controlled variable for the specific process.

The length of the relay experiment considers the convergence of the limit cycle. Despite a large quantity of literature using relay autotuning, there is a scarcity in a methodology that quantifies how long the relay autotuning procedure should be based on convergence of the limit cycle. However, Berner (2015) quantified the relay convergence using the period of the limit cycle, specifically the error between consecutive period values calculated had to be less than a specific threshold value. In contrast, most literature sources used a graphical interpretation of the limit cycle as a feasible means to evaluate convergence.

The relay amplitude takes into consideration the limits to which the controlled variable is allowed to oscillate. The amplitude of the oscillations for the controlled variable is a major factor and could lead to potential economic penalties if incorrectly selected. For example, a unit could be overflowed if the inlet flow rate, used to control the level, is too high. Despite the potential ramifications, few guidelines are presented from literature sources in selecting a relay amplitude. Generally, selection is based on the system with the only clear requirement being, the relay amplitude should be selected to overcome the user specified hysteresis band. As a result, the sensor noise level is a key parameter in the selection of the relay amplitude as sensor noise is prevalent in industry. Therefore, for industrial application, the relay with hysteresis would be the most applicable procedure. The presence of sensor noise further limits modified relay procedures such as the saturated relay as formulation of the critical gain disregards noise. However, the preload relay can be applied and application with noise is a potential area of further research due to the shortage of literature studies.

Further limitation to relay autotuning can be observed from the MIMO extension to the methodology. With several control loops present on processing plants, applying relay autotuning to each control loop would require time which could affect production or variables controlled for stability. Therefore, a trade-off needs analysing between manually tuning each control loop with potential for error, or applying relay autotuning to each control loop. Nonetheless, the MIMO extension adds complexity in evaluating relay autotuning due to the assessment of interacting control loops.

Chapter 3
Control Performance Monitoring

Chapter overview

Chapter 3 discusses control performance monitoring. The guidelines generally followed for control performance monitoring are proposed through a background section. Subsequently, the Harris index is identified as a key theoretical performance criteria. Thereafter practical alternatives such as historical benchmarking is discussed. Lastly, controller performance techniques are assessed for the methodology.

3.1. Background

As mentioned previously, processing industries have large quantities of control loops present, depending on the size and function of the plant. Therefore, it is necessary to monitor these process controllers and assess their control performance such that control objectives (e.g. product quality or stability) for all control loops are met (Gao *et al.*, 2016). Within control performance monitoring several frameworks have been designed in assessing poorly performing control loops (Jelali, 2006).

Conventionally the frameworks consist of identifying poorly performing control loops, determining the root cause of the fault and then implementing countermeasures to rectify the fault. Subsequently, the control performance of the control loops are analysed, to assess if improvements are observed after the countermeasures were implemented (Jelali, 2006). Consequently, controller performance evaluation plays an important role in two steps of the framework, namely identifying poorly performing control loops and assessing control loop improvement after rectification of the fault.

Due to the importance of identifying poorly performing process controllers in CPM, Jelali (2006) stated the control performance of a control system should be assessed on its ability to nullify set point deviations of controlled variables. Furthermore, the assessment should be quantified by a single number known as the control performance index (CPI or η) and is shown in equation 3-1 (Jelali, 2006). From the equation, J_{des} and J_{act} refer to the desired and actual controller performance respectively. Furthermore, the CPI is bounded between 0 and 1, where values closer to 1 indicate an optimal control system (Huang *et al.*, 1997; Huang, Shah and Kwok, 1997).

$$\eta = \frac{J_{des}}{J_{act}} \qquad \textbf{Equation 3-1}$$

Several CPI values have been used in industry (Bauer and Craig, 2008). However, the most widespread performance criterion utilizes the variance of the controlled variable, defined in equation 3-2 (Jelali, 2006). The terms N and $\bar{y}$ refer to the number of samples and sample mean respectively. The common usage of variance, as a performance criterion, is due to its inherent representation of the product quality consistency. Furthermore, the reduction in the variance of controlled variables indicates an increase in product quality and the possibility of operating near constraints that increase product throughput, reduce energy consumption and raw material usage (Jelali, 2006).

$$\sigma^2{}_y = \frac{1}{N-1}\sum_{k=1}^{N}(y(k)-\bar{y})^2 \qquad \textbf{Equation 3-2}$$

3.2. Harris index

The variance of the controlled variable has to be compared to a desired performance criterion ($\sigma^2{}_{des}$). Therefore, for any process there is a theoretical minimum variance ($\sigma^2{}_{MV}$) to which performance can be compared to irrespective of the controller. As a result, a control performance index namely, the Harris index, is formulated from the ratio of the theoretical minimum variance and the controlled variable's variance (Huang, Shah and Kwok, 1997):

$$\eta_{Harris} = \frac{\sigma^2{}_{MV}}{\sigma^2{}_y} \qquad \textbf{Equation 3-3}$$

Operating at the point of the minimum variance is known as minimum variance control (MVC). Despite benefits such as reduction in the variance and possible economic benefits from operating near control limits, obtaining the minimum variance requires process information and assumptions. The minimum variance can be obtained from process data provided the time delay (τ) is known or can be estimated to a degree of accuracy. Furthermore, a linear time invariant model for the process output y is required (Jelali, 2013). A discrete model such as the autoregressive model can be used to describe the process model. The following is an autoregressive moving average with exogenous inputs model (ARMAX):

$$A(q)y(k) = q^{-\tau}B(q)u(k) + C(q)\varepsilon(k) \qquad \textbf{Equation 3-4}$$

From equation 3-4, k indicates a certain time step, $u(k)$ is the manipulated variable at time increment k, $y(k)$ is the controlled variable at k and $\varepsilon(k)$ indicates the unmeasured disturbance at k. The unmeasured disturbance is assumed to be white noise with a mean of 0. Furthermore, the terms $A(q)$, $B(q)$ and $C(q)$ are defined as polynomials in q^{-1} of order n, m and p.

$$A(q) = 1 + a_1 q^{-1} + a_2 q^{-2} + \cdots + a_n q^{-n} \quad \textbf{Equation 3-5}$$

$$B(q) = b_0 + b_1 q^{-1} + b_2 q^{-2} + \cdots + b_m q^{-m} \quad \textbf{Equation 3-6}$$

$$C(q) = 1 + c_1 q^{-1} + c_2 q^{-2} + \cdots + c_p q^{-p} \quad \textbf{Equation 3-7}$$

From equation 3-5, 3-6 and 3-7 the q^{-1} operator is defined as unit delay or backwards shift operator. The following equation displays how the q operator is used to represent a previous value of y.

$$q^{-1} y(k) = y(k-1) \quad \textbf{Equation 3-8}$$

3.2.1. Determination from time-series analysis

Time series analysis can be used to determine the minimum variance. Consider a time series model estimated from closed loop plant data, the disturbance model is evaluated as:

$$y(k) = \frac{C(q)}{A(q)} \varepsilon(k) \quad \textbf{Equation 3-9}$$

An impulse response of the time series disturbance model yields:

$$y(k) = \left(\sum_{i=0}^{\infty} e_i q^{-i} \right) \varepsilon(k) \quad \textbf{Equation 3-10}$$

Where:

$$e_i = \frac{C(i)}{A(i)} \quad \textbf{Equation 3-11}$$

From the impulse response, the impulse response coefficients (e_i) before the time delay (τ) has been reached, are not dependent on the process controller:

$$y(k)_{Invariant} = (e_0 + e_1 q^{-1} + \cdots + e_{\tau-1} q^{-(\tau-1)}) \varepsilon(k) \quad \textbf{Equation 3-12}$$

$$y(k)_{variant} = (e_\tau q^{-\tau} + e_{\tau-1} q^{-(\tau-1)} + \cdots) \varepsilon(k) \quad \textbf{Equation 3-13}$$

The feedback invariant terms are, therefore, not a function of the process model or the process controller, but only dependent on the characteristics of the disturbances acting upon the system. As a result, the minimum variance is calculated from the first τ terms that are feedback invariant. Subsequently, the first τ impulse response coefficients can therefore be calculated through long division of $C(q)$ and $A(q)$.

$$\sigma_{MV}^2 = \sum_{i=0}^{\tau-1} e_i^2 \sigma_\varepsilon^2 \qquad \textbf{Equation 3-14}$$

3.2.2. Estimation algorithms

In contrast to time-series analysis, algorithms have been designed to determine the Harris index without the need for determining the impulse response coefficients for the disturbance model. Methods such as direct least-squares estimation, online least-squares estimation, and the filtering and correlation analysis (FCOR) method have been proposed for determining the Harris index. Despite the numerous methods, the FCOR method is commonly used for determining the Harris index (Wei and Craig, 2009a). The FCOR method involves two stages. Initially the process output is filtered. Filtering involves determining the white noise excitation:

$$\varepsilon = \frac{A(q)}{C(q)} y \qquad \textbf{Equation 3-15}$$

The aim of filtering is to determine the source of disturbances within the process. Following filtering the expected value or mean ($r_{y\varepsilon}$) of the process output multiplied by the error term, from $\varepsilon(k)$ until $\varepsilon\big(k-(\tau-1)\big)$, is evaluated:

$$r_{y\varepsilon}(0) = E\{y(k)\varepsilon(k)\} = e_0\sigma_\varepsilon^2$$
$$r_{y\varepsilon}(1) = E\{y(k)\varepsilon(k-1)\} = e_1\sigma_\varepsilon^2$$
$$\vdots$$
$$r_{y\varepsilon}(\tau-1) = E\big\{y(k)\varepsilon\big(k-(\tau-1)\big)\big\} = e_{\tau-1}\sigma_\varepsilon^2 \qquad \textbf{Equation 3-16}$$

Substituting the expected/mean value into equation 3-14, for determining the minimum variance, yields the following:

$$\sigma_{MV}^2 = \sum_{i=0}^{\tau-1} e_i^2\sigma_\varepsilon^2 = \sum_{i=0}^{\tau-1} \left(\frac{r_{y\varepsilon}(i)}{\sigma_\varepsilon^2}\right)^2 \sigma_\varepsilon^2 = \sum_{i=0}^{\tau-1} \frac{r_{y\varepsilon}(i)^2}{\sigma_\varepsilon^2} \qquad \textbf{Equation 3-17}$$

Cross correlation coefficient (ρ_{ij}) is defined as the ratio of the covariance (γ_{ij}) between two variables and their root mean squared (Boyd, 2001):

$$\rho_{ij} = \frac{\gamma_{ij}}{\sqrt{\sigma_i^2 \sigma_j^2}} \qquad \textbf{Equation 3-18}$$

Where the covariance is defined as the expected value of $x(k)$ from its mean and $y(k)$ from its mean (Boyd, 2001):

$$\gamma_{ij} = E\{[x(k) - \bar{x}][y(k) - \bar{y}]\} \qquad \textbf{Equation 3-19}$$

$$\gamma_{ij} = \frac{1}{N}\sum_{k=1}^{N}[(x(k) - \bar{x})(y(k) - \bar{y})] \qquad \textbf{Equation 3-20}$$

Both the cross correlation and covariance are described as the similarity between two variables (Jelali, 2013). Through manipulation of equation 3-17 and the cross correlation coefficient, the Harris index can be defined as the inner product of the matrix Z:

$$\eta_{MV,cor} = \sum_{i=0}^{\tau-1} \frac{r_{y\varepsilon}(i)^2}{\sigma_y^2 \sigma_\varepsilon^2} = \sum_{i=0}^{\tau-1} \rho_{y\varepsilon}^2 = Z^T Z \qquad \textbf{Equation 3-21}$$

Where Z is a vector consisting of the cross correlation of y and ε before the time delay:

$$Z = \left[\, \rho_{y\varepsilon}(0), \rho_{y\varepsilon}(1), \ldots, \rho_{y\varepsilon}(\tau - 1)\right]^T \qquad \textbf{Equation 3-22}$$

3.3. Historical data benchmarks

Although there are benefits to the Harris Index, the Harris index as a benchmark focuses on the controlled variable's variance and does not take the controller action into account. As a result, improving the control performance to the point of minimum variance control often leads to excessive controller action and control performance assessment based off the Harris index can potentially be overaggressive for a control system (Zhao *et al.*, 2009). Consequently, the inability to take into account the controller action, therefore, leads to minimum variance control potentially having poor robustness (Ko and Edgar, 2001; Huang and Shah, 2012). In addition to poor robustness, using a linear time invariant model may not be a suitable assumption as in most cases process variables have dependencies on time. Furthermore, the linear time invariant model requires knowledge of the time delay which is not always available.

In response, it is often decided to use historical data from when control performance was performing well as a benchmark. The performance index below is described as a baseline, reference data set or historical benchmark, where J_{his} indicates a user defined performance benchmark value where control was considered good.

$$\eta_{his} = \frac{J_{his}}{J_{act}} \qquad \textbf{Equation 3-23}$$

The user specified benchmark can therefore be applied to variance as shown by equation 3-24. The user specified benchmark can now be larger than unity, indicating that the current controller is performing better than what is desired.

$$\eta_{his} = \frac{{\sigma^2}_{user}}{{\sigma^2}_{y}} \qquad \textbf{Equation 3-24}$$

3.4. Set point response metrics

In contrast to using the variance as a performance indicator, the set point tracking of the controlled variable is often used. Therefore, the performance of a process controller can be evaluated based on the response to a set point or a disturbance change. Table 3-1 shows the metrics used to calculate deviations from the set point for a controlled variable. Along with these performance metrics, the rise time, settling time, decay ratio, overshoot and steady state error can also be evaluate in assessing controller performance. Of the set point response metrics, the IAE has been argued a good economic performance indicator because the size and length of the error is directly proportional to losses in revenue.

Table 3-1: Set point response metrics (adapted from Jelali, 2013)

Metric	Formula	Comment
Integral of the squared error (ISE)	$\int_0^\infty e^2(t)dt$	Penalises large error terms
Integral of the absolute value of the error (IAE)	$\int_0^\infty \lvert e^2(t)\rvert dt$	-
Integral of the time weighted absolute error (ITAE)	$\int_0^\infty t\lvert e^2(t)\rvert dt$	Penalises error that persists over time
Integral of the multiplied error (ITNAE)	$\int_0^\infty t^n\lvert e^2(t)\rvert dt$	Penalises error that persists over time
Quadratic error	$\int_0^\infty (e^2(t) + \rho u^2(t))dt$	-

3.5. Evaluation of control performance techniques

Jelali (2013) indicated an extensive list of CPM methods that utilize the variance and set point tracking of the controlled variable, which have been further discussed in chapter 3. However, Bauer *et al* (2016) performed a survey which determined which CPM techniques were used in several industries. The CPM techniques were divided into the categories displayed in table 3-2. In addition, examples were stated of methodologies belonging to each category.

Table 3-2: Mathematical methods utilized in CPM (Obtained from Bauer *et al* (2016))

Category	Methods
Operating mode statistics	Time in manual versus time in automatic mode, number of changes in tuning parameters. Control loops in saturation
Basic statistics	Crossings of minimum/maximum boundaries, standard deviation, mean values
Algorithm indices	Integrated absolute error (IAE), scatter plot of manipulated variable against the controlled variable
Model-based techniques	Autoregressive models
Multivariate statistics	Principal component analysis
Minimum variance techniques	Harris index
Advanced statistics	Probability density function

From the literature survey, mathematical techniques such as operating mode, basic and algorithm indices statistics were found more useful in industry due to easier computation and interpretability. In contrast, the Harris index is found to be a useful technique in explaining CPM through theoretical aspects, however, in industry most signals are time variant and time delays are not always known. Therefore, the Harris index is rarely used in an industrial setting, due to assumptions, but is well known in academic literature.

Due to the limitations with the Harris Index, the historical benchmark is seen as an alternative. However, the historical benchmark has shortcomings too. Despite being easier to implement in industry, which is more popular from the literature survey, the historical benchmark is subjective. Interpreting a period of good performance is dependent on the knowledge of the person doing the assessment, instead of a theoretical minimum variance. As a result, there is limited studies applicable towards historical benchmarking (Rato and Reis, 2010).

In contrast to the variance based performance indicators presented by Jelali (2013), it's suggested that analyses of time trends as well as the fault detected is performed (Bauer *et al.*, 2016; Gao *et al.*, 2016). Therefore, the control performance can be based on the observed process data trends. These trends can be classified as saturation, sinusoidal oscillation, manual control, sluggish behaviour, nonlinear oscillations (Bauer *et al.*, 2016). In addition, the control performance can be classified based on the frequency of faults observed. In industry, the most frequent observed fault in processing is incorrect tuning settings despite autotuning settings on modern controllers. In addition, frequently observed faults can be extended to valve stiction, actuator faults, sensor faults interacting loops and equipment degradation.

Chapter 4
Economic Performance Assessment

Chapter overview

Chapter 4 provides the basis for economic performance assessment. Initially a theoretical introduction into economic performance assessment is discussed, providing details on economic performance functions. Subsequently, economic performance assessment with respect to milling circuits is presented. Lastly, the economic performance assessment for milling circuits are described with case studies which highlight key aspects.

4.1. Economic performance assessment of process control

Control systems are implemented to increase profits and system efficiencies by maintaining controlled variables near their optimal set points and improving production capacity (Seborg *et al.*, 2011). However, not all implementations of process control can be seen as economically viable. Therefore, a framework in establishing whether implementing a control system is feasible would be beneficial. Economic performance assessments (EPA) is a framework that is becoming increasingly important in evaluating the benefit of implementing control systems (Brisk, 2004; Martin, 2004; Friedmann, 2006)

The conventional technique in determining the benefits of a control system is reducing the variability of the controlled variable and shifting operating conditions closer to specification limits (Bauer *et al.*, 2007). To determine the benefit of shifting operating conditions, the relationship between the controlled variable and its economic effect needs to be established. Performance functions (PFs) relate controlled variables to their monetary values, furthermore, they determine either a profit or loss as the controlled variable deviates from the optimal set point (Stout and Cline, 1976; Bawden, 1993; Bauer and Craig, 2008). Therefore, EPAs conventionally involve the construction of performance functions (Wei and Craig, 2009a).

Despite the ability to determine the economic significance in deviations from the optimal set point, general guidelines in formulating performance functions are difficult to construct. Formulation of performance functions require extensive knowledge of the process, therefore, the difficulties in formulating performance functions originate from the economic impact's dependency on the specific type of industry (Williams and Rameshni, 1998). Conventionally performance functions are constructed from plant experiments (Craig *et al.*, 1992), insight into the characteristics of the process combined with knowledge from literature sources (Craig and Koch, 2003), and evaluations from production costs versus product value (Zhou and Forbes, 2003).

Despite the shortage of literature that has produced clear guidelines on constructing performance functions, there are common performance functions used in industry. Three functional forms of economic performance functions have been discussed in literature namely, quadratic, linear and clifftent performance functions (Bauer *et al.*, 2007; Bauer and Craig, 2008; Wei and Craig, 2009a, 2009b). The following section further discusses these economic performance functions.

4.2. Performance functions

4.2.1. Linear performance functions

A linear performance function, with a constraint, can be used to relate a monetary value to a controlled variable, as is depicted in figure 4-1. The economic benefit increases linearly as the operating point of the controlled variable is shifted from x_1 to the maximum (ϑ_m) at x_m. As the operating point is shifted beyond x_m, the controlled variable becomes wasteful. Therefore, there is no economic benefit beyond x_m. Furthermore, in relation to application, linear performance functions have been applied to processes such as fuel oil blending industries (Bauer *et al.*, 2007). With respect to fuel oil blending processes, the profit increases linearly with an increase in the sulphur content. However, if the sulphur content increases beyond the threshold or set point, environmental regulations are violated and there will be no economic benefit.

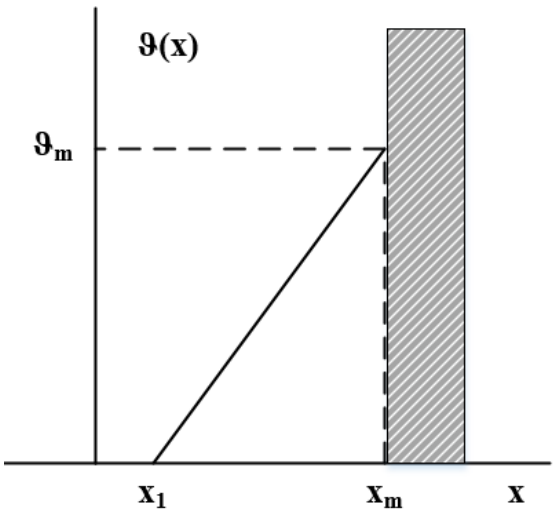

Figure 4-1: Linear performance function (adapted from Bauer *et al* (2007))

4.2.2. Clifftent performance functions

The clifftent performance function is depicted in figure 4-2 and further builds upon the linear performance function. The clifftent performance function is described by two linear functions, specifically a linear function that increases from x_1 to x_m and a linear function that decreases thereafter. Operating points x_1 and x_3 are points where the economic benefit for the process is 0. Furthermore, x_m is the operating point at which the maximum economic benefit (ϑ_m) is achieved. Application of the clifftent performance function can be observed with the mill load of a milling circuit (Wei and Craig, 2009a). The mill load is controlled between upper and lower limits. When these limits are exceeded there will be differing compensative actions. Therefore, depending on which boundary was exceeded, there will be a varying economic impact, as is shown by either side of x_m.

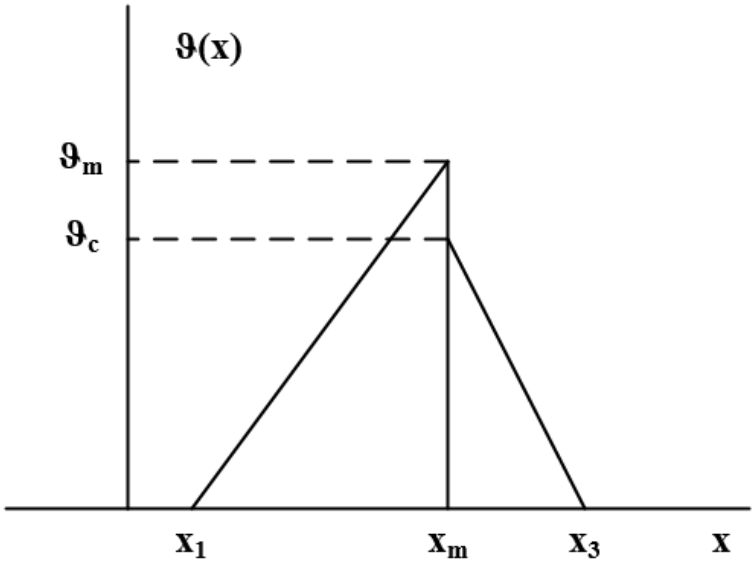

Figure 4-2: Clifftent performance function (adapted from Bauer *et al* (2007))

4.2.3. Quadratic performance functions

In contrast to the linear functions described, the quadratic performance function is depicted in figure 4-3. The maximum benefit (ϑ_m) is obtained when the controlled variable is at the optimal operating point (x_m) for the process. The economic benefit is decreased as the controlled variable shifts from the optimal operating point and reaches 0 once the controlled variable reaches x_1 or x_2. The quadratic performance function has been applied to a variety of processes. For example, an ammonia production process whereby the profit has a linear relationship with the throughput and further the throughput has a quadratic relationship with the composition ratio of the product (Bauer *et al.*, 2007). For the milling circuit, the quadratic performance function is used to describe the relationship between the product particle size and the flotation mineral recovery. The maximum benefit is obtained at an optimal point and performance deteriorates as the mill grind becomes either finer or coarser than the optimal product particle size (Wei and Craig, 2009a).

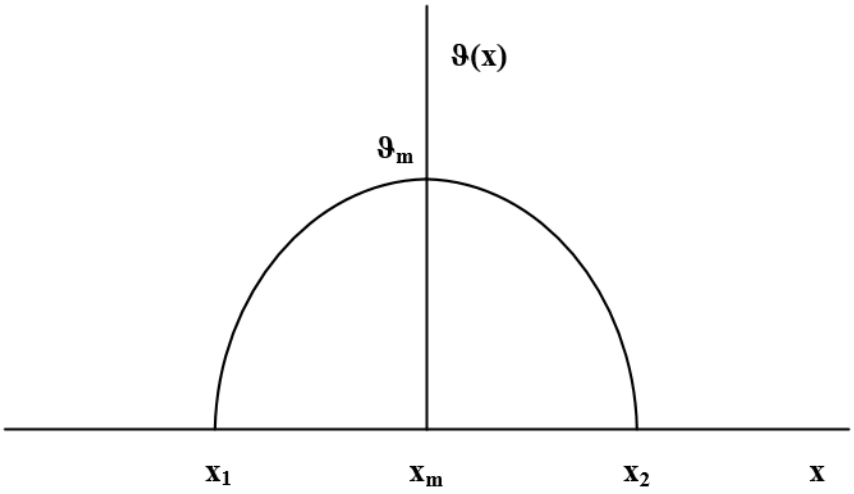

Figure 4-3: Quadratic performance function (adapted from Bauer *et al* (2007))

4.3. Overall economic performance index

As mentioned previously, performance functions relate the controlled variable to a monetary value. Therefore, historical data pertaining to profit or losses of the process can be produced from performance functions. Despite the availability of historical data obtained from PFs, the overall economic performance index (EPI), a single monetary value based on the historical data and performance functions of several process values, is often reported to summarise the economic performance of the process (Zhou and Forbes, 2003; Wei, Craig and Bauer, 2007).

An acceptable method in calculating the overall economic performance index is to use the product of the estimated process variable's probability density function and its performance function. Consequently, the calculation of the economic performance index requires an assumption to the probability density function of the process variable. Nonetheless, the probability density function of the process variable is assumed to follow a Gaussian distribution for simplicity in the calculation of the economic performance index (Bauer and Craig, 2008). Although several industrial process data do not necessarily follow a Gaussian distribution, this probability distribution provides a satisfactory estimation of the economic impact of the data (Zhou and Forbes, 2003). Therefore, once a performance function is obtained, the economic performance index of a controller (Ψ_{y_1}) for a controlled variable (y_1) can be calculated with the following equation (Wei and Craig, 2009a):

$$\Psi_{y_1} = \int_{-\infty}^{\infty} v(y_1) f(y_1) dy_1 \qquad \textbf{Equation 4-1}$$

The probability density function for the Gaussian distribution is defined as following:

$$f(y_1) = \frac{1}{\sqrt{2\pi}\sigma_{y_1}} \exp\left(-\frac{\left(y_1 - \mu_{y_1}\right)^2}{2{\sigma_{y_1}}^2}\right) \qquad \textbf{Equation 4-2}$$

Where μ_{y_1} and ${\sigma_{y_1}}^2$ are the mean and variance of the process variable y_1 respectively. Alternatively the product of a frequency distribution and the EPF can be used, further eliminating the assumption of a probability density function. Despite the assumption of a Gaussian distribution for a satisfactory estimation of the EPI, a non-Gaussian distribution of a control loop would indicate poor control performance of the control loop. Therefore assuming a Gaussian distribution requires careful assessment of the process behaviour (Bauer *et al.*, 2007).

4.4. Economic performance assessment of milling circuits

4.4.1. Background

Variations in milling circuits are a common challenge experienced in the minerals processing industry. Variations can occur from the feed ore properties such as the hardness, grade, and particle size. Compounded with the changing feed rate, these variables can affect process unit variables such as the mill load or sump levels and lastly the product particle size (Wei and Craig, 2009b). Therefore, factors such as the complexity of milling circuits in combination with cost-intensive process units, justify the importance of economic performance assessments applied to milling circuits (Hodouin *et al.*, 2001; Wills and Napier-munn, 2006).

The benefits to economic performance assessments can be observed from various literature studies. Wei and Craig (2009a) assessed the economic benefits of two controllers applied to their milling circuit simulation study. In contrast, Wakefield *et al* (2018) simulated different faults occurring in the milling circuit industry and their economic impact. Subsequently, the literature case studies highlight potential improvements to milling circuits, for example fault detection and advanced process control application.

However, despite the benefits to economic performance assessments, formulating economic performance functions for milling circuits is difficult. As mentioned previously, there are no clear guidelines in constructing performance functions. This can be observed in the survey of Wei and Craig (2009b), whereby for each controlled variable in the milling circuit, several different performance functions have been used in industry. To accommodate for the highly complex characteristics of economic impacts of variables, assumptions are made to simplify construction of performance functions (Zhou and Forbes, 2003; Oosthuizen, Craig and Pistorius, 2004). Therefore, with careful analysis of assumptions made, various economic performance assessments studies simplify complex processes by solely evaluating key process variables (Zhou and Forbes, 2003; Wei and Craig, 2009a; Steyn and Sandrock, 2013).

Selection of key process variables are dependent on their economic impact. Therefore, various literature studies neglect certain controlled variables in the economic performance assessment if their economic impact is insignificant. For example, Wei and Craig (2009a) assessed the economic impact of controlled variables such as the sump level and mill load were negligible because they are only controlled for stability, assuming they are controlled within a specific boundary. Finally, through synthesis of key economic variables identified, a single monetary value (overall EPI) is produced.

In the synthesis of key process variables, the product particle size, defined as the percentage mass of milling circuit product that is less than a specific size (e.g. 40% < 75 µm), is often chosen as a key process variable. Specifically the relationship between the product particle size obtained after comminution and the minerals recovery following the flotation circuit is utilized as a performance function. This important relationship is used to avoid economic assessments of both milling and flotation circuits. This is attributed to complexity associated with analysing both circuits (Craig and Henning, 2000). Furthermore, several studies have proven the consistency in using the product particle size to estimate the recovery (Wei and Craig, 2009a).

Therefore, economic performance assessments for milling circuits allow for the recovery to be analysed without additionally observing the flotation circuit. However, neglecting the factors associated with the flotation circuit remains a major limitation of milling circuit economic performance assessments. Nonetheless, milling circuit case studies have used the product particle size as a key variable representing the quality of the product. The following section further discusses milling circuit case studies and how certain assumptions made formulate their EPIs.

4.4.2. Milling circuit EPA case studies

As mentioned previously, for an economic case study an overall EPI is required. Steyn and Sandrock (2013) performed an economic impact study on an industrial autogenous (AG) mill, whereas Wei and Craig (2009a) performed a simulation based study on a semi-autogenous (SAG) mill. Despite differing types of mills, both literature studies based the overall EPI of the milling circuit on the profit:

$$Profit = R - C \qquad \textbf{Equation 4-3}$$

Where R is the revenue ($), and C is the cost ($). Furthermore the revenue is further evaluated as follows (Wei and Craig, 2009a; Steyn and Sandrock, 2013):

$$R = BP \times F \times HG \times MR \times t \qquad \textbf{Equation 4-4}$$

Whereby BP is the basket price of metal ($/g), F is the throughput (t/h), HG the head grade (g/ton), MR is the minerals recovery (%) and t the time duration (h). Despite a similar evaluation for the revenue and overall EPI, the contrast in evaluating the revenue is observed with the minerals recovery. Specifically the functional relationship between the flotation circuit recovery and product particle size after comminution differs. For example, Steyn and Sandrock (2013) used a linear relationship, derived from plant data, to relate the product particle size (PS) to the final minerals recovery from the flotation circuit (PR):

$$PR = 0.134PS + 79.61 \qquad \textbf{Equation 4-5}$$

Despite a linear relationship between the product particle size and the recovery, the product particle size is evaluated from empirically derived quadratic functions with the mill load and water inlet ratio to the mill. Furthermore, the quadratic functions derived from plant data has operating limitations for the mill load and water inlet ratio to the mill. Therefore, the economic performance of their product particle size is heavily dependent on these two factors.

Although Steyn and Sandrock (2013) evaluated the profit to the milling circuit with a linear relationship for the particle size and minerals recovery, there remains various other configurations for the relationship. Wei and Craig (2009a) used another common performance function, namely the quadratic function to relate the product particle size (y_1) to the minerals recovery ϑ_{y_1} in equation 4-6, whereby parameters a, b and c are defined as a = -0.009776, b = 1.705 and c = -2.955.

$$\vartheta_{y_1} = a{y_1}^2 + by_1 + c \qquad \textbf{Equation 4-6}$$

The quadratic function used by Wei and Craig (2009a) is depicted in figure 4-4. From observing the data, the maximum recovery obtained from the quadratic performance function is estimated to be 71.4% with a corresponding 87.2% of particles passing 75µm. Further observation of the quadratic performance function shows the dependencies of the recovery on factors influencing the product particle size from lab and plant experiments. Therefore, when evaluating the product particle size there are trade-offs. A finer product particle size (above particles passing 75 µm) results in larger recovery values at the expense of the throughput as well as an increase in energy costs involved with the mill. In contrast, a coarser product produced will result in a reduced concentrate grade due to the existence of middlings (Hodouin *et al.*, 2001; Wills and Napier-Munn, 2005). Consequently for both linear and quadratic performance functions, decisions based on operation and external economic factors need to be considered for analysing the product particle size.

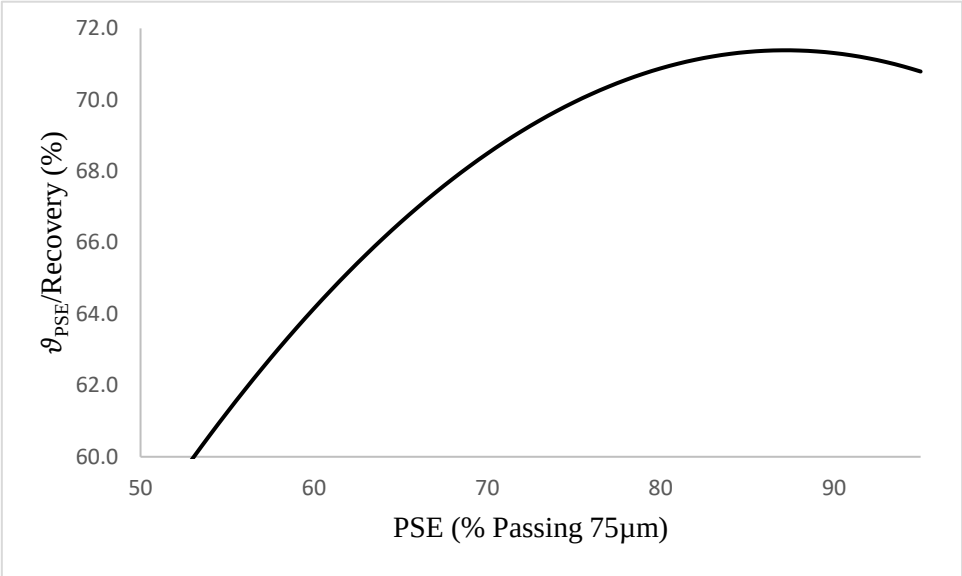

Figure 4-4: Performance function for the recovery (redrawn from Wei & Craig (2009))

In contrast to the product particle size, other controlled variables are assumed to be have an insignificant economic impact. Wei and Craig (2009a) assumed the mill load and sump level are controlled to ensure they stay within the stability limit of the system. When either of the controlled variables are greater or lower than their operating values the controller will rectify the error, however, countermeasures are only taken when these variables are outside predetermined limits (Wei and Craig, 2009a).

Figure 4-5 further illustrates the performance function for the sump level and would also be applicable for the mill load. The performance function is divided into three sections namely a middle range (operating range) and two ranges which exceed the upper or lower limit of the sump level. At the middle operating range there is no significant economic impact, however, if the boundary limits are violated the process operation must be stopped and remedial action taken which subsequently have different economic impacts. However, owing to the complexity

of milling circuit economic studies and differing assumptions, variables such as the mill load are not always neglected. This is evident in Steyn and Sandrock (2013) whereby the mill load effects are directly taken into account through the quadratic relationship with the product particle size.

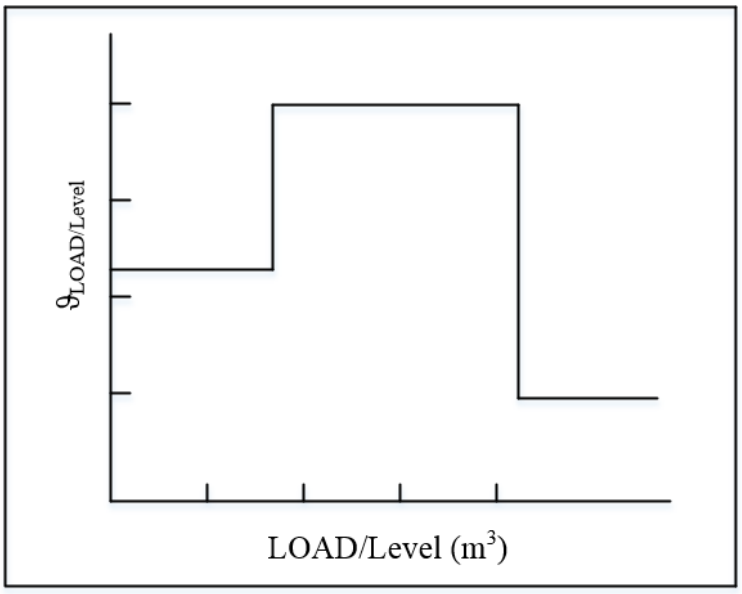

Figure 4-5: Performance function for the mill load and sump level (redrawn from Wei and Craig (2009a))

In addition, different assumptions can be observed in the assessment of the milling circuit costs. Similar to assumptions made for the construction of recovery versus product particle size performance functions, the flotation circuit operating costs are generally assumed constant for simplicity. However, the assumptions of the operating costs associated with the milling circuit differ for case studies. Wei and Craig (2009a) assumed the cost function is a constant for their case study. Although considering the high energy costs and complexity associated with comminution, this may not be a justifiable assumption. In contrast, other literature studies preferred to only incorporate the electricity costs of units in the milling circuit into their cost analysis as is shown in equation 4-7, where u is the unit cost of power and P is the power consumed (Matthews and Craig, 2012; Steyn and Sandrock, 2013). Therefore, the cost of grinding media is neglected. For cases such as Steyn and Sandrock (2013), this assumption is justified due to the mill being fully autogenous. However, despite evaluating a semi-autogenous mill, Wakefield *et al.*, (2018) still assumed the cost of grinding media is negligible and instead identified the energy consumption of the mill as the most important cost factor.

$$C = u \times P \times t \qquad \textbf{Equation 4-7}$$

Chapter 5
Methodology

Chapter overview

Chapter 5 provides a systemic outline of the methodology that will be applied such that each objective is achieved. Initially the milling circuit simulation model is motivated and described for its suitability. Subsequently, the objectives pertaining to implementing relay autotuning using CPM is described, including the degradation model and the CPI, based on historical benchmarking, to be used. Thereafter key parameters and factors to be evaluated for the relay autotuning procedure is discussed.

5.1. Case Study – Milling Circuit model

5.1.1. Motivation

A run-of-mine milling circuit simulation model designed in MATLAB® and Simulink® is used as a case study for relay autotuning. The milling circuit model has been presented in literature and has further been validated, using sampled plant data (Hulbert, 2005; Coetzee, Craig and Kerrigan, 2010; Le Roux *et al.*, 2013). As a result, literature sources have applied process control studies in combination with EPAs to the milling circuit (Wei and Craig, 2009a; Wakefield *et al.*, 2018). These factors validate the use of the simulation model to assess relay autotuning.

In contrast to literature sources applying relay autotuning to linearized models, the milling circuit is a non-linear system. Therefore, the effects of relay autotuning on a complex system can be evaluated, which has rarely been applied in research (refer to table 2-3). The simulation model also provides the possibility of assessing interacting control loops, once relay autotuning has been applied, due to the presence of multiple control loops. The factors mentioned culminate in a suitable environment with a simulation model that allows for evaluation of the research objectives.

5.1.2. Model description

Figure 5-1 shows the semi-autogenous (SAG) milling circuit model. The term semi-autogenous refers to a circuit that utilises the addition of steel balls and the ore itself for the breakage of ore. As a result, the milling circuit contains an additional state namely, steel balls for the mill. With the aid of the steel balls, the PSE can be obtained from the milling circuit. Despite the breakage of ore performed in the mill, process units such as a sump and hydrocyclone are required as a buffer and product separation unit respectively. Therefore, due to the process, five state variables are present within the milling circuit simulation model namely, water, steel balls, rocks, solids, fines and coarse ore.

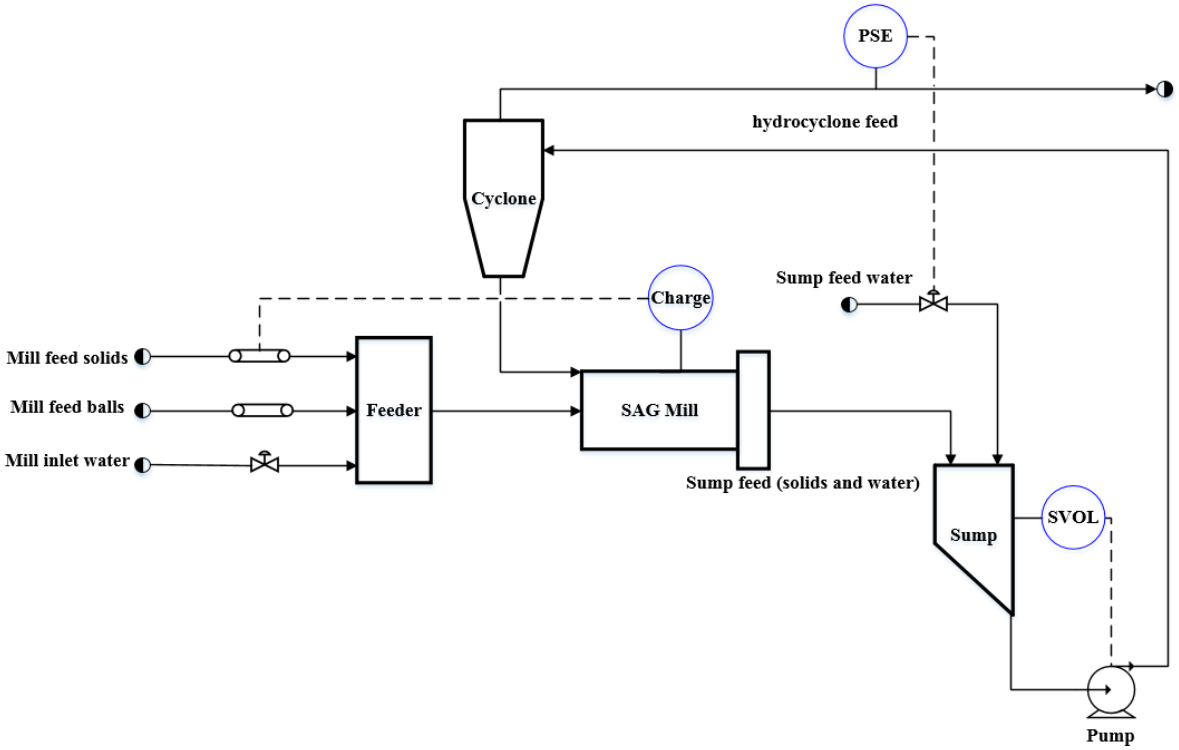

Figure 5-1: Milling circuit model (adapted from Le Roux *et al* (2013))

Rocks are defined as components which are too large to be discharged from the mill. Subsequently, solids are interpreted as components that pass through the mill and can further be assessed as the summation of fines and coarse ore. In contrast to coarse ore, the fines are described as particles which are smaller than a specific size range required for mineral liberation. Due to the importance of the PSE, the milling circuit's main objective is to maximise the fines produced with consideration to variables such as the electricity cost of the mill. Appendix A provides the equations implemented in Simulink such that simulated experiments can be performed. The following section further highlights the requirements needed from the simulation model such that realistic conditions are implemented in comparison to industry.

5.2. Data generation

5.2.1. Introduction

Ordinary differential equation (ODE) solvers enable users to evaluate and simulate process models. For this research study, MATLAB® and Simulink® are suitable software tools as they contain various ODE solvers such that the equations presented in appendix A can be evaluated. Furthermore, the simulation model presented in MATLAB® and Simulink® grant dynamic responses of the milling circuit model to perturbations and specifically relay autotuning in process control.

The milling circuit model in MATLAB® and Simulink® is further made realistic, to an industrial setting, through the addition of sensors with noise, input disturbances and regulatory control systems. The addition of these parameters, specifically noise and disturbances, allow for generation of unique data sets for experiments performed, due to the random number generators used. The seeds for these random number generators are changed for each experiments, therefore, altering the initialisation and sequence of random numbers generated. With each changing initialisation, a unique data set is produced for each experimental setting. Consequently, confidence in results can be obtained using unique data obtained, strengthening arguments proposed towards the thesis objectives. The additions of sensors with noise, input disturbance and regulatory control are further discussed, specifically applied to the milling circuit simulation model, in the following sections.

5.2.2. Sensors with noise

In an industrial setting, sensors allow process variables to be measured. Specifically for the milling circuit, sensors are used to measure flow rates, the particle size of stream or energy outputs associated with the mill. Most industrial sensors, however, experience noise. Sensor noise can be attributed to fast sampling rates and measurement errors (Wakefield, 2018). Despite the noise associated with the process variable reading, the measured value is generally close to the true value of the variable.

In comparison to an industrial sensor with noise, for the milling circuit model, sensor noise has been modelled by adding white noise to process variables measurements using a random number generator. Therefore, unique data sets can be obtained by altering of the seed of the random number generator. Furthermore, following equation 5-1, the sensor variance is modelled as a fraction of the process variable's operating value ($PV_{nominal}$). Whereby, n_L refers to a noise global fraction used for all sensors within the simulation model. For experimental purposes, n_L, is referred to as the sensor noise level because it's a variable that can be altered in evaluating the effects of the sensor noise level on relay autotuning.

$$\sigma^2_{sensor} = (n_L PV_{nominal})^2 \qquad \textbf{Equation 5-1}$$

5.2.3. Disturbances

Process disturbances are uncontrollable factors that vary within the process e.g. variations in feed flow rates, pressures, temperatures, and stream compositions. Within the milling circuit context, process variables such as the ore feed, steel ball and water flow rate can be upstream disturbances that could hinder optimal operation of controlled variables. In addition, within the ore feed, the rock hardness can vary depending on where the ore was obtained. Subsequently, variations in the ore hardness can translate to further disturbances such as the power required per mass of fines produced.

Nonetheless, for a realistic milling circuit simulation model, which adheres to an industrial setting, process disturbances such as the rock hardness as well as the power required per tonne of fines produced are implemented as bounded process disturbances. The disturbances have been modelled using one dimensional random walks (Lawler and Limic, 2012; Miskin, 2016). For a process variable $v(t)$, the process variable will increase or decrease depending on a gradient value s_i. Therefore, $v(t)$ is determined from integrating all s_i values up until time t:

$$v(t) = \sum_{i=1}^{t} s_i \Delta t + v(0) \qquad \textbf{Equation 5-2}$$

The gradient s_i is determined using a uniform discrete distribution to obtain a random number x_i which is bounded between 0 and 1. Depending on the value of x_i, the gradient is either positive or negative l. The random number generator, therefore, incorporates variations between experiments using the seed value. To avoid drifting of disturbances, the random walk needs to be bounded between an upper and lower limit. This is achieved by ensuring that v is at the boundary limit. Subsequently, decrease v with a negative gradient $(-l)$ if it has reached the upper boundary or increase v with a positive gradient $(+l)$ if it has reached the lower boundary.

$$s_i = \begin{cases} +l, & x_i < 0.5 \\ -l, & x_i \geq 0.5 \end{cases} \qquad \textbf{Equation 5-3}$$

5.2.4. Regulatory control

Process disturbances prevent system variables from reaching optimal operating conditions. To attenuate process disturbances, regulatory control is used. The introduction section highlighted the popular use of PID/PI control loops in attenuating process disturbances within industry. Equation 5-4 describes a PI controller which uses the error e between the controlled variable and its set point. The controller tuning parameters K_c and τ_I are selected such that set point tracking is optimal and the error reduced without excessive controller action. Fundamentally, the proportional term adjusts the manipulated variable proportionate to the error, thereafter, the integral term reduces steady state offset that occurs.

$$u(t) = K_c\left(e(t) + \frac{1}{\tau_I}\int_0^t e(t')\,dt'\right) + \bar{u} \qquad \textbf{Equation 5-4}$$

Within the milling circuit simulation model, three process control loops have been modelled. The sump water feed flow rate (SFW) is used to control the PSE, the cyclone feed flow rate (CFF) is used to control the sump volume (SVOL), and lastly the mill feed solids (MFS) is used to control the mill charge (the volumetric fraction of the mill that is filled). The control loops were designed based on common control loops used in industry (Wei and Craig, 2009b). Table 5-1 below shows the controller tuning parameters used for each PI control loop, and have been obtained using the Ciancone correlations. The obtained controller tuning parameters are conservative such that process disturbances are attenuated without excessive controller action.

Table 5-1: Controller tuning parameters for milling circuit simulation model

Control Loop	K_C	τ_I (h^{-1})	Set Point
SFW-PSE	928.6 ($m^3.s^{-1}.Pa^{-1}$)	4.54	0.67
CFF-SVOL	20 ($m^3.s^{-1}.Pa^{-1}$)	0.25	5.99 (m^3)
MFS-Mill charge	42.1 ($m^3.s^{-1}.Kw$)	9.46	0.34

Furthermore, the set points have been established in table 5-1. The mill charge and SVOL have been selected based on the stability of the process and require controllers because they are integrator processes. The PSE set point has been assessed from plant data and further indicate a set point away from the maximum achievable recovery (refer to figure 4-4). As mentioned previously, a set point at the maximum recovery introduces increased costs due to the power required for the mill.

Despite satisfactory controller tuning parameters that produces good control performance, the research project requires poorly performing control loops such that retuning is necessary. Nonetheless, the control loops are available and provide a platform such that process control research can be applied to the milling circuit simulation. Therefore, the following section discusses the methodology that will be followed, such that the research objectives are achieved, using the realistic milling circuit simulation model.

5.3. Implementing relay autotuning using CPM

5.3.1. Performance index

The aim of the literature study is to implement relay autotuning using CPM techniques. From chapter 3, variance based control performance indicators were discussed in order to obtain a suitable technique that evaluates poor controller performance. The Harris index was extensively discussed and the methodology as well as benefits to minimum variance control established. However, poor robustness and the use of linear time invariant models categorises the Harris index as a theoretical benchmark that describes CPM. Therefore, historical benchmarking is the appropriate substitute to the Harris index and, for the milling circuit simulation, historical benchmarking will serve as the CPI.

Using the historical benchmark requires evaluating which controlled variable should be used for the benchmark. As discussed in chapter 4, for milling circuit case studies, the key process variable established is the PSE, which is directly related to the recovery using performance functions. Therefore, through evaluation of literature, the historical CPI will be based on the variance of the PSE (σ_{PSE}^2) and the following equation is derived:

$$CPI = \frac{\sigma_{PSE}^2}{\sigma_{threshold}^2} \qquad \textbf{Equation 5-5}$$

From equation 5-5, the threshold PSE variance ($\sigma_{threshold}^2$) to which the current PSE variance is compared towards, is established. Generally for a historical benchmark, the current PSE variance would be compared to the variance at a period where control performance was evaluated as good. However, in this case $\sigma_{threshold}^2$ is referring to the 90th percentile of the PSE variance associated with the period where controller performance was assessed as satisfactory. This is performed such that the CPI can be used to implement relay autotuning when the current variance is above the threshold value.

Determining $\sigma_{threshold}^2$ requires a simulated period where no faults are occurring and the set point tracking of the PSE is acceptable. This period will be referred to as the normal operating condition (NOC). Therefore, the aim is to introduce a fault model such that the current controller tuning parameters would introduce poor controller performance. Poor controller performance will be characterised by σ_{PSE}^2 being larger than $\sigma_{threshold}^2$ for a significant period of time, resultantly, allowing the relay procedure to be introduced. Consequently, a fault model has to be chosen such that this is realizable. The following section further discusses the degradation model to be used within the study.

5.3.2. Degradation model

Controller performance can be classified based on the frequency of faults observed. In industry, the most frequently observed fault in processing is incorrect tuning settings despite autotuning settings on modern controllers. Other frequently observed faults include valve stiction, actuator faults, sensor faults and equipment degradation. Wei and Craig (2009b) further surveyed milling circuits specifically in order to determine frequently observed faults. The survey determined that process equipment found within the milling circuit, such as valves, particle size and other sensors were mostly experiencing faults. Furthermore, the faults were as a result of poor quality, outdated software as well as the abrasive and poor environment experienced in the milling circuit. Therefore, from the observed industrial faults, valve wear will be used as a degradation model within the study due to the abrasive nature of the milling circuit (Wei and Craig, 2009b).

Figure 5-2 illustrates valve degradation. The wearing of the valve plug allows for more slurry to flow between the valve seat and valve plug due to the abrasive nature of the milling circuit. As a result, the valve changes from linear to quick-opening characteristics. Therefore, the valve% is converted to the worn valve %, which is defined as the valve position without wear which would produce the same flow rate at the current valve state.

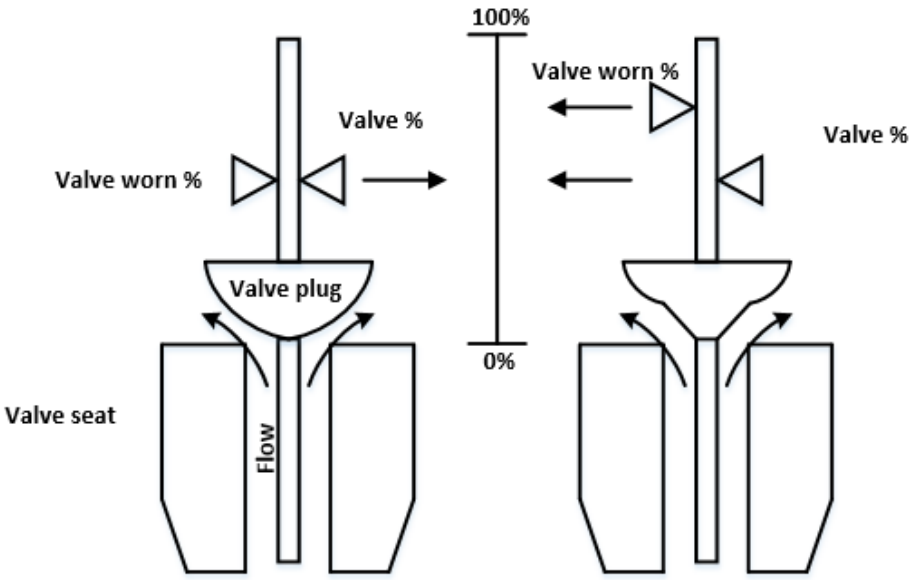

Figure 5-2: Valve before (left) and after (right) wearing (adapted from Miskin (2016))

Determining models for valve degradation is a complex process. Gaining detailed knowledge of slurry and valve characteristics, in order to fundamentally derive a valve wear model, would be a rigorous process. Therefore, equation 5-6 which describes valve wear, has been derived empirically from plant data (Miskin, 2016). Despite being used for a high pressure leaching simulation model, valve wear is assumed to be applicable due findings for literature sources justifying the abrasive nature of milling circuits. From equation 5-6, it can be shown that the worn valve percentage opening (valve worn%) is a function of the valve degradation (α(t)) and the unworn valve percentage opening (valve%) (Miskin, 2016).

$$valve\ worn\ \% = 100\ \times \left(\frac{valve\%}{100}\right)^{1-\ \alpha(t)} \qquad \textbf{Equation 5-6}$$

Equation 5-6 has been derived considering the following cases:

- 0% ≤ valve worn % ≤ 100%
- Valve worn % = 0% when the unworn valve% = 0%
- Valve worn % = 100% when the unworn valve% = 100%
- The valve worn % is a continuous function

Following the derivation of valve wear, an expression is required for determining the valve %. Miskin, (2016) empirically derived relationships relating the manipulated variable u, to the valve % through a gradient K_v for a high pressure leaching simulation model. Typically observed characteristics were linear valve relationship described by equation 5-7. As a result, the milling circuit simulation model will use the same linear valve relationship such that characteristics can alter from linear to quick opening.

$$valve\% = K_v\ \times u \qquad \textbf{Equation 5-7}$$

The valve wear model provides a means to implement poor controller performance. Nonetheless, assessment of which control loop to which valve wear will be implemented is required. Previously discussed reasoning have outlined the PSE as the important controlled variable. Therefore, for the milling circuit simulation model, valve wear will be applied to the SFW-PSE control loop valve. Despite the presence of water in this control loop, the assumption from an industrial point of view is that the SFW could potentially be a recycle stream containing ore that contributes to valve degradation.

Using the linear valve relationship as well as operating conditions obtained from Wei and Craig (2009a), it is assumed that for the nominal SFW operating condition of 267 $m^3.s^{-1}$ the valve% is at 50%, resultantly, the following relationship is adhered to in relating the valve% to the SFW.

$$valve\% = \frac{50}{267} \times SFW \qquad \textbf{Equation 5-8}$$

The information presented is synthesised into the following algorithm which details how valve degradation will be implemented into the milling circuit simulation experiments:

- For a given $\alpha(t)$ final value (e.g. 0.5) use a ramp function with a slope of 0.001hr^{-1} at simulation starting time 100 hours.
- Convert the SFW to valve% using equation 5-8.
- Once the starting time for valve degradation has been reached (100 hours), the valve% is converted to a quick opening characteristic through equation 5-6.

5.3.3. Relay execution using historical benchmarking

Following the derivation of the performance index, the valve wear model attempts to implement an environment that will indicate poor controller performance. Consequently, to achieve the research aim, a methodology has to be implemented such that poor controller performance is detected. Rato and Reis (2010) proposed a sliding window be used to evaluate controller performance over a certain period of time in their study relating to historical benchmarking. As a result, in order to determine the current variance of the process variable, a moving variance algorithm will be used within the simulation model.

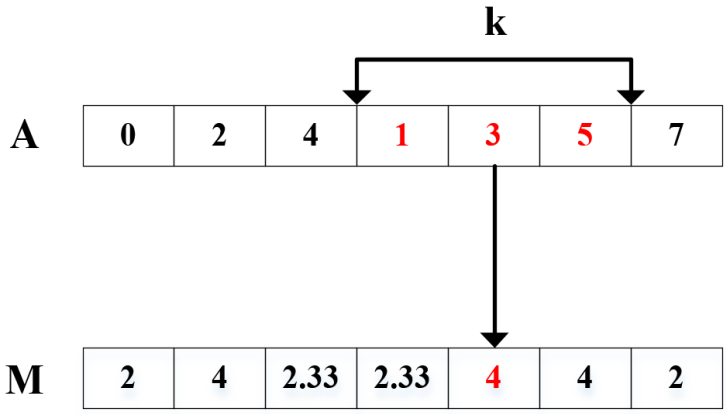

Figure 5-3: Sliding window method used to determine the moving variance

An example of how the sliding window/moving variance is performed is illustrated in figure 5-3. For a window length size (k) of 3, the moving variance calculates the variance over data set A and further translates the calculated value into a variance data set M. From the methodology, it is evident that the only parameter needed is the window length size. Generally there is no heuristic in determining the sliding window size k. However, the size should be within a range where a fault in the process such as a degrading element (e.g. valve degradation) is detected and results in a shift in the moving variance. Furthermore, caution should be taken for large window length sizes, considering most industries do not store large data sets. In the

interest of this study, a sensitivity analysis is performed before relay autotuning experiments such that a suitable sliding window length can be determined. The following algorithm will be used:

- In the presence of valve degradation vary the sliding window size
- Evaluate if there is a shift (an increase) in the moving variance, therefore, indicating a change in process conditions in comparison to the NOC.
- Evaluate feasibility of window size, for example if the window size is too small will it be able to detect changes in the process conditions, or if the window size is too large is it sensible in industry to evaluate such large data sets.

Subsequently, the sliding window in combination with the $\sigma^2_{threshold}$ will be used to initiate the relay autotuning procedure, therefore, providing a methodology for the objectives. Figure 5-4 depicts how the variance threshold value will be used to determine when to trigger the relay autotuning process. Procedurally, when σ^2_{PSE} is larger than the specified $\sigma^2_{threshold}$ value, for a specific number of time (t_{RS}), the relay autotuning procedure will be started. Currently there is no guideline to selecting a suitable t_{RS}, as a result, a subjective range of values will be used.

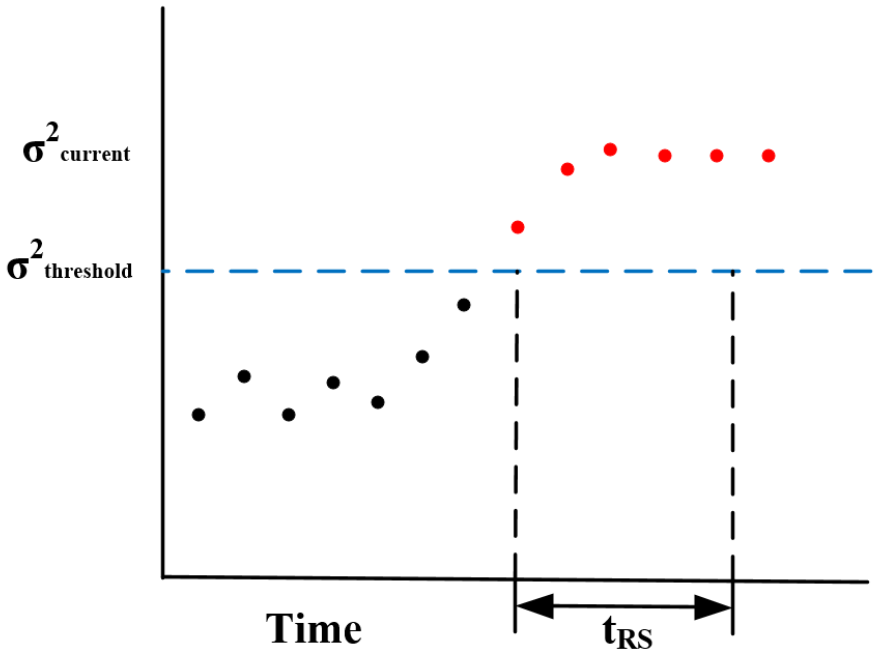

Figure 5-4: Control performance schematic illustrating the use of historical benchmarking in executing the relay autotuning procedure.

Based on the proposed control performance method, the following procedure will be used, in Simulink, to determining when to initiate the relay autotuner using the PSE.

- For NOC simulation conditions evaluate $\sigma^2_{threshold}$.
- Implement experiments with valve wear using the algorithm provided.
- Using $\sigma^2_{threshold}$ and σ^2_{PSE}, apply the principal based in figure 5-4. The relay autotuning procedure is triggered when σ^2_{PSE} has persistently been larger than $\sigma^2_{threshold}$ (region where process control is seen as poor). Resultantly, the following is observed for a specific number of time before the relay is initiated:

$$\sigma^2_{PSE} > \sigma^2_{threshold}$$

In addition to the triggering of the relay autotuner, an average CPI will be used to determine the controller performance for the two month period. Therefore, using the average of the calculated moving variance data set and equation 5-5, the average CPI can be evaluated. Logistically, if the average CPI value is larger than 1, for the two month period, controller performance was poor, as a result of the variance being larger than the 90th percentile for NOC.

5.4. Evaluation of relay autotuning

5.4.1. Key parameters

ANOVA is a useful technique whereby the mean of different sample populations can be compared, specifically on the performance criteria. ANOVA answers the question of whether factor means are truly different, therefore, allowing a comprehensive assessment of factors which could be useful for implementation of relay autotuning in industry. The objectives require evaluation of key parameters for implementing relay autotuning. As a result, ANOVA and Fischer LSD will be utilised such that key parameters can be assessed. Using the statistical analyses, a full factorial design of four factors with three levels will be performed. Therefore, with 10 repetitions, 810 experiments will be simulated for the ANOVA and Fischer LSD analyses. Selection of critical parameters have been analysed based on the findings from chapter 2 and 3. The critical factors as well as their levels have been summated in table 5-2.

Table 5-2: Key parameters and their levels that have been selected for the ANOVA

Factor	Levels
Sensor noise level (n_L)	0.0075 0.0100 0.0125
Valve degradation (α)	0.35 0.40 0.45
Relay start time (t_{RS})	3h 4h 5h
Relay amplitude factor (f_{RA})	0.40 0.50 0.60

As previously discussed, the relay autotuning literature has brought forward several variables that need consideration when applying the procedure. Factors and parameters such as the type of relay procedure, relay amplitude, convergence of the relay autotuner, tuning parameters, hysteresis levels, sensor noise level and MIMO procedures have been identified as variables that need consideration. For the project, relay with hysteresis was selected as a suitable procedure due the presence of sensor noise within industry. Despite the numerous variables, only the relay amplitude and the sensor noise level were selected as factors used for the ANOVA. The sensor noise level was selected based on the shortage of literature pertaining to realistic industrial conditions where sensor noise is present. Similarly, the relay amplitude was chosen to provide an industrial guideline for implementation of the relay with hysteresis. However, the tuning relationships as well as the sequential relay autotuning will be assessed separately in a supplementary evaluation.

In addition to the variables associated with relay autotuning, the proposed research provided a CPM technique, based on historical benchmarking, to execute relay autotuning. Resultantly, the relay start time is analysed in the ANOVA. Defined as the allowable time period of poor controller performance before relay autotuning is initiated, the assessment allows for analyses of the CPM technique in combination with relay autotuning variables. Therefore, the assessment could have potential importance in application of the proposed methodology. For example, earlier execution of the relay autotuner (i.e. smaller t_{RS}) could be more beneficial towards the performance criteria.

Furthermore, valve degradation has been defined within the methodology. The degree of valve degradation, specifically α, could have potential implications on the performance criteria. Therefore, assessing the intensity of the fault provides a differing perspective to the application of relay autotuning. It answers the question as to whether retuning is necessary depending on the extent/degree of valve wear. In addition, relay autotuning can be assessed against none retuning conditions. Therefore, at each α value experiments are simulated without retuning for 10 repetitions.

5.4.2. Pre-experimental procedure

The following section summarises the preliminary experimental procedures to be implemented. Before the relay autotuning simulations are evaluated, preliminary variables are required, as discussed in table 5-3. The sliding window size for the moving variance needs to be selected such that changes in the process due to valve degradation can be translated into a shift in the moving variance (i.e. detection of the fault). As a result, a sensitivity analysis is performed on selecting the sliding window size. Additionally, the variance threshold value falls into the preliminary category because it is evaluated at NOC whereby no valve degradation occurs. Lastly, n_O is required for determining the hysteresis limits. Therefore, for each n_L, the observed noise is determined such that the hysteresis limits can be obtained. Overall at each n_L, for NOC, 10 repeats are performed to obtain an average value for the preliminary variables.

Table 5-3: Preliminary relay autotuning experiments

Target variable	Varying variable	Range	Details
Desired sliding window size	Sliding window size	1 h 6 h 12 h	Evaluate the variance before and after valve degradation with a saturation of 0.5 has been implemented.
$\sigma^2_{threshold}$	n_L	0.0075 0.0100 0.0125	Used to evaluate if control performance is poor.
PSE_{UL} and PSE_{LL}	n_L	0.0075 0.0100 0.0125	The hysteresis limits are required for the switching of relay amplitudes in the presence of a noisy system.

5.4.3. Analysis of key parameters overview

Figure 5-5 shows the overall experimental flow sheet for the ANOVA analysis. The initial phase is obtaining pre-relay autotuning experimental data, namely the sliding window size, hysteresis upper and lower limits for the PSE. Lastly $\sigma^2_{threshold}$ is required for detecting poor controller performance. The CPI and EPI obtained from the NOC experiments are also required for comparison between valve degradation with and without relay autotuning experiments (as mentioned previously, for 10 repetitions at each sensor noise level). Subsequently, the ANOVA experiments are performed and the significant effects of the factors evaluated on the CPI and EPI.

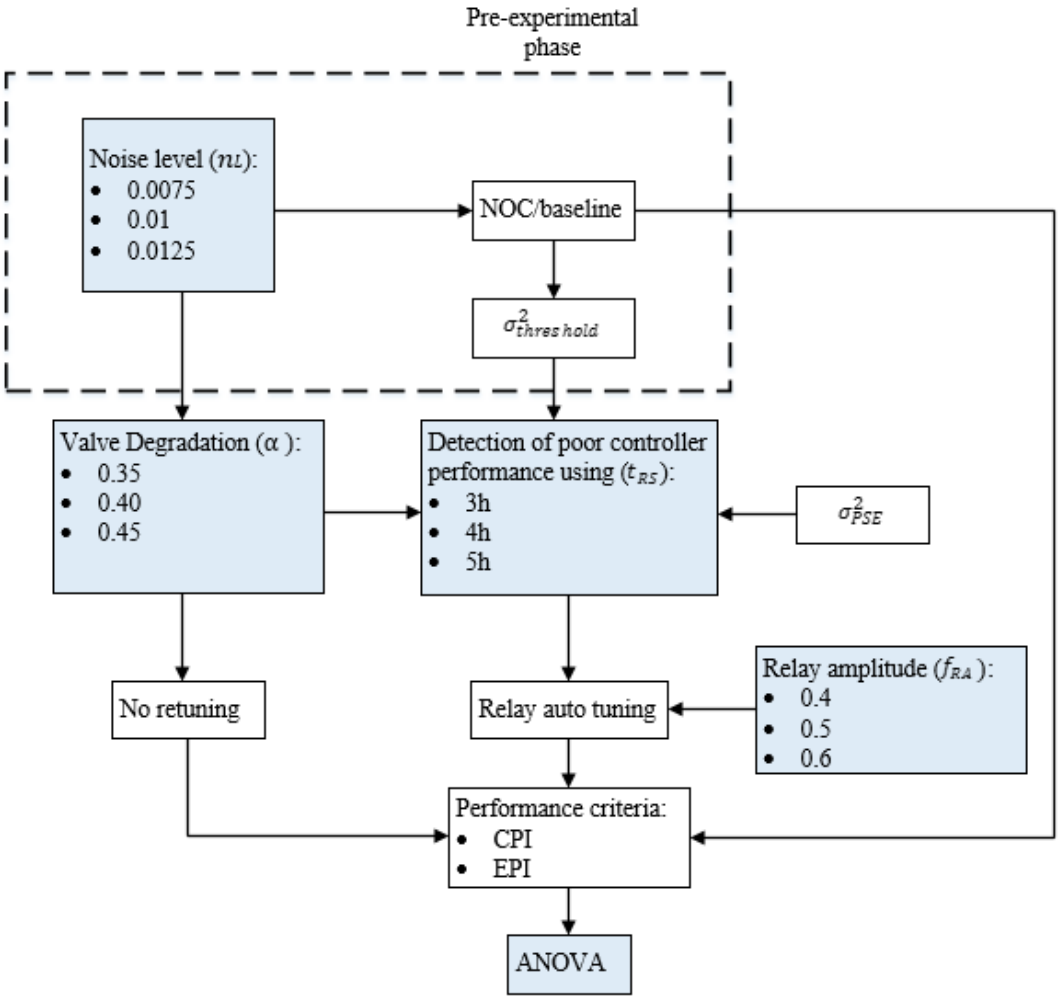

Figure 5-5: Flow sheet for the evaluation of relay autotuning and ANOVA variables

5.4.4. Supplementary assessment of relay autotuning

The ANOVA analysis provides a framework for identifying the best performing factors and their interactions, with respect to the CPI and EPI. However, there is an opportunity to assess variables that weren't evaluated in the ANOVA. As a result, this section defines supplementary relay autotuning experiments for further evaluation of the relay autotuning procedure.

Valve degradation is a fault frequently observed in industry. As will be observed in the results and discussion section, valve degradation introduces oscillations if the controller tuning parameters are too aggressive. The oscillatory behaviour can lead to high valve reversals. Valve reversals are described as the changing in direction of the valve. High valve reversals can result in static friction within the valve and further indicate additional faults such as valve sticking and valve stiction (Miskin, 2016). Similarly to valve degradation, valve stiction and sticking are commonly occurring faults within industry. Therefore, valve degradation in combination with valve sticking will be assessed.

Within Simulink, valve sticking can be simulated by adding a time delay to the SFW valve. The time delay models the internal static friction effects which introduce a phase lag in the controller action. Procedurally the experiment can be assessed as follows, using 10 repeated experiments: implement a time delay of 30s to the valve, evaluate the effects of the time delay on the CPI and EPI with and without valve degradation, lastly evaluate the effects of retuning in the presence of valve degradation and valve sticking.

The tuning parameters provided are the Ziegler-Nichols tuning parameters. However, the Tyreus-Luyben tuning parameters have been designed for MIMO control loops with interacting control loops. A comparative assessment of tuning relations will be performed and their respective effects on the controller performance, for a system experiencing valve degradation, assessed. Therefore, comparing the two tuning relationships will be performed using the ideal factor levels obtained from the ANOVA. Using 10 repeats, the effects of both tuning relationships will be evaluated on the CPI.

Procedurally, for a MIMO control loop, sequential relay autotuning is a procedure which retunes each control loop consecutively. This procedure is performed to account for interacting control loops. The sequential relay autotuning will be assessed by retuning the SFW-PSE control loop and subsequently the CFF-SVOL thereafter. For the current assessment, convergence of the initial control loop's tuning parameters will be ignored. The sequential relay autotuning procedure will be assessed at $t_{RS} = 3h$, $n_L = 0.01$ and $\alpha = 0.45$. In contrast, f_{RA} will be varied, with 10 repetitions for each relay amplitude. Furthermore, it's assumed both control loops will use the same t_{RS} and f_{RA} values.

5.5. Relay autotuner procedure

5.5.1. Overview

The objectives require implementation of relay autotuning within the Simulink milling circuit model. The poor controller performance detection technique has been provided, nonetheless, a structured procedure for relay autotuning is required. As mentioned previously, the SFW-PSE control loop will experience valve degradation and, subsequently, retuning. Conventionally, the remaining control loops would require retuning for a MIMO system. However, the proposed methodology assumes the remaining control loops do not require controller retuning. The assumption will be evaluated in the results and discussion section. The following procedure will be used to retune a SISO, namely the SFW-PSE control loop:

- Implementation of valve degradation.
- Detection of poor controller performance using the PSE variance.
- Determine the sensor noise level and, subsequently, the hysteresis band.
- All other control loops (CFF-SVOL and MFS-LOAD) are put in manual mode i.e. kept constant for the process
- Increase the manipulated variable to the upper amplitude (d_1).
- Once the controlled variable has reached the upper hysteresis level, shift the manipulated variable to the lower relay amplitude (d_2).
- Continue switching of relay amplitude until convergence of the limit cycle
- Once convergence of the limit cycle has occurred, the relay autotuner is switched off.
- The amplitude and period of the limit cycle are used to calculate the critical gain and period using equation 2-15.
- Using tuning rules such as the Ziegler Nichols, the new tuning parameters are calculated.
- Control is switched back from relay mode to PI control.

The following sections discuss the sensor noise level, hysteresis, relay amplitude, relay convergence and controller tuning, specifically for a simulation model.

5.5.2. Observed noise level & hysteresis limits

From the evaluation of literature, few literature sources applied relay autotuning with hysteresis. In industry, noise is prevalent and, therefore, the applications of relay autotuning within literature studies are unrealistic. As a result, there is a shortage of techniques used for determining the noise for the hysteresis band. Nonetheless, Berner, Hägglund and Åström, 2016 provided a technique in determining the observed noise level (n_O) by calculating the maximum deviation (y_{max}) and minimum deviation (y_{min}) of the process output at steady state. Equation 5-9 describes the calculation of n_o. The observed noise level is assumed as an average distance away from the steady state value using y_{max} and y_{min}. Industrially, the calculation of system noise using this method is not robust and does not factor process drift i.e. non-steady state evaluation. Nonetheless, the technique will be implemented in the Simulink model under the assumption the fault introduced does not induce process drift. The calculation of the procedure will be further evaluated in the results and discussion section.

$$n_O = \frac{(y_{max} - y_{min})}{2} \qquad \textbf{Equation 5-9}$$

Furthermore, based on the relay with hysteresis procedure, ε is required and should range between two to three times to observed noise level. For the current study, the selected ε value will be two times n_O. The value has been selected from an engineering view point whereby minimal drift in the controlled variable is favourable. For the current system, the SFW directly affects the SVOL and, therefore, it is desirable to implement a smaller ε . Therefore, for the Simulink model at steady state, the following methodology is used in determining the hysteresis upper and lower limits for the PSE, PSE_{UL} and PSE_{LL} respectively:

- Measure y_{max} and y_{min}.
- Using equation 5-9, calculate n_o.
- Using n_o determine the hysteresis level by multiplying the n_o :

$$\varepsilon = 2n_o \qquad \textbf{Equation 5-10}$$

- Add to hysteresis level to the PSE steady state value to obtain PSE_{UL} and PSE_{LL}:

$$PSE_{UL} = \varepsilon + PSE_{setpoint} = \varepsilon + 0.67 \qquad \textbf{Equation 5-11}$$

$$PSE_{LL} = PSE_{setpoint} - \varepsilon = 0.67 - \varepsilon \qquad \textbf{Equation 5-12}$$

5.5.3. Relay amplitude

The relay amplitude was identified as a key parameter in the relay autotuning procedure. Despite the importance of the relay amplitude, there is no substantial literature that provides a guideline to selecting a relay amplitude required to obtain a limit cycle for the controlled variable. Nonetheless, the required relay amplitude should be larger than ε and can be characterised using equation 5-13.

$$\left|K_p \mathrm{d}\right| > \varepsilon \qquad \textbf{Equation 5-13}$$

The heuristic requires the process gain (K_p) to be known beforehand. Industrially, the process gain can be obtained with a step test. As a result, a limitation to relay autotuning is determining a relay amplitude that would oscillate the controlled variable beyond the hysteresis upper and lower limit. Process knowledge is required which is a limitation for an automatic procedure which aims to reduce the knowledge required for operators.

For the current study various relay amplitudes will be evaluated such that the effects of the relay amplitude can be observed on the performance criteria. With respect to the Simulink model, the effects of the relay amplitude will be observed by increasing the manipulated variable SFW at the relay start time (t_{RS}) to the upper relay amplitude d_1, and decreasing the SFW to the lower relay amplitude d_2 by using relay amplitude factor (f_{RA}). Therefore, using the fractions provided in table 5-2, several relay amplitudes can be assessed.

$$d_1 = SFW \times (1 + f_{RA}) \qquad \textbf{Equation 5-14}$$

$$d_2 = SFW \times (1 - f_{RA}) \qquad \textbf{Equation 5-15}$$

The range selected for the relay amplitudes fractions were 0.4, 0.5 and 0.6 respectively. The chosen ranges considers the interaction between the SFW and the SVOL as well as ε. Referring to figure 5-1, the SFW directly affects the SVOL. Compounded with the CFF in manual mode (i.e. constant), selection of an incorrect f_{RA} can induce instability and violation of boundary conditions. Therefore, considering operating conditions provided by (Wei and Craig, 2009a) the f_{RA} range was selected such that the SFW does not exceed boundary conditions. Inherently, using a literature source further highlights the requirement of process knowledge and, resultantly, is a shortcoming of relay autotuning.

5.5.4. Relay convergence

Similarly to the relay amplitude, there is a shortage of literature that provide knowledge on procedurally terminating the relay autotuning process once convergence has occurred. From the literature sources, one analytic method was identified that provide a limit cycle convergence methodology. In contrast, several other sources used a graphical interpretation, which would require an operator to observe the controlled variable, for industrial application. Therefore, the analytical method proposed by Berner, Hägglund and Åström (2016) is beneficial in eliminating decision making for an operator.

The proposed methodology uses the time the current period takes (t_p) and compares it to the time the previous period took ($t_p{}^*$). If the absolute error between the two values is less than a certain threshold value ($P_{threshold}$), the limit cycle has converged. The following equation shows the proposed calculation for convergence (Berner, Hägglund and Åström, 2016).

$$\left|\frac{t_p - t_p{}^*}{t_p}\right| \leq P_{threshold} \qquad \textbf{Equation 5-16}$$

Selecting $P_{threshold}$ is a design criteria for the relay autotuning procedure. Berner, Hägglund and Åström (2016) evaluated three threshold values, such that accurate process models can be obtained. The analysed $P_{threshold}$ were 0.005, 0.01 and 0.05. Their results indicated that the accuracy of models were identical for each $P_{threshold}$. However, selecting $P_{threshold}$ affects the length of the relay experiment which could have an impact on the economic and controller performance. With this in consideration, for the Simulink model, the $P_{threshold}$ chosen is 0.05. The largest error tolerance has been selected which potentially removes prolonged relay experiments.

The period convergence method is a useful technique, however, application of the period convergence alone has potential flaws. Early convergence of the period does not account for the convergence of the amplitude of oscillations, especially considering the largest error tolerance was selected. If the amplitude of oscillations for the PSE has not converged, the calculated K_u can potentially exhibit inflated error. Therefore, the calculation of the amplitude of oscillations, within Simulink, will be based on the average of the peaks obtained. Furthermore, in combination with the period convergence, a minimum of five output sinusoidal peaks will be used. As a result, an average of the sinusoidal amplitude can be used once the limit cycle has converged, such that an accurate $K_u$can be obtained. The convergence of the limit cycle within Simulink can be summated as follows:

- Calculate the current period and previous period of the limit cycle.
- Determine if the limit cycle has converged using equation 5-16.
- If the limit cycle has at least 5 peaks, and the period has converged, calculate the new tuning parameters.

5.5.5. Controller tuning

Controller tuning methods consist of model based and Ziegler-Nichols type tuning relations. Model based tuning methods are more advanced, however, they require model validation before tuning parameters can be obtained. The objectives outlined do not require determining the most ideal tuning parameters but rather a method for implementing retuning. Nevertheless, evaluating model based tuning in comparison to the Ziegler-Nichols type tuning relations should be performed in future research for a comprehensive study.

The Ziegler-Nichols tuning relationships will be used to obtain the new tuning parameters once relay autotuning has been applied. Table 5-4 shows two possible relationships that can be used for the retuning of the controller. Tyreus-Luyben can be used directly for multivariate systems, however, the Ziegler-Nichols tuning relationship requires a detuning factor. The detuning factor allows the Ziegler-Nichols tuning parameters to be conservative for interacting MIMO control loops.

Table 5-4: Tuning Relations used for relay autotuner

Ziegler-Nichols	K_C	τ_I
PI	$K_u/2.2$	$P_u/1.2$
Tyreus-Luyben		
PI	$K_u/3.2$	$P_u/0.45$

The detuning factor f is described in equation 5-17 and 5-18 for the Ziegler-Nichols tuning relationship (Luyben, 1986). For the simulation experiments, the Ziegler-Nichols tuning detuned with f equal to 2.5, as is recommended from Yu (2006), will be used for the retuned system. As a result, the obtained tuning parameters will be more conservative than the Tyreus-Luyben but similarly account for interacting control loops.

$$Kc = \frac{K_{c,ZN}}{f} \qquad \textbf{Equation 5-17}$$

$$\tau_I = f\tau_{I,ZN} \qquad \textbf{Equation 5-18}$$

5.6. Economic performance

From the objectives, the project requires economic performance assessment of relay autotuning. Chapter 4 extensively discussed formulation of EPI relating to the milling circuit. For the purpose of this study, the approach used by Wakefield *et al.*, (2018), whereby an instantaneous EPI is determined using equation 5-19, will be used. The instantaneous EPI values are calculated under the assumption that the comminution is applied to a platinum mining process. Therefore, the following parameters are used: HG of 3g/ton, BP of US$35.3/g and an electricity cost of US$0.06/kWh (standard tariff used in previous studies). The instantaneous EPI was chosen to avoid assuming the data follows a Gaussian distribution. The presence of faults such as valve wear introduce non-linearity, as a result, the methodology used in section 4.3 cannot be used because the data does not follow a Gaussian distribution.

The EPI incorporates both revenue and costs in contrast to the method used by Wei and Craig (2009a), where cost was assumed constant. Therefore, the cost incorporates the power used by the mill (P_{mill}) for a comprehensive cost analysis. However, evaluating the costs associated with mill in isolation is a potential limitation to the study. For future studies further equipment cost analysis should be investigated. In contrast to the cost analysis, studies performed on the milling circuit simulation model all incorporate the recovery translated from the PSE using the quadratic performance function (Wei and Craig, 2009a; Matthews and Craig, 2012; Wakefield *et al.*, 2018). Therefore, the quadratic performance function is used for this thesis.

$$EPI\ (\$/h) = R - C \qquad \textbf{Equation 5-19}$$

$$R(\$/h) = BP \times MFS \times HG \times MR \qquad \textbf{Equation 5-20}$$

$$C\ (\$/h) = u \times P_{mill} \qquad \textbf{Equation 5-21}$$

The Simulink model operates with a sampling time of 1 minute. Consequently, the instantaneous EPI calculated requires a unit conversion such that the accumulated EPI for the 2 month simulation period can be evaluated. Equation 5-22 is the adjusted EPI calculation implemented in MATLAB to determine the accumulated EPI for the 2 month period.

- Determine the PSE, MFS, and P_{mill} at each sampling time.
- Using the PSE and quadratic performance function, calculate the MR.
- Determine the instantaneous EPI using equation 5-19.
- Determine the EPI for the simulated time period using equation 5-22

$$EPI\ (\$) = \left(\sum_{t=0}^{stop\ time} EPI_{inst} \right) \frac{1}{60} \qquad \textbf{Equation 5-22}$$

Chapter 6
Results and Discussion

Chapter Overview

Chapter 6 provides the results obtained from the experiments performed using the methodology. Initially the valve degradation model with application towards the milling circuit is discussed. Subsequently, control performance monitoring with respect to valve degradation and relay autotuning is assessed. The ANOVA results are then evaluated with respect to the CPI. Thereafter economic performance assessment of relay autotuning is discussed. Lastly, supplementary relay autotuning experiments were evaluated

6.1. Valve degradation applied to the milling circuit

6.1.1. Product particle size

The following sections provides an overview of valve degradation evaluated on the milling circuit simulation model. The valve degradation model has never been applied to the milling circuit simulation model and, therefore, requires assessment. From experiments, figure 6-1 depicts the effects valve degradation has on the PSE in comparison to Figure B-2.

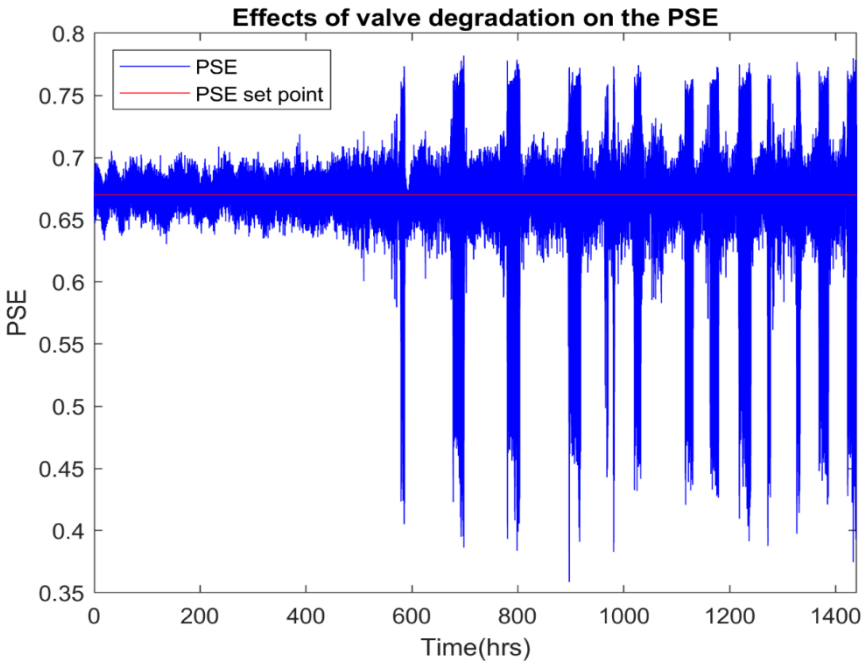

Figure 6-1: Effects of valve degradation on the PSE for $\alpha = 0.45$ and $n_L = 0.01$

The implementation of valve wear introduces oscillations into the system. This is attributed to the valve characteristics shifting from linear to quick opening behaviour. As a result of wearing to the valve seat, more flow is allowed through the valve for the controller action. In addition, it can be shown that the same behaviour observed in the milling circuit, once valve wear has been introduced, is displayed for the high pressure leaching simulation model used by Miskin (2016). In addition to introducing oscillations within the PSE-SFW control loop, the valve wear inherently generates another commonly found problem in industry, namely wrongful controller tuning. Due to the incorrect controller tuning parameters, specifically large controller gains, as valve wear is implemented the excessive controller action is further intensified. Therefore, the maintenance of controllers is important for industry and the observed effects highlight the necessity for regular retuning of controllers.

Furthermore, assessment of increasing the extent of valve degradation is depicted in figure B-25 (refer to appendix B, 'extent of valve degradation'). From the figure, low and medium extents of valve degradation do not produce large fluctuations. However, at $\alpha = 0.45$ extreme oscillations are observed, which is further shown in figure 6-1 at a system with larger sensor noise. The increase in oscillations can be explained with the wearing of the valve seat. Increasing α allows more flow through the valve and, as a result, increases in overshoots are perceived.

Referring to appendix A, the coarse ore split is modelled to incorporate the effects of the fraction of solids within the hydrocyclone feed (F_i). Specifically from the Plitt equation, an increase in F_i increases the corrected size classification (d_{50c}), defined as the particle size whereby 50% of the specific particle size entering the hydrocyclone would report to the overflow and underflow. An increase in d_{50c} would allow more coarse particles to be observed in the overflow (product stream). An increase in the SFW reduces F_i which results in an increase in the PSE, therefore, the SFW is proportional to the PSE i.e. a positive gain is assessed. Due to this relationship, correct controller tuning parameters are vital in maintaining the PSE at its set point.

However, when degradation is implemented on the SFW valve, as is shown in figure 6-2, the oscillations for the PSE is produced due to their proportionate relationship. As the controller attempts to maintain the PSE at its set point value, with the current controller tuning parameters, the valve % opening is constantly changed to compensate for the overflow. This is attributed to the linear valve conversion to quick opening characteristics. In addition to the excessive changes in the SFW, large travel distances are produced with valve degradation (e.g. flow rate changing from 0 $m^3.s^{-1}$ to values above 250 $m^3.s^{-1}$) which has potential to degrade the valve further.

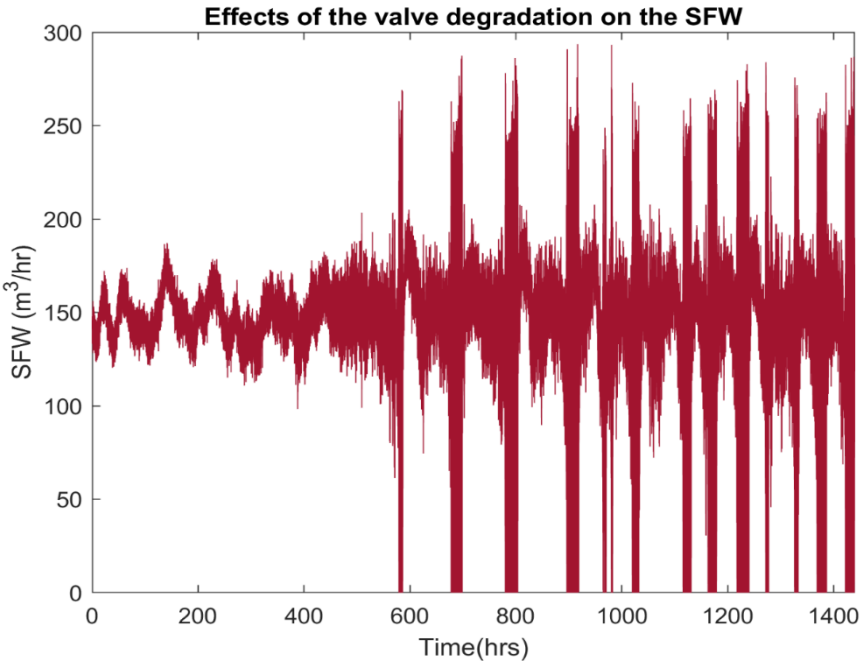

Figure 6-2: The SFW for $\alpha = 0.45$ and $n_L = 0.01$

Although the SFW varies between 0 and 300 $m^3.s^{-1}$, the resultant effect on the PSE is an asymmetrical oscillation around the set point (0.67). The decreases in the SFW introduce a larger deviation from the set point than for increases in the SFW. Similar effects are shown for relay autotuning, whereby the symmetrical relay heights introduce asymmetry in the PSE i.e. larger decreases than increases. The effects are attributed to the current system parameters, specifically with respect to the parameters associated with the coarse particle split in the hydrocyclone. As a result, the PSE is bounded to an upper limit of 0.8. However, the lower boundary is 0.35. Therefore, valve degradation for the current system produces a bias towards larger decreases from the set point, than increases, for the PSE. Evaluation of figure B-38 (refer to appendix B, 'hydrocyclone flow rates' section) further illustrates the tendency for a larger increase in fines reporting to the underflow, which would reduce the PSE.

6.1.2. Sump volume

Similarly to the PSE-SFW control loop, the fluctuations can be noticed for the SVOL-CFF control loop. The effects are due to the SFW's relationship with the SVOL. From the process model, it can also be shown that the SFW is proportional to the SVOL. An increase in the SFW would increase the volume of water within the sump and, as a result, the CFF would increase to reduce the sump volume to the set point. The fluctuations produces a SFW that behaves as an oscillating disturbance to the SVOL-CFF control loop. Referring to figure 6-3, similar behaviour to the PSE is observed for the SVOL whereby the CFF is unable to attenuate the oscillatory SFW disturbance. Therefore, poor set point tracking is induced.

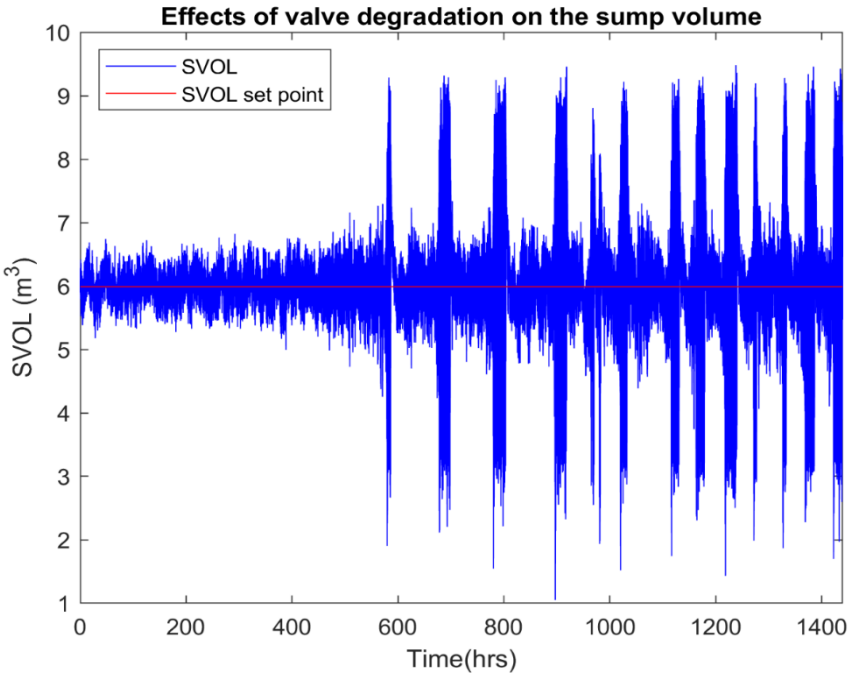

Figure 6-3: Effects of valve degradation on the SVOL for $\alpha = 0.45$ and $n_L = 0.01$

Additionally, the CFF contributes to the oscillations that occur within the system. Referring to appendix A, the coarse ore split is modelled to incorporate the effects of the CFF. From the Plitt equation, an increase in CFF decreases d_{50c}. As a result, less coarse particles report to the overflow. The reduction in the number of coarse particles in the overflow directly increases the PSE. From a controller perspective, if the SFW is increased, the CFF decreases to maintain the SVOL at its set point. The decrease in CFF, therefore, further increases the PSE. These relationships show the interactions between control loops are significant for the milling circuit and provide a complex overall assessment to the effects of valve degradation due to the CFF oscillations depicted in figure B-13 (refer to in appendix B,'SVOL control loop').

6.1.3. Mill charge and power draw

The effects of the valve degradation system can further be evaluated on the mill. The SFW is directly proportionate to the mill load due to the recycle stream containing water and solids. Increasing the SFW directly increases the mill LOAD. As a result, the oscillations from figure 6-2 are directly observed for the mill charge, as is illustrated by figure B-15. Despite the large fluctuations observed for the PSE and SVOL, the mill charge does not have large fluctuations from its set point. This is illustrated by comparing the effects of valve degradation in comparison to NOC, as is shown with figure B-7 and B-15.

The degree to which the variance of the mill charge increases can be assessed and is shown in figure 6-4. The variation observed for the 10 experimental runs, at each condition, indicate that the oscillations produced in the SFW result in minimal variation in mill charge control loop. Based on the data from the figure, at the largest extent of valve degradation, the variance in the mill charge is only increased by approximately 0.0002. Furthermore, the mean value of the mill charge is 0.34 for each condition which indicates minimal process drift for the mill charge once valve degradation is implemented.

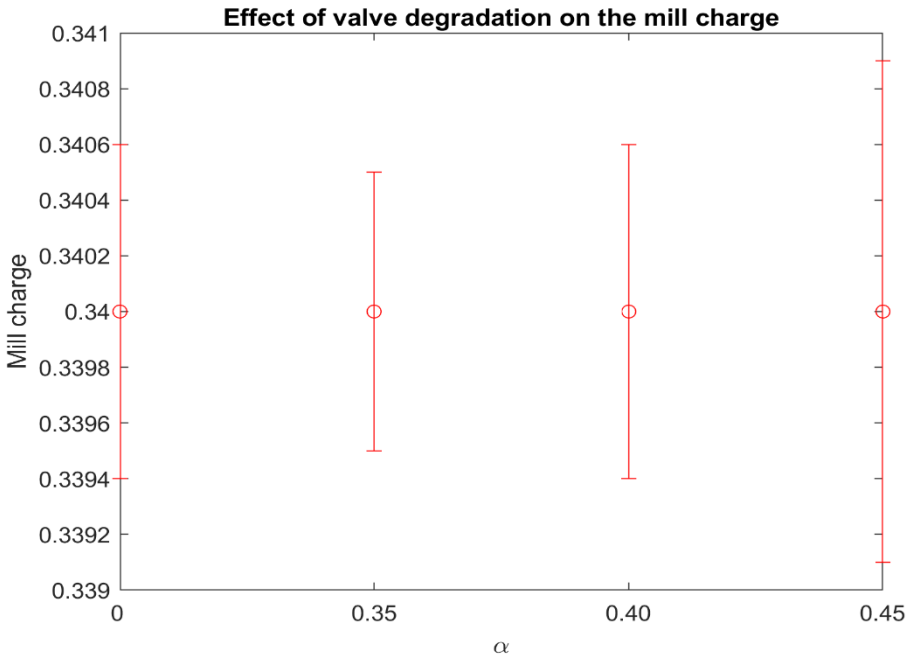

Figure 6-4: Effect of the extent of valve degradation on the mean value of the mill charge, with 2σ

Assessment of the MFS should indicate a bias towards larger increases in comparison to NOC, in the presence of valve degradation. The predicted tendency for larger increases in the MFS is resultant from the system conditions. Figure B-34 and B-32 illustrate larger decreases in the solids and water in the recycle stream. Furthermore a larger portion of coarse particles report to the overflow, resulting in the large negative deviations in the PSE from its set point. The combination of larger decreases in the recycle water and solids should result in larger increases in the MFS to attenuate the change in the mill charge. However, from figure 6-5, the results indicate no significant increase in the average MFS as α increases. Furthermore, there is no identifiable increase in the variance of the MFS from NOC. The data justifies the similar trend observed between figure B-8 (NOC for MFS) and the effects of valve degradation on the MFS in figure B-16. Therefore, valve degradation has no perceivable effect on the throughput of the milling circuit simulation model. In comparison to the CFF and SFW, the MFS is not affected by the wearing of the valve.

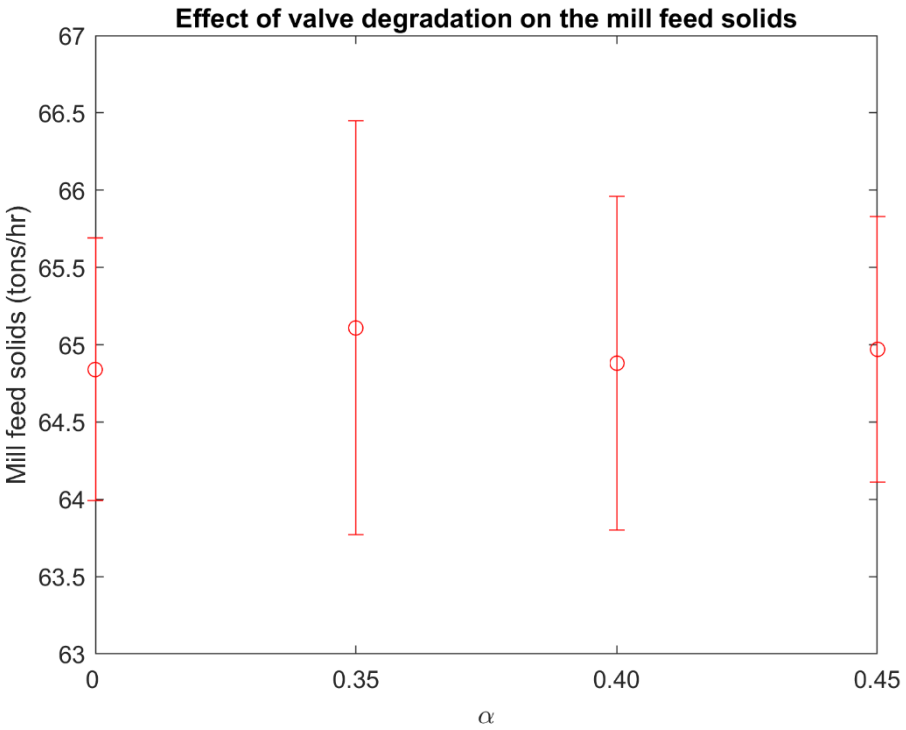

Figure 6-5: Effect of the extent of valve degradation on the mean MFS, with 2σ

The increase in the variance of the mill charge has a significant effect on P_{mill}, as a result of the changing slurry characteristics. The P_{mill} model is designed to be low for a high and low water content within the mill. For a LOAD containing a high water content, the slurry forms a puddle at the bottom of the mill. In contrast, a low water content would produce a ball of mud. Despite the differing characteristics, they both absorb smaller quantities of energy. Therefore, P_{mill} depends on the rheology (φ) and the mill LOAD respectively. It is expected that when the extent of valve degradation is large, the mill power draw is lowered as the SFW oscillates i.e. when the SFW induces high and low water contents within the mill due to the recycle stream. Figure 6-6 highlights the slight decrease in the grand mean observed for P_{mill} at each α condition. The decreases in P_{mill} are expected due to the large reduction in water within the recycle stream to the mill (refer to figure B-32). In addition, the variance of P_{mill} increases due to the oscillations the SFW produce for the mill recycle stream.

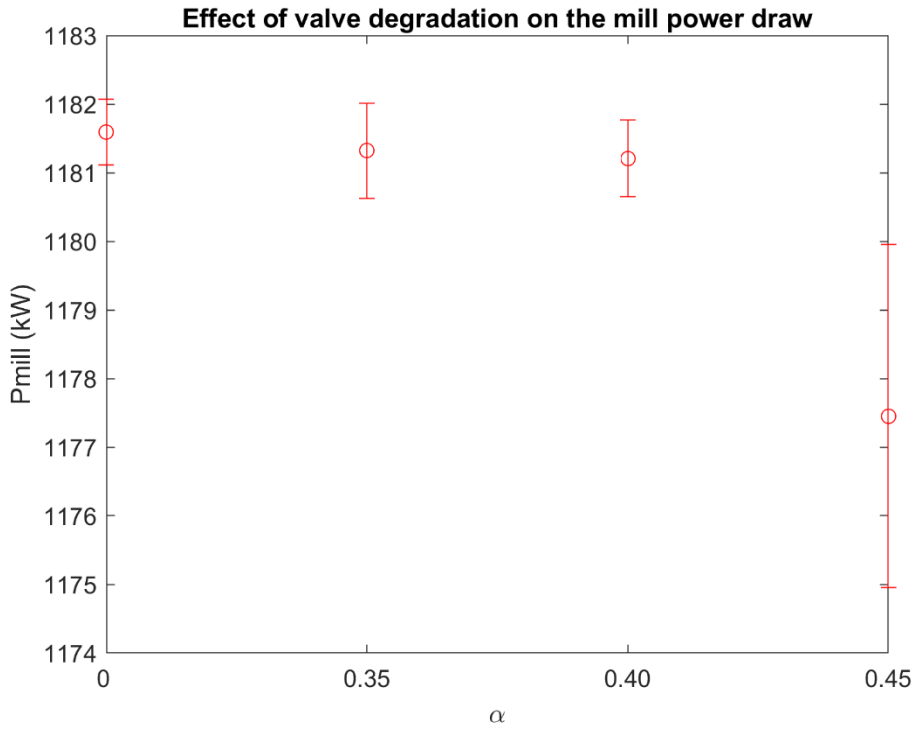

Figure 6-6: Effect of the extent of valve degradation on the mean P_{mill}, with 2σ

Furthermore, assessment of figure B-20 indicates the conditions for the maximum mill power draw does not occur. For P_{mill} to increase to the maximum mill power draw (P_{max}), the effects of the rheology (Z_r) and the LOAD (Z_x) need to equate to 0. These cases both occur when φ equals the rheology at the maximum power draw (φ_{Pmax}) and the mill charge within the mill equates to the charge at the maximum power draw (v_{Pmax}) simultaneously. A separate evaluation on φ, Z_r and Z_x indicate the rapid changes of the SFW translates to these variables, as is shown with figure B-22, B-23 and B-24 in appendix B (refer to mill power draw section). However, Z_r and Z_x never equate to 0 simultaneously. As a result, for extreme oscillations in the SFW, the range at which the mill charge and φ are affected introduce reductions in P_{mill} and limits the current P_{mill} to a maximum of P_{mill} at NOC (roughly 1220kW).

6.2. Control performance monitoring

The following section discusses controller performance holistically in terms of historical benchmarking. Initially the historical benchmark is assessed towards its adequacy in detection of poor controller performance, an important criteria established by Rato and Reis (2010). Subsequently, the effects of valve degradation is evaluated with respect to the historical benchmark. Lastly, relay autotuning is compared towards none retuning simulations in the presence of valve wear.

6.2.1. Historical benchmarking as a CPI

It is evident that valve wear has an oscillatory effect on the PSE-SFW control loop. Therefore, retuning of the process controller is required to reduce the aggressive controller action. Historical benchmarking and the subsequent use of a sliding window is required to detect the effects of valve wear through observation of the moving variance. Furthermore, It is required that the relay autotuning procedure can be initiated using the CPM technique. From the analysis of valve wear on the moving variance, for a sliding window of 1 hour, figure 6-7 is produced for $\alpha = 0.45$.

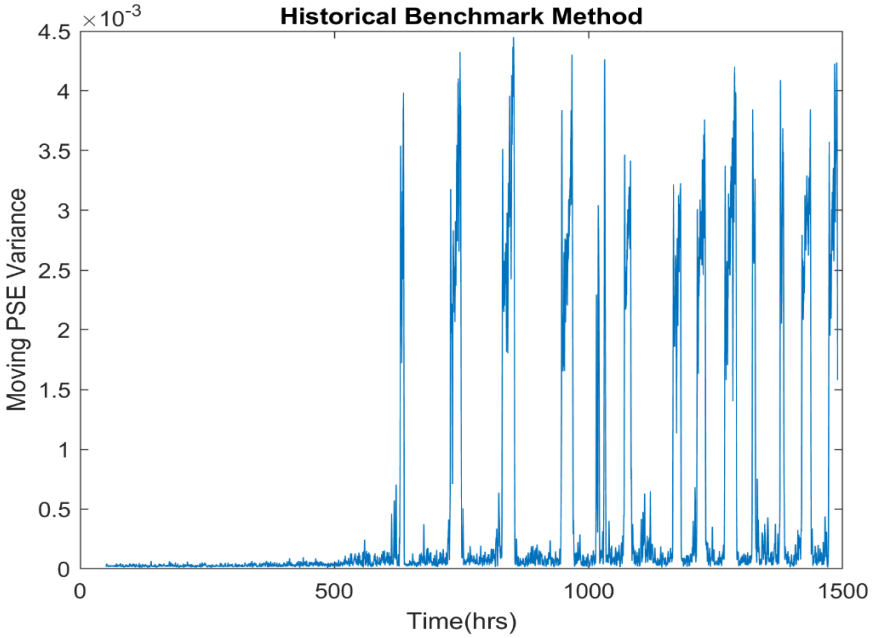

Figure 6-7: Historical benchmark method illustrating the shift in the moving variance once $\alpha = 0.45$ for $n_L = 0.01$

At a sliding window length of 1, a shift in the variance, after valve degradation has been introduced, can be observed. There is a clear increase in the moving variance values as time progresses. In addition the detection of low extents of valve degradation ($\alpha = 0.35$) was compared for 1hr, 6hr and 12hrs and is shown in appendix B (refer to historical benchmark section). The data indicates all sliding windows are able to detect lower extents of valve degradation which would visually depict similar to behaviour to NOC.

Detection of changes in process conditions, due to persistent faults, is one of the determining factors in selecting the sliding window length (Rato and Reis, 2010). The moving variance methodology is able to detect the underlying fault behaviour at various sliding windows, however, a choice on the sliding window size has to be made. Currently there is no clear guideline on choice of the sliding window length, however, a subjective decision can be made. For the current study, the choice of a 1 hour sliding window was assessed as suitable. This is justified in industry, whereby larger data sets are rarely used (Bauer *et al.*, 2016). In addition, a larger sliding window size would, inherently, detect persistent faults later than a small sliding window size. In contrast, a larger sliding window length is insensitive to smaller changes in the process system. A smaller sliding window length would be sensitive to faults that do not persist. For example, a change in system conditions that only occurred for an hour and affects the system variance, would be significant for a smaller sliding window.

For the current methodology, although the 1hr sliding window is smaller and more sensitive to smaller changes in the system, the relay autotuning procedure is aided with t_{RS}. As a result, faults that do not persist within the system, which could trigger the relay procedure, can be avoided due to the threshold time required before the relay procedure can be initiated.

6.2.2. Valve degradation

Using the 1 hour sliding window, the average CPI for the 2 month period can be assessed. Table 6-1 quantitatively displays the effects the extent of valve degradation has on the average CPI in comparison to the baseline experiment at each noise level. From the data, an increase in the average CPI in comparison to the baseline/NOC experiment, at each sensor noise level, is observed. The increase in the average CPI is due to the fluctuations occurring, therefore, an increase in the moving variance values (refer to figure 6-7). Assessment of low and medium extents of valve on the obtained CPI values indicated values relatively close to the CPI at NOC ($\alpha = 0$). These values are further justified with figure B-25, whereby at a low and medium α value, the perturbations are visually minimal. However, at $\alpha = 0.45$ extreme oscillations are observed which translate to relatively larger CPI values.

Table 6-1: Effect of varying α on the CPI at each n_L

n_L	α	CPI
0.0075	0.00	0.61
0.0075	0.35	0.98
0.0075	0.40	1.38
0.0075	0.45	22.87
0.0100	0.00	0.63
0.0100	0.35	0.94
0.0100	0.40	1.27
0.0100	0.45	8.46
0.0125	0.00	0.62
0.0125	0.35	0.99
0.0125	0.40	1.44
0.0125	0.45	9.91

The benefits of the historical benchmarking methodology is exemplified from the increasing CPI values. The increasing CPI values could be favourable in industry if detection of poor controller performance is necessary. The methodology is specifically favourable in the detection of changes in the variance and, subsequently, the product quality. However, caution should be taken with using the variance. Valve degradation does not induce process drift. Process drift is a result of the controlled variable persistently deviating from its set point. With process drift, the variance can be constant during process drift. Therefore, the historical benchmarking methodology is only viable if the variance differs in cases where the process behaviour is oscillatory or the controller is too aggressive. The problem can be attenuated by changing the basis of the CPI from the variance to an upper or lower threshold value from the mean.

Although the problem is not associated with the controller tuning parameters, Wakefield *et al* (2018) evaluated that the MFS continually decreases as mill liner wear is implemented. Wearing of the mill liner reduces the energy transferred to ore. As a result, there is a gradual accumulation of rocks within the mill. To attenuate increasing the LOAD, the MFS decreases. The MFS is an important criteria in the economic performance assessment as it is used as the throughput. Using the mean as a historical benchmark, the gradual decline of the throughput can be detected, which could have significant impact on the economic performance if mill liner wear is detected early and attenuated. In contrast, the variance of the MFS wouldn't reflect the decrease in the MFS, therefore, the selection of a user defined historical benchmark is important for the type of fault present

6.2.3. Relay autotuning

Due to the aggressive controller action, the controller requires retuning such that oscillations within the PSE-SFW control loop can be reduced. Using the t_{RS}, a certain period of time is allowed before the relay autotuning procedure can be initiated. Furthermore, various time delays, whereby a certain time period above the moving variance threshold was allowed such that a false alarm wouldn't be triggered. The resultant effect of retuning is displayed with figure 6-8.

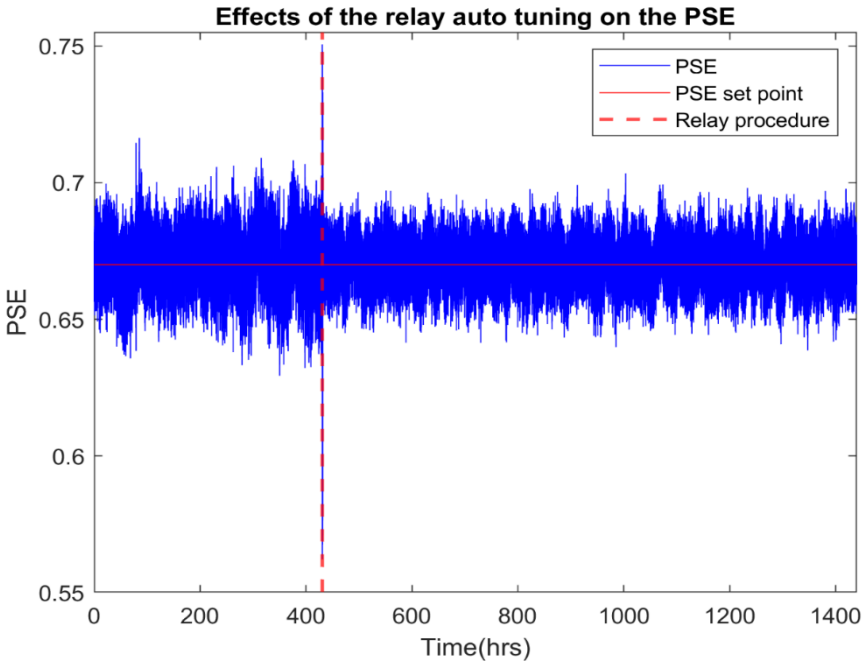

Figure 6-8: Effects of relay autotuning on the PSE for $\alpha = 0.45, t_{RS} = 3hr, f_{RA} = 0.4$ and $n_L = 0.01$

Figure 6-8 does not clearly show the relay autotuning procedure due to the time steps used, instead the PSE before and after relay autotuning (red dotted line) can be distinguished. In contrast, figure B-10 and B-11 in appendix B provide a clearer illustration of the specific relay autotuning procedure shown in figure 6-8. The graphical data depicts a reduction in the oscillatory effects and magnitude of deviations observed in figure 6-1, when relay autotuning is implemented. Therefore, set point tracking with relay autotuning has improved. In addition, using an historical benchmark allowed for quick detection of the valve degradation fault, such that none of the oscillations in figure 6-1 are observed.

Quantitatively, the new controller tuning parameters after relay autotuning is shown in table 6-2. From the data, the controller gain is reduced to values ranging from 200 to 300 ($m^3.s^{-1}.Pa^{-1}$). With the new tuning parameters obtained, the average CPI observed is reduced, which indicates better controller performance than without retuning (refer to table 6-1). These values are effective because, in the presence of valve degradation, the critical gain where oscillations occur is determined and a reduced controller tuning parameter is evaluated using the Ziegler-Nichols tuning parameters. Table 6-2 shows the critical gain in the presence of the varying

extents to valve degradation is in a range between 1000 and 1500 ($m^3.s^{-1}.Pa^{-1}$) for the PSE-SFW control loop. The original controller gain is 928.6 ($m^3.s^{-1}.Pa^{-1}$) which is close to the range of the critical gain of the system, as a result, aggressive controller action is observed without retuning. The reduction in oscillations and variance observed can be translated to a broader analysis of relay autotuning. Potentially for several systems, whereby tighter controller constraints are needed, relay autotuning can improve the overall controller performance, if controller performance is based on the variance.

Table 6-2: Average CPI as well as controller tuning parameter values obtained at various f_{RA} and n_L values for $t_{RS} = 5hrs$ and $\alpha = 0.45$

f_{RA}	n_L	K_C	τ_I	Average CPI
0.5	0.0075	243.9	2.90	0.61
0.6	0.0075	271.9	3.29	0.63
0.5	0.0100	229.9	2.70	0.58
0.6	0.0100	241.3	2.83	0.58
0.5	0.0125	218.4	2.41	0.57
0.6	0.0125	216.4	2.51	0.57

Additionally, in the presence of valve degradation, satisfactory controller action can be observed, as is shown in figure 6-9 in comparison to figure 6-2. With respect to the SFW, a less aggressive process controller reduces the valve travel distances which could potentially decrease the acceleration of valve degradation.

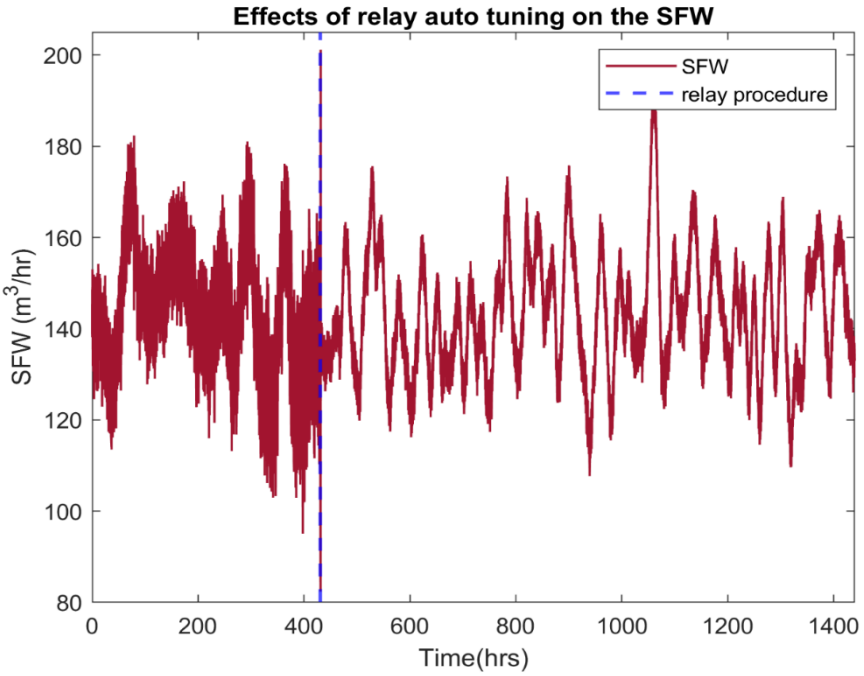

Figure 6-9: Effects of relay autotuning on the SFW for $\alpha = 0.45$, $t_{RS} = 3hr$, $f_{RA} = 0.4$ and $n_L = 0.01$

The reduction in oscillations to the SFW has positive knock-on effects. As mentioned previously, the milling circuit is a complex system with multiple control loops that have potential interactions. From appendix A, the addition of valve degradation on the SFW valve has a direct influence on the SVOL. The oscillations that occur with the SFW directly impact the SVOL control loop. However, the relay autotuning on the SFW-PSE control loop attenuates the oscillations, as is illustrated in figure 6-10. Therefore, relay autotuning has potential in remedial action of retuning MIMO control loops. Specifically through retuning the control loop where valve degradation has been implemented only. As a result, retuning several control loops in the MIMO case can be avoided.

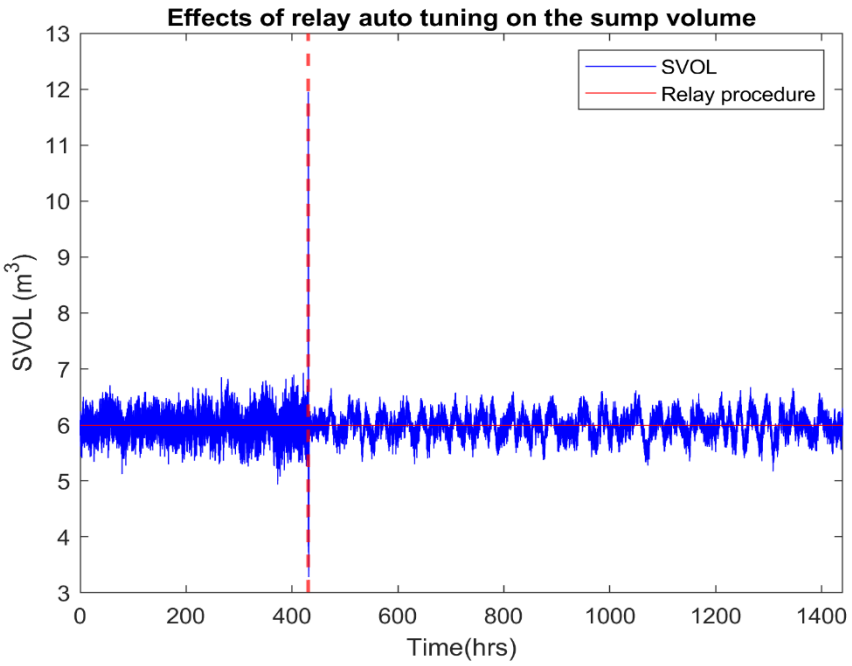

Figure 6-10: Effects of relay autotuning on the SVOL for $\alpha = 0.45$, $t_{RS} = 3hr$, $f_{RA} = 0.4$ and $n_L = 0.01$

The effects of retuning can further be seen from the milling unit. From figure B-17 in appendix B, the reduction in the oscillations on the SFW directly reduces the slight oscillations produced in the mill charge. The reduction in the variance is shown with figure 6-11 for relay amplitude experiments assessed in the ANOVA. The data indicates a reduction in the variance from $1.83(10^{-7})$ without retuning to values close to $8.90(10^{-8})$ at $\alpha = 0.45$. Despite the minimal reduction in variance of the mill charge, the benefits of relay autotuning for the single control loop can be assessed as beneficial for MIMO systems for the CFF-SVOL and SFW-PSE control loop.

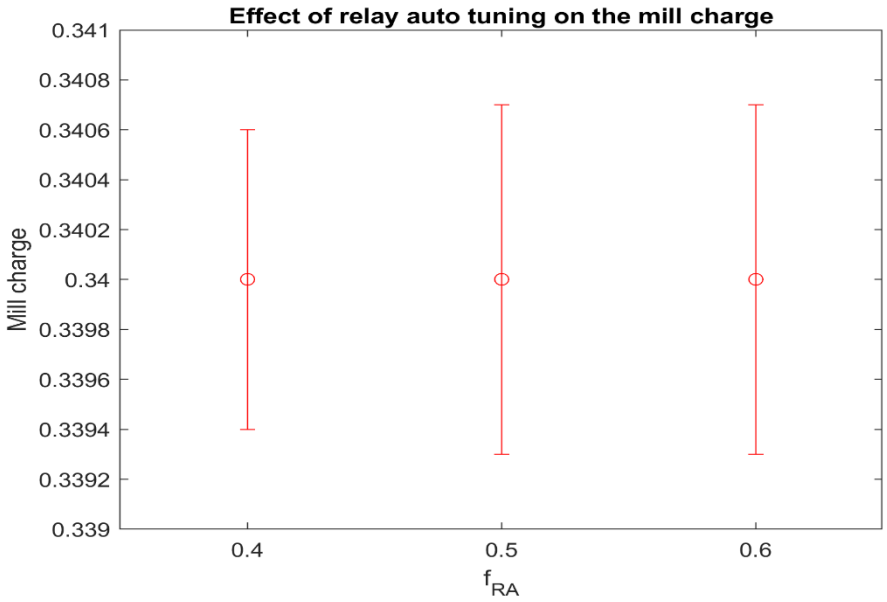

Figure 6-11: Effects of relay autotuning on the mean mill charge values for various f_{RA} at $\alpha = 0.45$ and $n_L = 0.0075$, with 2σ

As mentioned previously, the effects within the mill directly affect the mill power draw. The reduction in oscillations for the SFW reduces the propagation of fluctuations to φ and the LOAD within the mill. As a result, the average mean for P_{mill} is not reduced due to the rheology and LOAD effects and is shown in figure 6-12. In addition, the reduction in the oscillations reduces the observed variation for P_{mill} at large α values.

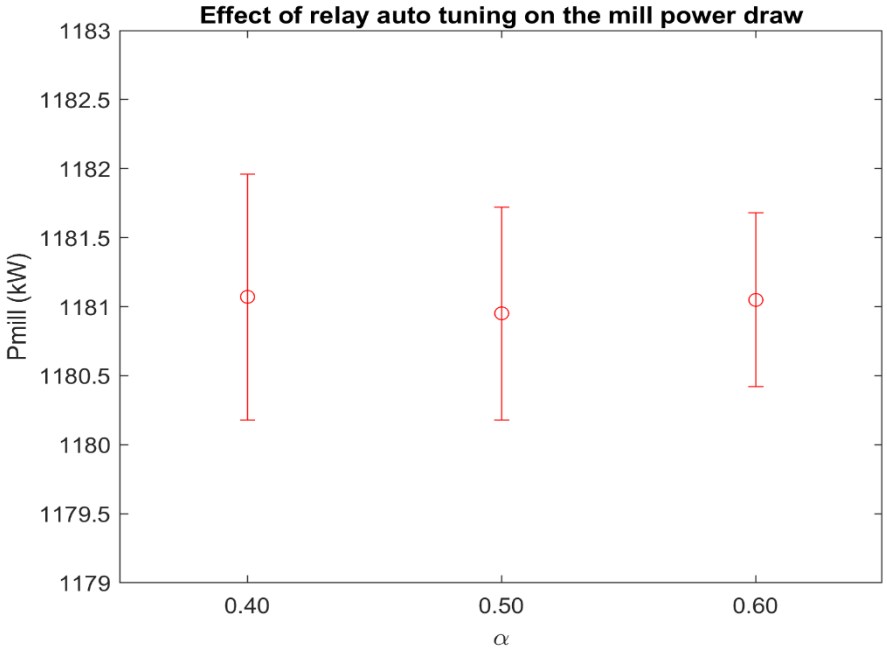

Figure 6-12: Effects of relay autotuning on the mean P_{mill} values for various f_{RA} at $\alpha = 0.45$ and $n_L = 0.0075$, with 2σ

6.3. Control performance analysis of key parameters

6.3.1. Overview

The objectives required the analysis of key parameters such that a robust technique for implementing relay autotuning can be presented. An ANOVA was performed using a full factorial design of four key parameters, with each factor assessed with three levels. Resultantly, with 10 repetitions at each experimental case, 810 experiments were used for the ANOVA. The overall ANOVA results indicating the effect the four factors have on the CPI is shown in Table 6-3. A p-value less than 0.05 indicates there is a significant effect on the CPI for a specific level within the factor. As a result, based on the p-value, valve degradation, relay start, noise and the relay amplitude all indicate significance with respect to the CPI. In addition, the combination of changes in the sensor noise level and the relay amplitude selected have a distinguishable effect of the controller performance. In contrast, the residual combination of factors have p-values greater than 0.05 and is by far larger in comparison to the p-values obtained by the singular factors. Therefore, the results indicate an insignificant impact on the CPI for most interaction between factors. The following section discusses specifically which means differ using the post hoc analysis (Fischer LSD test).

Table 6-3: ANOVA of the CPI

Factor	Sum Sq.	d.f.	Mean Sq.	F	P-value
α	0.5007	2	0.2504	80.68	0.0000
t_{RS}	0.6628	2	0.3314	106.80	0.0000
n_L	0.1347	2	0.0673	21.70	0.0000
f_{RA}	0.1402	2	0.0701	22.60	0.0000
$\alpha \times t_{RS}$	0.5332	4	0.1333	42.96	0.0000
$\alpha \times n_L$	0.0120	4	0.0030	0.97	0.4248
$\alpha \times f_{RA}$	0.0018	4	0.0005	0.15	0.9648
$t_{RS} \times n_L$	0.0186	4	0.0046	1.50	0.2013
$t_{RS} \times f_{RA}$	0.0204	4	0.0051	1.65	0.1610
$n_L \times f_{RA}$	0.0675	4	0.0169	5.44	0.0003
$\alpha \times t_{RS} \times n_L$	0.0441	8	0.0055	1.78	0.0784
$\alpha \times t_{RS} \times f_{RA}$	0.0300	8	0.0037	1.21	0.2919
$\alpha \times n_L \times f_{RA}$	0.0339	8	0.0042	1.37	0.2079
$t_{RS} \times n_L \times f_{RA}$	0.0151	8	0.0019	0.61	0.7715
$\alpha \times t_{RS} \times n_L \times f_{RA}$	0.0620	16	0.0039	1.25	0.2251
Error	2.2621	729	0.0031		
Total	4.5391	809			

6.3.2. Extent of valve degradation

The ANOVA presented in table 6-3 indicated that valve degradation was a significant factor in relation to the CPI values. Furthermore, limited interactions between valve degradation and the remaining factors were observed. As a result, the valve degradation can be assessed on its own. Therefore, following the ANOVA calculation the trend observed between levels within the valve degradation is illustrated in figure 6-13. The trend shows, as the extent of valve degradation is increased, the obtained CPI values are less once relay autotuning is implemented. Specifically the average CPI observed for $\alpha = 0.35$ is larger in comparison to $\alpha = 0.40$ and $\alpha = 0.45$.

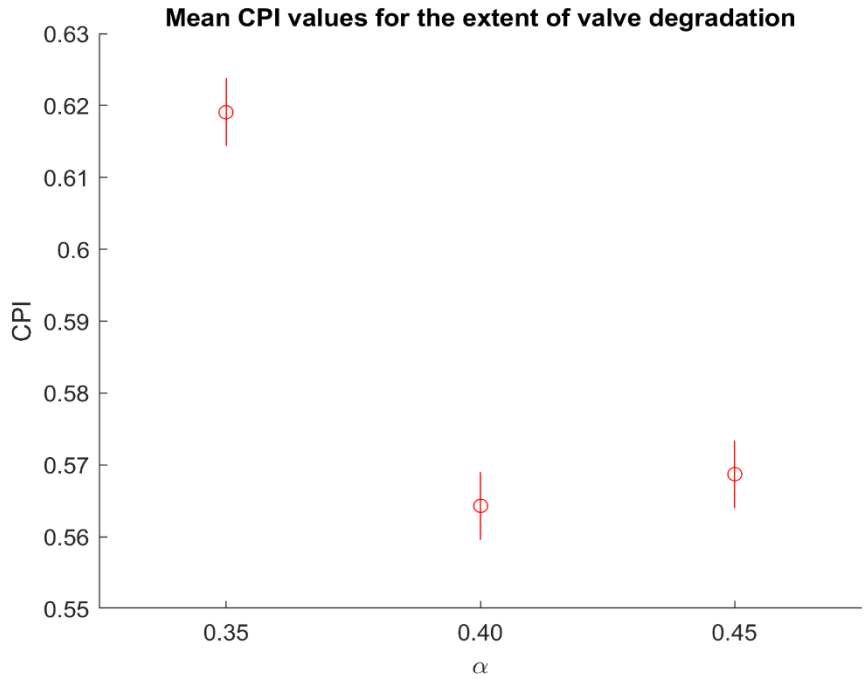

Figure 6-13: Mean CPI values for changes in α, with the standard error

From the methodology section, a larger CPI value indicates poorer controller performance. The perceived poorer controller performance indicates the new tuning parameters are, to a small degree, conservative at $\alpha = 0.35$ or controlled variables variances which are closer to NOC. Nonetheless, in comparison to the old tuning parameters in table 6-1, the conservative tuning parameters achieve a better controller performance. However, the deviation in the variance from non-tuning scenarios is the smallest at $\alpha = 0.35$ in comparison to $\alpha = 0.45$. As a result, in industry it is possible to avoid retuning the control system at low α values. Due to the inability to quantify valve wear in industry, to avoid initialising the relay autotuning procedure at low α values, the threshold variance should be increased. Lastly, despite clear benefits from controller performance at larger valve degradation values, caution should be taken. A valve that has degraded more performs better with retuning, however, there is degradation present which could further deteriorate. As a result, there could be a trade-off between retuning and replacing the valve, where retuning would reduce oscillations at the expense of using a worn valve.

6.3.3. Relay start time

The ANOVA results indicated that t_{RS} was a significant factor in relation to the CPI values. In addition, there was limited interactions between the relay start and the remaining factors. As a result, the relay start has been assessed on its own. The trend observed between levels within t_{RS} is illustrated in figure 6-14. The trend shows, at increasing relay start hours, the obtained average CPI values increases. As a result, increasing t_{RS} leads to a slight deterioration in the observed controller performance over the 2 month period.

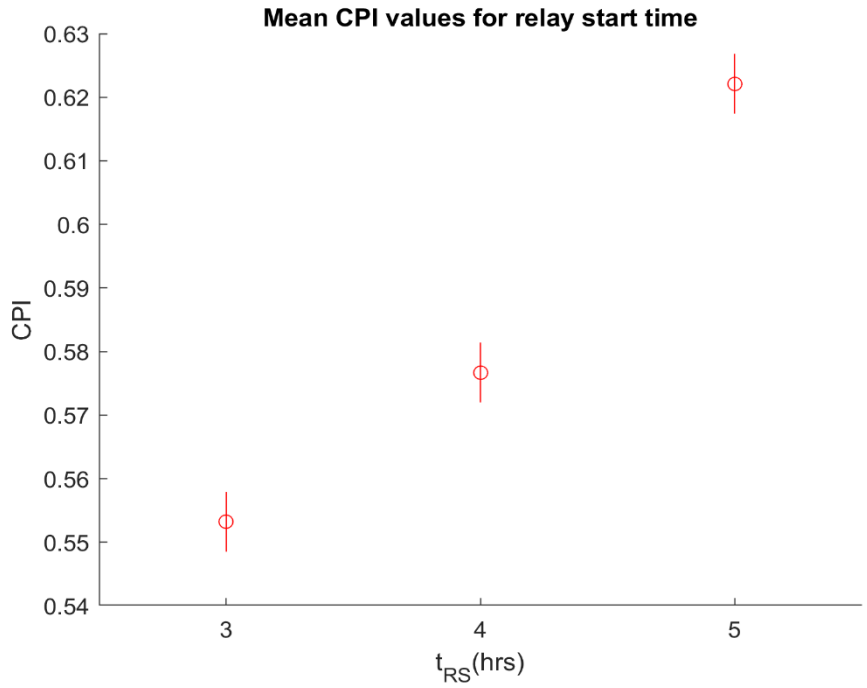

Figure 6-14: Mean CPI values for changes in t_{RS}, with the standard error

The observed trend is expected, as increasing the number of hours for the system to be above the threshold variance would increase the number of observed moving variance values larger than the threshold for that period of time. Therefore, application of relay autotuning using controller performance, specifically the variance, could be beneficial with early initialisation of relay autotuning (a smaller t_{RS}). Early execution of relay autotuning can be beneficial in two ways, namely a smaller CPI value for the period of interest, as well as early detection of valve degradation. A smaller CPI value translates to better product quality if the CPI is based on the variance. In addition, early detection of valve degradation could prevent further wearing of the valve through retuning. This is possible through reduction of valve travel distances.

The evaluation of the t_{RS} in relation to the CPI demonstrates how relay autotuning can be implemented using controller performance. The results indicate that at earlier detection controller performance improves. However, the decision on how long poor controller performance is allowed before retuning is subjective and could potentially lead to a false triggering of the relay if the incorrect relay start time is used.

6.3.4. Sensor noise level

The ANOVA results indicated that n_L was a significant factor in relation to the CPI values. The trend observed between levels within the sensor noise levels is illustrated in figure 6-15. The trend shows, when n_L is increased, the obtained CPI values decreases once relay autotuning is implemented.

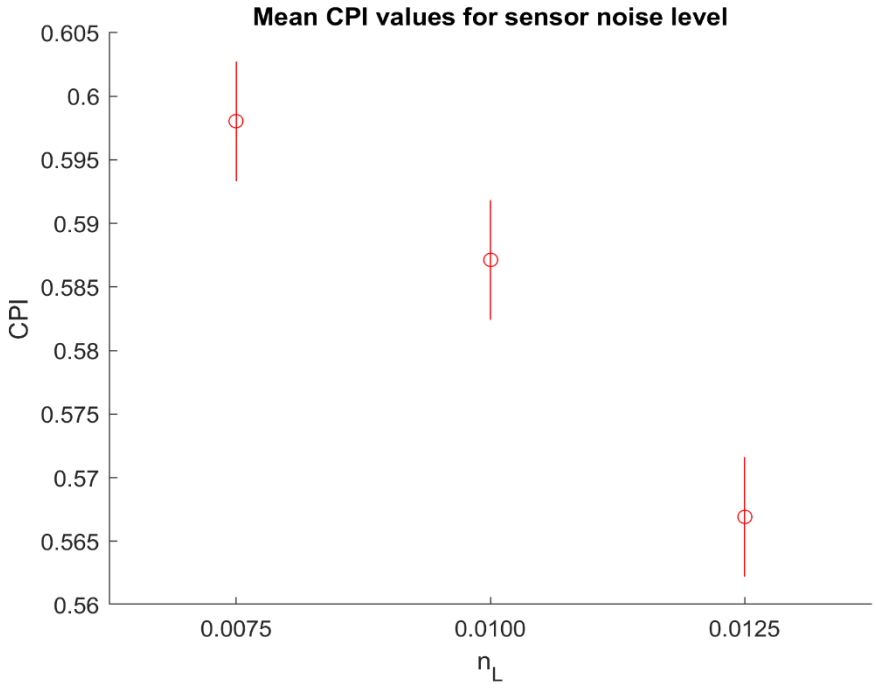

Figure 6-15: Mean CPI values for changes in n_L, with the standard error

The observed trend is expected and can be explained from table 6-1. At the lowest sensor noise level ($n_L = 0.0075$), valve degradation has a larger effect on the average CPI in comparison to the larger noise levels. Furthermore, at the noise level of 0.0075, the PSE variance threshold value is at a low value of 2.14×10^{-5}, in comparison to the PSE variance threshold values of 3.75×10^{-5} and 5.87×10^{-5}, for the noise levels of 0.01 and 0.0125 respectively. This is inherent from a system with less noisy data. Despite the lowest threshold value, the degree to which oscillations occur between noise levels is the same i.e. the amplitude of oscillations are the same (refer to figure 6-1, B-29 and B-30). Therefore, the effects of valve degradation increases the observed CPI value for a system that is less noisy due to the configuration of the historical benchmark.

In addition, a less noisy sensor level would increase the observed critical gain from equation 2-15. The amplitude of the controlled variable is less due to the reduction of the sensor noise. As a result of reducing ‘a’, the critical gain is increased. The increased critical gain would produce a more aggressive controller and, subsequently, result in a larger CPI. Therefore, despite the desirability for a less noisy sensor level within industry, the calculation of the critical gain is inflated for the relay autotuning procedure.

Although the low sensor noise level would produce a larger gain for the controller system, the solution is to change the relay amplitude, specifically decrease the relay amplitude. Further justification of the importance of the relay amplitude selected and the sensor noise level is highlighted in table 6-3. The following section further discusses the solitary effect of the relay amplitude on the CPI as well as the effect of the interaction between the relay amplitude and noise.

6.3.5. Relay amplitude

The ANOVA results indicated that f_{RA} was a significant factor with respect to the CPI values. The trend observed between levels within the relay amplitude parameter is illustrated in figure 6-16. The trend shows, when f_{RA} is increased, the obtained CPI values increases once relay autotuning is implemented. Therefore, control performance worsens as the selected relay amplitude is increased.

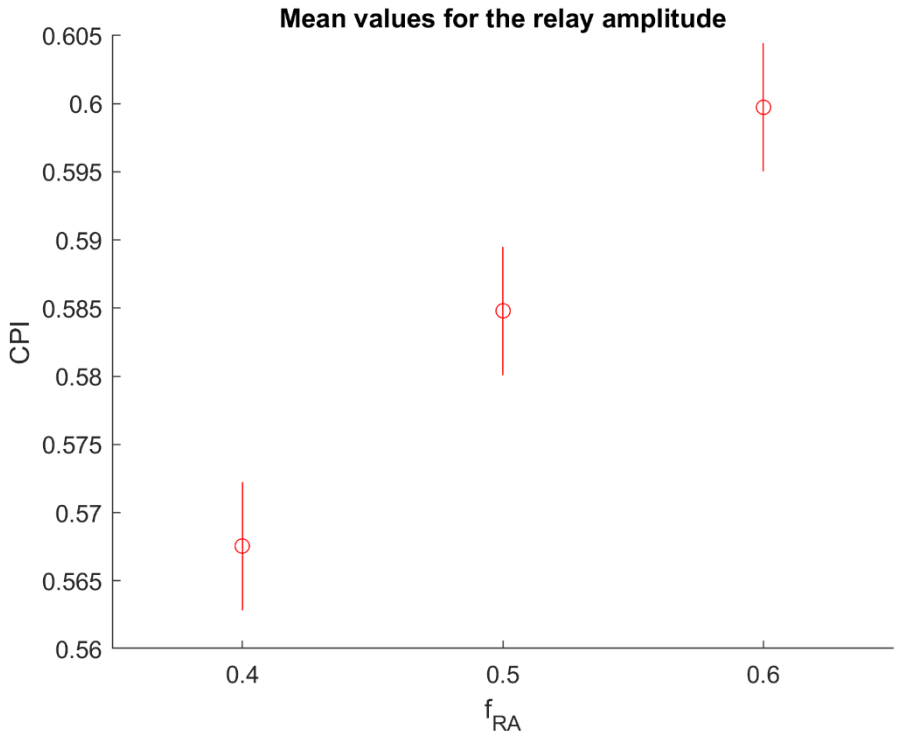

Figure 6-16: Mean CPI values for changes in f_{RA}, with the standard error

The observed trend is expected and can be analysed using the equation 2-15 obtained for determining the critical gain. Despite an increase in the PSE amplitude, the hysteresis band is kept constant. As a result, the critical gain is increased due to an increase in 'd'. Therefore, the larger tuning parameters produce a more aggressive controller and, subsequently, a larger CPI in the presence of valve degradation.

The industrial application of relay autotuning would suit the use of smaller relay amplitudes. A smaller relay amplitude results in less drift from the set point for the controlled variable. Furthermore, it is beneficial for interacting control loops, whereby operating constraints are required for residual control loops. With respect to the milling circuit, as the relay amplitude is increased, the drift of the SVOL from its set point is increased.

However, for sensors with large noise, larger relay amplitudes are required such that the hysteresis band is overcame. As a result, a less noisy sensor would be favourable for implementation of relay autotuning in terms of the required relay amplitude. Nonetheless, a noisier process system can be counteracted with a sensor filter which reduces noise and smoothens data. Therefore, there is potential to avoid the use of larger relay amplitudes.

The ANOVA results indicated that the interaction between the sensor noise level and relay amplitude factor had a significant impact on the CPI. At the lowest sensor noise value and increasing relay amplitudes, the CPI values increased. The values can be explained with the tuning parameters observed from table 6-4. The controller tuning parameters become larger as the relay amplitude increases and the noise level decreases. For industrial application of relay autotuning a better controller performance is required. However, the results obtained indicate that a larger sensor level would result in a better controller performance due to the obtained tuning parameters. Despite the results, a noisier sensor would be less desirable in industry. The reasonable solution is, therefore, improving controller performance for low sensor noise levels by selecting a smaller relay amplitude.

Table 6-4: Controller tuning parameters obtained after retuning, for $t_{RS} = 3h$ and $\alpha = 0.35$

f_{RA}	K_C	τ_I
$n_L = 0.0075$		
0.4	211.4	2.34
0.5	252.3	2.85
0.6	273.5	3.19
$n_L = 0.01$		
0.4	192.8	2.05
0.5	219.1	2.38
0.6	243.5	2.88
$n_L = 0.0125$		
0.4	183.4	1.86
0.5	201.8	2.23
0.6	221.3	2.38

6.4. Economic performance assessment

6.4.1. Overview

The benefits and shortcomings of relay autotuning have been observed from the controller performance. Nonetheless, the last objective requires evaluating relay autotuning using EPA. Specifically using the EPI determined from the methodology. Table 6-5 contains results comparing the economic effects of relay autotuning and valve degradation. From the data, simulations were performed to determine the overall throughput (MFS), electricity costs and EPI. Thereafter, the average recovery is back-calculated from the EPI formula in the methodology.

Table 6-5*:* EPI breakdown for various f_{RA} at $n_L = 0.01$, $t_{RS} = 3hrs$ and $\alpha = 0.45$ as well as for increasing α without retuning

Conditions	MFS (tons×10^3)	Average Recovery	Revenue ($×$10^5$)	Electricity cost ($×$10^5$)	EPI ($×$10^5$)
NOC	93.4	0.674	66.7	1.02	65.7
$\alpha = 0.35$	93.8	0.674	66.9	1.02	65.9
$\alpha = 0.40$	93.4	0.674	66.7	1.02	65.7
$\alpha = 0.45$	94.0	0.672	66.9	1.02	65.9
Relay autotuning					
$f_{RA} = 0.4$	93.4	0.674	66.7	1.02	65.6
$f_{RA} = 0.5$	94.0	0.674	67.1	1.02	66.1
$f_{RA} = 0.6$	93.1	0.674	66.4	1.02	65.4

From the methodology section, the EPI is affected by the throughput (MFS), PSE/Recovery and the electricity costs associated with the mill (specifically P_{mill}). Assessment of valve degradation showed the introduction of oscillations within the system, which increased the variance of the PSE and, to a smaller extent, the mill charge and P_{mill}. From figure 6-1, the PSE does not reach the maximum recovery point, therefore, the revenue is directly proportional to the PSE. As mentioned previously, for current system, the degree to which the PSE decreases from its set point is larger in comparison to the increases. As a result, table 6-5 indicates a tendency for the recovery to be lower for a large α, without retuning, in comparison to NOC. In contrast, for low and medium α values, the system has similar observable PSE values as NOC. Despite the bias towards larger decreases for a large α, the decrease is relatively smaller in comparison to NOC and relay autotuning scenarios. The slight decrease can be attributed to the frequency of larger PSE values over the 2 month period which offset against the smaller PSE values.

Furthermore, the fluctuations that occur with the SFW slightly increased the variance of the mill charge. Observation of the rheology and LOAD within the mill, once valve degradation is implemented, indicates variation for φ, Z_x and Z_r. The variations never produce an increase in P_{mill} towards P_{max}, instead the maximum observed P_{mill} is the same for P_{mill} at NOC. In addition, the trend shows a bias towards decreases in the electricity costs for valve degradation in comparison to the retuned system. This is due to the variations of the LOAD and φ at the current system conditions. However, the electricity costs observed in table 6-5 indicate the reduction of the electricity costs due to valve degradation is indistinguishable for the economic comparison with relay autotuning scenarios.

As a result of indistinguishable recoveries and electricity costs, when comparing valve degradation effects to NOC as well as relay autotuning cases, the EPI values obtained are significantly affected by the throughput (MFS). As mentioned previously, valve degradation produces a bias towards larger decreases in the SFW. The resultant effect is a bias towards larger decreases observed in the recycle stream flow to the mill (refer to appendix B, 'hydrocyclone flow rates'). Due to the larger reductions for the flow rates in the recycle stream, valve degradation effects should favour a larger overall throughput. However, from figure 6-5, the results indicate no significant increase in the average MFS to attenuate the mill charge as α increases. This is attributed to the similar mean and variance observed for MFS sample populations. Therefore, despite the larger throughput at $\alpha = 0.45$ in table 6-5, the increase in the MFS cannot be attributed to valve degradation.

Evaluation within relay autotuning, from table 6-5, further highlights the dependencies of the EPI on the MFS. For retuning at $\alpha = 0.45$, the control systems follows NOC at each f_{RA}. However, the fluctuations in the MFS differ despite the same average recovery and similar electricity costs. In contrast to the valve degradation, the SFW oscillations are reduced for relay autotuning, therefore, the fluctuations on the mill charge are random and dependent on the disturbances. This can be shown with comparison of figure B-7 and B-17, which differ due to the disturbances within the mill i.e. the random walks designed for ϕ_f and α_r. Furthermore, assessment of the variation of the MFS for the data obtained in table 6-5 is shown in figure B-19. The results indicate no discernible difference in the obtained MFS when evaluating the change in the relay amplitude. This is attributed to the similar mean and variance observed for sample populations. The following section further discusses the effect key parameters associated with relay autotuning on the EPI.

6.4.2. Economic performance of key parameters

The overall ANOVA results indicating the effect that the four factors have on the EPI is shown in table 6-6. Based on the p-value, valve degradation, relay start time and the sensor noise level indicate insignificance with respect to the EPI. This is due to the p-value being larger than the 0.05 confidence criteria. However, f_{RA} as well as the interaction effects between α and n_L, show marginal values close to 0.05. With marginal cases it is subjective as to whether or not they have a significant impact.

Table 6-6: ANOVA results for the EPI

Factor	Sum Sq. ($\times 10^9$)	d.f.	Mean Sq. ($\times 10^9$)	F	P-value
α	2.15	2	1.07	0.3853	0.6804
t_{RS}	5.40	2	2.70	0.9685	0.3801
n_L	10.2	2	5.11	1.8308	0.1610
f_{RA}	13.0	2	6.51	2.3350	0.0975
$\alpha \times t_{RS}$	13.0	4	3.25	1.1669	0.3241
$\alpha \times n_L$	23.1	4	5.78	2.0730	0.0826
$\alpha \times f_{RA}$	2.70	4	6.74	0.2418	0.9147
$t_{RS} \times n_L$	4.97	4	1.24	0.4451	0.7760
$t_{RS} \times f_{RA}$	9.09	4	2.27	0.8149	0.5158
$n_L \times f_{RA}$	7.60	4	1.90	0.6812	0.6051
$\alpha \times t_{RS} \times n_L$	12.8	8	1.59	0.5720	0.8014
$\alpha \times t_{RS} \times f_{RA}$	34.8	8	4.35	1.5596	0.1333
$\alpha \times n_L \times f_{RA}$	22.8	8	2.85	1.0207	0.4186
$t_{RS} \times n_L \times f_{RA}$	22.1	8	2.76	0.9907	0.4418
$\alpha \times t_{RS} \times n_L \times f_{RA}$	30.6	16	1.91	0.6852	0.8103
Error	2030	729	2.79		
Total	2250	809			

The Fischer LSD analyses of the relay amplitude levels on the EPI is illustrated in figure 6-17. From the figure, the distinguishable levels are for f_{RA} equal to 0.4 and 0.6 respectively. The data indicates larger profit margins at a lower selected relay amplitudes. Despite the observed effects, the results are arguably unreliable due to the data from table 6-5 which indicated the assessment of key parameters were dependent on the MFS. Furthermore, separate assessment of the spread of the MFS was performed and shown in figure B-19. The data indicates there is no distinguishing difference in the MFS as the relay amplitude is increased, due to the overlapping standard deviations. In addition, observable from figure 6-17 is a large standard error for f_{RA} equal to 0.4 and 0.6 ($3200). From the figure, the mean and standard errors for both cases are fairly close to overlapping, which would indicate insignificance. Resultantly, from these factors and the p-values, the assessment of key parameters is not possible and it is assumed all cases were insignificant for the milling circuit simulation model.

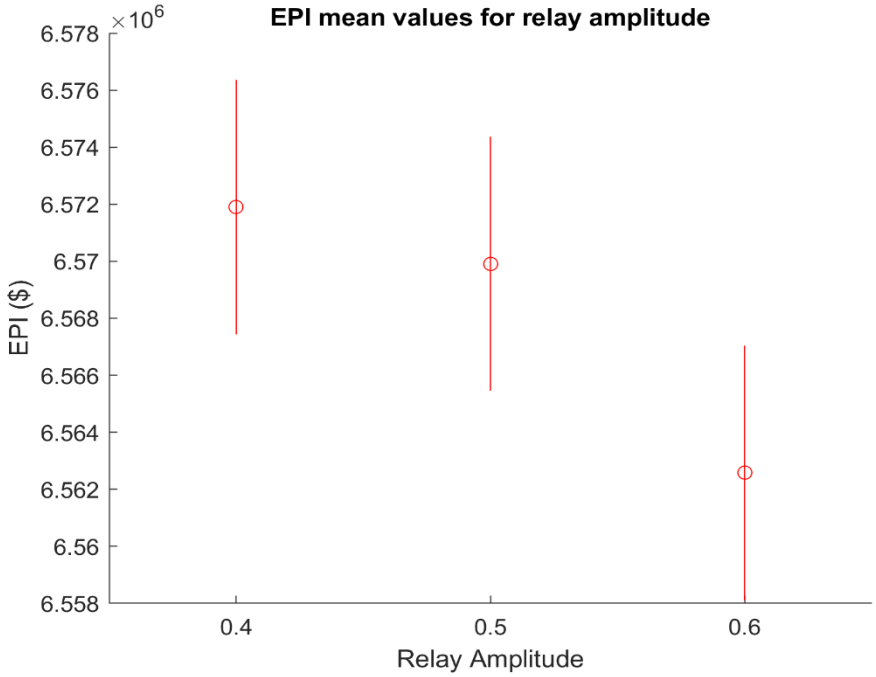

Figure 6-17: Effect of relay amplitude on the EPI, with standard error

6.4.3. Remarks

Despite the inability to distinguish EPI values when comparing valve degradation to relay autotuning, the effects of valve degradation could have a negative impact in the economic performance of the plant. Further valve degradation can results in costs associated with valve replacement if the valve is not usable. In addition, the oscillations produced from valve degradation, could result in plant shutdown, due to instability, and revenue loss for the shutdown period. For the milling circuit, if the upper or lower boundaries of the sump level are violated, it is assumed that countermeasures are implemented which have economic costs.

Olivier and Craig (2017) extensively discussed if a fault was detected and isolated, whether operating with the fault is more economically viable than plant shutdown. Although the comparison is a complex procedure, for the milling circuit, the economic benefits of relay autotuning can be observed inherently through better controller performance. Reduction in the controller action has potential to reduce the further wearing of the valve. Therefore, there is an opportunity to prevent plant shutdown, due to instability, or costs associated with replacing the valve. In addition, the results indicate the operability of the plant regardless of the worn valve with no justifiable negative impact on the EPI. Alternatively, it can be argued that relay autotuning is a procedure that improves controller performance, by shifting the controlled variable away from its set point, while having no significant impact on the EPI for that period.

Assessment of the key parameters and their economic impact showed insignificance for α, t_{RS} and n_L due to the large and overlapping standard errors. Furthermore, the standard error is affected by the large variation in the MFS as a result of the mill disturbances. However, from an industrial perspective these variables cannot be argued as insignificant. A smaller t_{RS} would result in faster detection of faults and retuning of the system. As mentioned previously, earlier initialisation could prevent further wearing of the valve or valve replacement. In addition, the sensor noise resulted in inflated controller tuning parameters. As a result, selection of a smaller relay amplitude would reduce the new tuning parameters. Therefore, controller performance could be improved. Reduction in the system variance for the system indicates better set point tracking. Despite the current systems unreliability, for an alternative system the improvements could result in better product quality as well as a reliable increase in the profits. Furthermore, selection of a relay amplitude requires careful consideration of economic boundaries placed on interacting control loops. This can be argued with the effect the SFW has on the SVOL which has economic penalties if boundaries are violated. Lastly, assessment of smaller values of α, indicated retuning could possibly be too conservative for the system and result in increased variance. The increased variance could have a significant impact on alternative process systems. Resultantly, these parameters cannot be evaluated as economically insignificant.

6.5. Supplementary evaluation of relay autotuning

6.5.1. Valve degradation with time delay

The valve degradation experiments indicated an increase in oscillations for the specific control loop. The oscillatory behaviour can lead to high valve reversals and static friction within the valve. Resultantly, additional faults such as valve sticking and valve stiction can occur. Therefore, further experiments were performed, whereby relay autotuning and valve degradation were performed on the SFW-PSE control loop, with the addition of a 30s time delay to simulate valve sticking. The results are shown in table 6-7:

Table 6-7: CPI values results obtained from the added 30s time delay to the SFW valve

Experiment	CPI	EPI ($\$ \times 10^5$)
Valve sticking	1.33	66.1
Retuning system with valve sticking	0.45	65.8
Adjusted $\sigma^2_{threshold}$	0.49	65.9
Valve degradation with time delay	3.73	65.8
Retuning system with valve degradation and time delay	0.26	65.8

The results indicate that with the addition of solely a time delay to the valve, the controller performance observed is worsened in comparison to the NOC due to the CPI increase from 1.33 from 0.63 (refer to table 6-1). Therefore, the effects of the time delay on the variance can be observed and detecting valve sticking effects is possible with the historical benchmark. This indicates that retuning is necessary due to the aggressive tuning parameters at the current system conditions. As a result of relay autotuning performed on the valve sticking, the CPI decreases from 1.33 to 0.45. The reduction in the CPI, provides further benefits of relay autotuning observed with incorrect tuning parameters applied to a system with a valve with time delay.

Following the detection of the time delay, $\sigma^2_{threshold}$ is recalibrated to incorporate the fault, such that valve degradation would be the isolated fault detected. From the results obtained, with the system having a time delay and valve degradation, there is an expected increase in the CPI from 0.49 to 3.73. Furthermore, the results indicates at a lower α value of 0.35, the oscillations observed are intensified in comparison to a system without a time delay. The observed oscillations are on par with larger valve degradation values without the time delay. Therefore, as is shown in figure 6-18, the time delay amplifies the effects of valve degradation due to the transport delay which results in further overshoots.

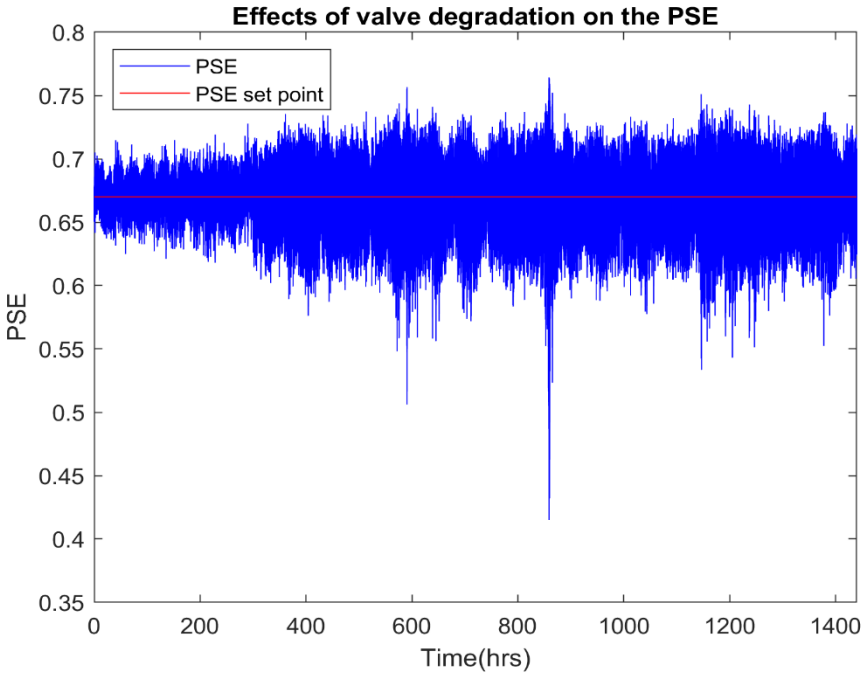

Figure 6-18: Effect of valve degradation and a 30s time delay on the PSE for $\alpha = 0.35$ at $n_L = 0.01$

Subsequently, with the addition of retuning, the tuning parameters are reduced and the observed controller performance is improved i.e. CPI reduced. As mentioned previously, the economic effects of oscillations could not be distinguished against relay autotuning for the milling circuit. Therefore, the economic effects cannot be distinguished with and without retuning of the system at the various conditions because the time delay produces oscillatory behaviour.

6.5.2. Tuning parameter relations

The methodology outlined experiments to be followed after the ANOVA such that further effects can be evaluated. An investigation was performed on using the Tyreus-Luyben tuning relations, in comparison to the Ziegler-Nichols tuning. The results shown in table 6-8 indicate, at the same parameter conditions, the Ziegler-Nichols tuning relationship performs better, as is shown with the CPI. The better CPI can be attributed to the controller tuning parameters obtained after using each tuning relationship. The Tyreus-Luyben is a conservative tuning relationship and can be used for MIMO controllers. However, the tuning parameters obtained are larger than the Ziegler Nichols tuning parameters due to the detuning factor used. Therefore, in the presence of valve degradation, the slightly more aggressive tuning parameters would obtain a larger CPI value.

Table 6-8: Comparison of the Tyreus-Luyben and Ziegler-Nichols rules at various f_{RA} for $n_L = 0.01$, $\alpha = 0.45$ and $t_{RS} = 3h$

f_{RA}	K_C	τ_I	CPI
Tyreus-Luyben			
0.4	327.2	1.95	0.59
0.5	390.3	2.43	0.60
0.6	423.5	2.85	0.63
Ziegler-Nichols			
0.4	202.2	2.29	0.55
0.5	223.9	2.61	0.57
0.6	250.7	3.32	0.60

The benefit of using the Tyreus-Luyben tuning relationship can be observed from the detuning factor. The detuning factor requires process knowledge in order to obtain good controller tuning parameters for multi-loop controllers. The Tyreus-Luyben tuning relationships perform satisfactorily for multi-loop controllers and, therefore, do not require a detuning factor. From an industrial perspective, this could remove selection criteria for relay autotuning and further promote the use of automatic retuning techniques. In addition, it can be argued that the larger tuning parameters obtained from the Tyreus-Luyben relationship performs only slightly worse than the Ziegler-Nichols tuning parameters and, therefore, does not rule out its potential in control performance.

6.5.3. Sequential relay autotuning

Despite the benefits of single loop relay autotuning, the shortcoming within industry is characterised with the control performance technique used. The interacting control loops of the PSE and SVOL loops indicate that retuning on both control loops are required if the fault cannot be isolated to the SFW control valve. Although the CPI can incorporate both controlled variables and oscillations would indicate poor controller performance, the technique is not robust to detect which control loop should solely require retuning. Nonetheless, the limitation can be overlooked if fault isolation is performed. Alternatively, sequential relay autotuning can be performed, whereby the SVOL control loop is retuned after the PSE control loop has undergone relay autotuning. Figure 6-19 illustrates the sequential relay autotuning of the SVOL once the PSE control loop has been retuned.

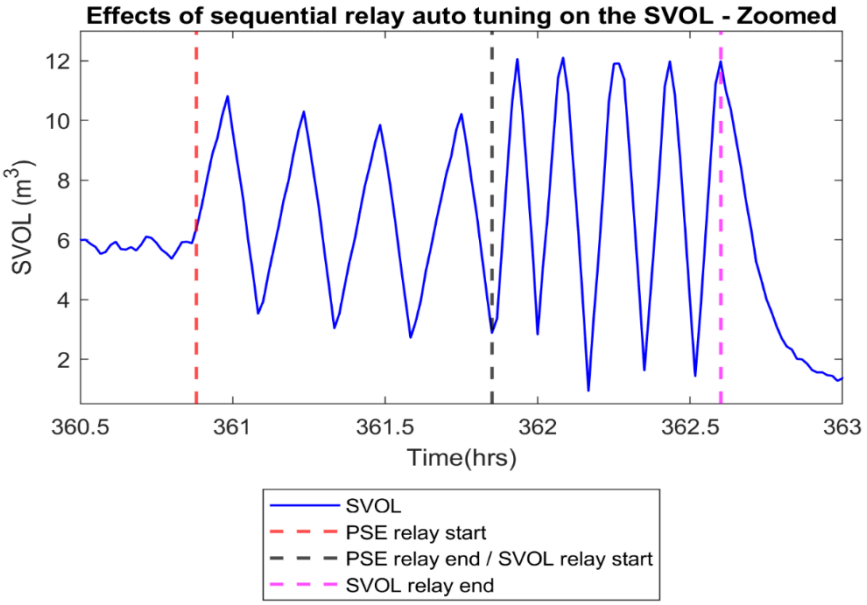

Figure 6-19: Sequential relay autotuning of the SVOL for $n_L = 0.01, f_{RA} = 0.4, t_{RS} = 3hrs$ and $\alpha = 0.45$

Contrasting the relay autotuning procedure for the PSE and SVOL indicates the differing controller relationships. The sinusoidal wave produced in figure 6-19 indicates a more triangular wave form when the SVOL undergoes retuning in comparison to the PSE. Research on the relay wave form's shape indicated additional process information can be obtained (Luyben, 2001; Thyagarajan and Yu, 2002). Consequently, a triangular wave form indicates a time constant dominant relationship for the SVOL. In contrast, it is probable the PSE control loop has a proportionate dead time to time constant ratio. The relationships are further justified with the transfer functions calculated by Matthews and Craig (2012) for the linearised milling circuit simulation model. Therefore, the relay wave form can provide additional benefits of relay autotuning, specifically for process characteristics as well as system identification.

Assessment of the retuned SVOL indicates a reduction in the controller gain from 20 to values ranging from 9.01 to 14.2 in table 6-9. In contrast, the integral time is increased from 0.25 to values ranging from 2.84 to 3.53. Similarly from the data obtained in 6.3.5, an increase in the f_{RA} resulted in poorer controller performance due to the controller tuning parameters being relatively more aggressive. However, comparing the CPI values obtained in table 6-9 to table B-1 shows the sequential relay autotuning performs worse at each f_{RA}. The data suggests that retuning the SVOL would produce more variation within the process. This is attributed to the reduction in the controller tuning parameters, which produces a more conservative SVOL-CFF control loop that is sluggish towards disturbances. As a result, detuning a single control loop, which is oscillatory, using relay autotuning for a MIMO system could be sufficient without further detuning residual control loops.

Table 6-9: Average CPI as well as controller tuning parameter values obtained using sequential relay autotuning at various f_{RA} for $n_L = 0.01$, $t_{RS} = 3hrs$ and $\alpha = 0.45$

f_{RA}	K_C	τ_I	CPI
0.4	9.01	2.84	0.80
0.5	11.3	3.08	0.90
0.6	14.2	3.53	1.01

Despite the poorer controller performance in comparison to single loop retuning, the CPI performs better than the controllers without retuning (refer to table 6-1). In addition, sequential relay autotuning allows for fault isolation to be avoided for the current CPM technique used to automate the relay autotuning procedure.

Economic evaluation of sequential relay autotuning can be shown in table 6-10. The data shows similar trends shown from section 6.4.1, whereby the dominating variable in the EPI is the throughput. Initial assessment of the results indicates as f_{RA} is increased, the MFS increases. However, the increase in the MFS and tendency to increase due to poorer controller performance cannot be justified with table 6-10 due to the large variance of the MFS data in figure B-43. As a result, the economic effects of sequential relay autotuning cannot be assessed. Although the economic effects of sequential relay autotuning cannot be quantified, the procedure can be assessed. The MIMO procedure introduces an extra relay step within the process and as a result approximately an extra hour of relay autotuning is required. The shifting of the process conditions for a longer period of time could possibly have a significant economic effect for another system in contrast to the milling circuit model.

Table 6-10: EPI breakdown of sequential relay autotuning for various f_{RA} at $n_L = 0.01$, $t_{RS} = 3hrs$ and $\alpha = 0.45$

f_{RA}	MFS (tons×10^3)	Average Recovery	Revenue ($\times 10^5$)	electricity cost ($\times 10^4$)	Average EPI ($\times 10^5$)
0.4	93.2	0.674	66.5	10.2	65.5
0.5	93.3	0.674	66.6	10.2	65.6
0.6	93.6	0.674	66.8	10.2	65.8

Chapter 7
Conclusions

The aim of the project was to design a procedure that automates relay autotuning, using CPM to detect poor controller performance due to incorrect tuning parameters. Furthermore, the case study for the project was a milling circuit simulation model. To achieve the aim a relay autotuning procedure was designed and implemented into the Simulink and MATLAB milling circuit model. Using CPM literature, the relay autotuning procedure was initiated using historical benchmarking. Subsequently, the following objectives were established.

- Evaluate the CPM technique (historical benchmarking) in the detection of a poorly performing control loop due to the fault implemented in the milling circuit simulation model.
- Evaluate relay autotuning and key parameters with respect to controller and economic performance.

The following sections conclude the results obtained for the mentioned objectives.

7.1. Assessment of historical benchmarking technique

The CPM technique uses historical benchmarking to initiate the relay autotuning procedure. The 90^{th} percentile of the PSE's variance was used as a benchmark to assess current control towards. Subsequently, a valve degradation model was used to simulate conditions whereby the current controller tuning parameters are unable to provide satisfactory set point tracking for the PSE. Utilising the historical benchmarking method as well as the degradation model, a platform for assessing relay autotuning was provided.

The historical benchmarking method required selection of a suitable moving variance size. For the project, the choice of a 1 hour sliding window was assessed as suitable. The 1 hour sliding window was able to detect the oscillations that occur for the PSE. Furthermore, the shift in the variance was a satisfactory method used to initiate relay autotuning. Despite the ability to detect a shift in the variance, the CPM methodology is not suitable for faults whereby process drift is observed and the variance of the variable remains constant. Therefore, for faults whereby the variance is constant and retuning is required, the historical benchmarking method is unable to initiate relay autotuning.

7.2. Performance assessment of relay autotuning

The relay autotuning procedure was evaluated as beneficial in the reduction of variance when valve degradation was implemented. The effects of relay autotuning were observed with the CPI values obtained in comparison to none retuning conditions. The CPIs were reduced which indicates similar control performance to the NOC i.e. a period of interest where control performance was assessed as good. Therefore, relay autotuning can attenuate faults which introduce oscillations into the process if the original tuning parameters are too aggressive.

The relay autotuning procedure initiated with historical benchmarking presented several variables that needed consideration for application within industry. The relay autotuning configuration selected was the relay autotuner with hysteresis as a result of alternative relay autotuning procedures not considering sensor noise in the calculation of the critical gain. Furthermore, the relay autotuner with hysteresis had fewer parameter selection requirements for the automated procedure. Therefore, based on these factors, the relay autotuner with hysteresis was assessed as suitable for industrial application.

In addition to the relay autotuning configuration, the relay amplitude, convergence of the relay autotuner, tuning parameters, sensor noise levels and MIMO procedures were identified as key factors and parameters. For this project, the relay amplitude, tuning parameters, sensor noise levels and MIMO procedures were assessed towards their controller performance. The factors and parameters were specifically evaluated for relay autotuning applied to a system experiencing oscillations due to valve wear.

Control performance assessment of the sensor noise level indicated marginally poorer performance for lower sensor noise levels. The results are due to the larger and more aggressive tuning parameters obtained at lower sensor noise levels which produce a slightly more aggressive controller in the presence of valve degradation. In contrast, at a larger sensor noise level the controller performance is better due to the more conservative tuning parameters obtained. Within industry, the sensor noise level is difficult to change and high sensor noise isn’t favourable. However, the results indicated the selected relay amplitude and sensor noise level interaction have a significant effect on the controller performance.

Isolated assessment of the relay amplitudes effect on the CPI indicated at larger relay amplitudes, the control performance is slightly worse due to the larger and more aggressive controller tuning parameters obtained. In contrast to the sensor noise level, the relay amplitude is a parameter that can be changed. The results showed at the lowest sensor noise level and increasing relay amplitudes, the controller performance worsened. Similarly this is attributed to the larger and more aggressive tuning parameters obtained. Therefore, for an industrial application of the relay autotuner applied to an aggressive controller, the selected relay amplitude should be as small as possible but able to overcome the hysteresis band.

The assessment of the relay amplitude and sensor noise level showed the tuning parameters obtained are important in the controller performance obtained. However, the type of controller tuning relationships used is a significant factor in the relay autotuning procedure. The Tyreus-Luyben tuning relationships were compared to the Ziegler-Nichols tuning relationships (with a detuning factor of 2.5). For a system experiencing valve wear, a larger controller gain and integral time introduce more variation within the system. Therefore, due to the Tyreus-Luyben

tuning relationship being marginally more aggressive than the Ziegler-Nichols tuning relationship with a detuning factor, the controller performance is slightly worse. However, the Tyreus-Luyben reduces design selection criteria for a MIMO system as it is designed to be conservative for a MIMO system. As a result, selecting a detuning factor is not required.

The last factor evaluated specifically for relay autotuning was sequential relay autotuning for a MIMO system. The CFF-SVOL control loop was additionally retuned after the SFW-PSE, using sequential relay autotuning. The results indicate, to an extent, poorer controller performance if the CFF-SVOL control loop is retuned. The reduction in the CFF-SVOL controller tuning parameters results in a sluggish controller. Therefore, sequential relay autotuning is not be necessary for MIMO systems if the control loop experiencing the valve degradation fault is attenuated i.e. SISO is applied to the controller with valve wear. However, sequential relay autotuning is beneficial for the historical benchmarking method used to initiate relay autotuning. Historical benchmarking does not isolate the fault and, therefore, it would not be known which manipulated variable is experiencing valve degradation for interacting control loops. As a result, fault isolation can be avoided using sequential relay autotuning.

In contrast to the factors parameters associated with relay autotuning, the fault used was examined i.e. the extent of valve wear. The average CPI for varying the extent of valve degradation, with relay autotuning applied, indicated at low extents of valve degradation control performance was marginally worse. The results suggest that if the extent of valve wear is close to the NOC, the controller performance is slightly worse due to the sluggish new tuning parameters obtained from relay autotuning. For the current case study, without retuning the system, the original tuning parameters are too aggressive and produce oscillations for the system at large degree of valve degradation. However, at lower extents of valve degradation, the system shows similar behaviour to NOC, which indicates the original tuning parameters are satisfactory. Since the extent of valve wear cannot be determined in industry, an alternative method is required where a satisfactory shift in the variance (degree of oscillations) would not require relay autotuning.

In addition to varying the degree of valve wear, an extension to the fault was implemented. The oscillatory behaviour introduced by valve wear can lead to high valve reversals and static friction within the valve. Resultantly, additional faults such as valve sticking and valve stiction can occur. Further relay autotuning experiments were performed whereby valve degradation was performed on the SFW-PSE control loop with the addition of a 30s time delay to simulate valve sticking. The data indicated improved controller performance through retuning of the controller for cases where only a time delay was applied as well as the combination of valve wear and the time delay. Therefore, relay autotuning is seen as beneficial in attenuating an aggressive controller due to valve sticking and/or valve wear.

The final parameter considered for the project was the relay start time, which is an assessment of the CPM technique used to initiate relay autotuning. The control performance of the relay start time showed for a smaller period of allowable poor control performance (i.e. a small relay start time), controller performance for the 2 month period was better. As the relay start time is increased the controller performance for the 2 month period is slightly worsened. This is observed with the increasing CPI value for the simulation experiments. As a result, earlier initiation of the relay autotuning using a 1 hour sliding window, is desirable for industrial application.

Contrasting to controller performance, economic comparison of relay autotuning to none retuning conditions, in the presence of valve wear, were inconclusive. Valve wear introduced large variations in the PSE and slight variations in the mill charge and power draw. Despite the variations, there was no discernible decrease or increase in the overall PSE, as well as the mill power draw. As a result, the throughput was the most influential variable on the EPI. However, there was no observable trend for the MFS for relay autotuning scenarios as well as none retuning cases in the presence of valve wear. Furthermore, economic assessment of changing key parameters and factors were inconclusive due to the MFS which showed no significant trend.

7.3. Recommendations

Based on the conclusions the following recommendations for future work are proposed:

- An alternative CPM technique should be evaluated that utilising both the mean and the variance of the controlled variable. Incorporating both terms allows detection of oscillations as well as process drift.
- The current research was applied for a fault where the initial tuning parameters are too aggressive, however, relay autotuning applied to sluggish incorrect tuning parameters should be assessed for a complete evaluation of relay autotuning.
- The relay autotuning literature requires further control and economic performance assessment for the convergence of the limit cycle, relay configurations applicable in industry (e.g. preload relay autotuner), MIMO procedures and model versus relation based tuning methods.
- Economic performance assessment for the milling circuit case study was inconclusive, therefore, future relay autotuning research should be applied to different case studies that are realistic for industry. The proposed research should attempt to correlate improved controller performance, due to relay autotuning, with the economic benefits associated with better control of variables. As a result, key variables can be successfully evaluated which aids in producing a robust relay autotuning procedure.

References

Åström, Karl Johan, T. H. (1995) 'PID controllers: Theory, design and tuning', *Instrument Society of America*, p. 343.

Åström, K. J. *et al.* (1993) 'Automatic tuning and adaptation for PID controllers - a survey', *Control Engineering Practice*, 1(4), pp. 699–714.

Åström, K. J. and Hägglund, T. (2006) 'Advanced PID control', *IEEE Control Systems*, pp. 98–101.

Åström, K. J. and Hägglund, T. (2017) 'Automatic Tuning of Simple Regulations for Phase and Amplitude Margins Specifications', *IFAC Proceedings Volumes*, 16(9), pp. 271–276.

Åström, K. and Lee, T. (1995) 'Recent advances in relay feedback methods-a survey', *1995 IEEE International Conference on Systems, Man and Cybernetics. Intelligent Systems for the 21st Century*.

Bauer, M. *et al.* (2007) 'A Profit Index for Assessing the Benefits of Process Control', *Industrial & Engineering Chemistry Research*, 46(17), pp. 5614–5623.

Bauer, M. *et al.* (2016) 'The current state of control loop performance monitoring - A survey of application in industry', *Journal of Process Control*. Elsevier Ltd, 38, pp. 1–10.

Bauer, M. and Craig, I. K. (2008) 'Economic assessment of advanced process control - A survey and framework', *Journal of Process Control*, 18(1), pp. 2–18.

Bawden, N. M. (1993) *The prediction, quantification and evaluation of advanced control benefits*. University of Witwatersrand.

Berner, J. (2015) *Automatic Tuning of PID Controllers based on Asymmetric Relay Feedback*. Lund University.

Berner, J., Åström, K. J. and Hägglund, T. (2014) 'Towards a new generation of relay autotuners', *IFAC Proceedings Volumes (IFAC-PapersOnline)*, 19, pp. 11288–11293.

Berner, J., Hägglund, T. and Åström, K. J. (2016) 'Asymmetric relay autotuning – Practical features for industrial use', *Control Engineering Practice*, 54, pp. 231–245.

Boyd, D. W. (2001) 'Stochastic Analysis', *Systems Analysis and Modeling*, pp. 211–227.

Brisk, M. L. (2004) 'Process Control: Potential Benefits and Wasted Opportunities', in, p. 10–16 Vol.1.

Cheng, Y. C. and Yu, C. C. (2000) 'Relay feedback identification for actuators with hysteresis', *Industrial and Engineering Chemistry Research*, 39(11), pp. 4239–4249.

Coetzee, L. C., Craig, I. K. and Kerrigan, E. C. (2010) 'Robust nonlinear model predictive control of a run-of-mine ore milling circuit', *IEEE Transactions on Control Systems Technology*, 18(1), pp. 222–229.

Craig, I. K. *et al.* (1992) 'Optimised multivariable control of an industrial run-of-mine milling circuit', *Journal of the Southern African Institute of Mining and Metallurgy*. Sabinet, 92(6), pp. 169–176.

Craig, I. K. and Henning, R. G. D. (2000) 'Evaluation of advanced industrial control projects: A framework for determining economic benefits', *Control Engineering Practice*, 8(7), pp. 769–780.

Craig, I. K. and Koch, I. (2003) 'Experimental design for the economic performance evaluation of industrial controllers', *Control Engineering Practice*. Elsevier, 11(1), pp. 57–66.

Desborough, L. and Miller, R. (2002) 'Increasing Customer Value of Industrial Control Performance Monitoring — Honeywell's Experience', *AIChE Symposium Series*, (Figure 1), pp. 153–186.

Ender, B. D. B. (1993) 'Process Control Performance : Not as Good as you Think', *Control Engineering*, 40(September), pp. 180–190.

Friedmann, P. G. (2006) *Automation and Control Systems Economics*. Second Ed. The Instrumentation, Systems, and Automation Society.

Gao, X. *et al.* (2016) 'A review of control loop monitoring and diagnosis: Prospects of controller maintenance in big data era', *Chinese Journal of Chemical Engineering*. Elsevier B.V., 24(8), pp. 952–962.

Gelb, A. and Vander Velde, W. E. (1968) *Multiple-input describing functions and nonlinear system design*. McGraw-Hill (McGraw-Hill electronic sciences series).

Hang, C. C. *et al.* (1993) *Adaptive Control*. Instrument Society of America (Independent learning module from the Instrument Society of America).

Hang, C. C., Åström, K. J. and Ho, W. K. (1993) 'Relay auto-tuning in the presence of static load disturbance', *Automatica*, 29(2), pp. 563–564.

Hang, C. C., Åström, K. J. and Wang, Q. G. (2002) 'Relay feedback auto-tuning of process controllers - A tutorial review', *Journal of Process Control*, 12(1), pp. 143–162.

Ho, W. K. *et al.* (2003) 'Relay auto-tuning of PID controllers using iterative feedback tuning', *Automatica*, 39(1), pp. 149–157.

Hodouin, D. *et al.* (2001) 'State of the art and challenges in mineral processing control', *Control Engineering Practice*, 9(9), pp. 995–1005.

Huang, B. *et al.* (1997) 'Performance Assessment of Multivariate Control Loops on a Paper-Machine Headbox', *Canadian Journal of Chemical Engineering*, pp. 134–142.

Huang, B. and Shah, S. L. (2012) *Performance Assessment of Control Loops: Theory and Applications*. Springer London (Advances in Industrial Control).

Huang, B., Shah, S. L. and Kwok, E. K. (1997) 'Good, bad or optimal? Performance assessment of multivariable processes', *Automatica*, 33(6), pp. 1175–1183.

Hulbert, D. G. (2005) 'Simulation of milling circuits: Part 1 & 2', *tech. rep.*

Jelali, M. (2006) 'An overview of control performance assessment technology and industrial applications', *Control Engineering Practice*, 14(5), pp. 441–466.

Jelali, M. (2013) *Control Performance Management in Industrial Automation*.

Ko, B. and Edgar, T. F. (2001) 'Performance Assessment of Constrained Model Predictive Control Systems', 47(6), pp. 1363–1371.

Lawler, G. F. and Limic, V. (2012) *Random Walk: A Modern Introduction*, *Random Walk: A Modern Introduction*.

Levy, S. *et al.* (2012) 'PID autotuning using relay feedback', *2012 IEEE 27th Convention of Electrical and Electronics Engineers in Israel, IEEEI 2012*. IEEE, pp. 1–4.

Li, W., Eskinat, E. and Luyben, W. L. (1991) 'An Improved Autotune Identification Method', *Industrial and Engineering Chemistry Research*, 30(7), pp. 1530–1541.

Li, Z. *et al.* (2014) 'Process identification using relay feedback with a fractional order integrator', *IFAC Proceedings Volumes (IFAC-PapersOnline)*, 19(December), pp. 2010–2015.

Loh, A. P. *et al.* (1993) 'Autotuning of Multiloop Proportional-Integral Controllers Using Relay Feedback', *Industrial and Engineering Chemistry Research*, 32(6), pp. 1102–1107.

Luyben, W. L. (1986) 'Simple Method for Tuning SISO Controllers in Multivariable Systems', *Industrial and Engineering Chemistry Process Design and Development*, 25(3), pp. 654–660.

Luyben, W. L. (2001) 'Getting more information from relay-feedback tests', *Industrial and Engineering Chemistry Research*, 40(20), pp. 4391–4402.

Martin, G. (2004) 'Understand control benefits estimates: here's how the five popular methods work', *Hydrocarbon Processing*. Gulf Publishing Co., 83(10), pp. 43–47.

Matthews, B. and Craig, I. K. (2012) 'Demand side management by load shifting a run-of-mine ore milling circuit', *IFAC Proceedings Volumes (IFAC-PapersOnline)*, pp. 84–89.

Miskin, J. J. (2016) *Control performance assessment for a high pressure leaching process by means of fault database creation and simulation*. Stellenbosch University.

Olivier, L. E. and Craig, I. K. (2017) 'Should I shut down my processing plant? An analysis in the presence of faults', *Journal of Process Control*. Elsevier Ltd, 56, pp. 35–47.

Oosthuizen, D. J., Craig, I. K. and Pistorius, P. C. (2004) 'Economic evaluation and design of an electric arc furnace controller based on economic objectives', *Control engineering practice*. Elsevier, 12(3), pp. 253–265.

Rato, T. J. and Reis, M. S. (2010) 'Statistical monitoring of control loops performance: An improved historical-data benchmark index', *Quality and Reliability Engineering International*, 26(8), pp. 831–844.

Ren-Chiou, C., Shih-Haur, S. and Cheng-Ching, Y. (1992) 'Derivation of Transfer Function from Relay Feedback Systems', *Industrial and Engineering Chemistry Research*, 31(3), pp. 855–860.

Rivera, D. E., Morarl, M. and Skogestad, S. (1986) 'Internal Model Control: Pid Controller Design', *Industrial and Engineering Chemistry Process Design and Development*, 25(1), pp. 252–265.

Le Roux, J. D. *et al.* (2013) 'Analysis and validation of a run-of-mine ore grinding mill circuit model for process control', *Minerals Engineering*, 43–44, pp. 121–134.

Ruel, M. (2002) 'Learn How To Assess And Improve Control Loop Performance', *Technical Papers-Isa*, 423, pp. 351–356.

Seborg, D. *et al.* (2011) *Process Dynamics and Control (3rd Edition), John Wiley & Sons*.

Shen, S. H., Wu, J. S. and Yu, C. C. (1996) 'Use of Biased-Relay Feedback for System

Identification', *AIChE Journal*, 42(4), pp. 1174–1180.

Skogestad, S. (2004) 'Simple analytic rules for model reduction and PID controller tuning', *Modeling, Identification and Control*, 25(2), pp. 85–120.

Soltesz, K., Mercader, P. and Baños, A. (2017) 'An automatic tuner with short experiment and probabilistic plant parameterization', *International Journal of Robust and Nonlinear Control*, 27(11), pp. 1857–1873.

Sommer, S. and Kienle, A. (2012) 'Auto-tuning of multivariable pid controllers using iterative feedback tuning', *At-Automatisierungstechnik*, 60(1), pp. 20–27.

Steyn, C. W. and Sandrock, C. (2013) 'Benefits of optimisation and model predictive control on a fully autogenous mill with variable speed', *Minerals Engineering*. Elsevier Ltd, 53, pp. 113–123.

Stout, T. M. and Cline, R. P. (1976) 'Control-system justification', *Instrumentation Technology*, 23(9), pp. 51–58.

Sung, S. W. and Lee, J. (2006) 'Relay feedback method under large static disturbances', *Automatica*, 42(2), pp. 353–356.

Sung, S. W., Park, J. H. and Lee, I. B. (1995) 'Modified Relay Feedback Method', *Industrial and Engineering Chemistry Research*, 34(11), pp. 4133–4135.

Tan, K. K. *et al.* (2006) 'Improved critical point estimation using a preload relay', *Journal of Process Control*, 16(5), pp. 445–455.

Thyagarajan, T. and Yu, C. C. (2002) 'Improved autotuning using shape factor from relay feedback', *IFAC Proceedings Volumes (IFAC-PapersOnline)*, 15(1), pp. 443–448.

Vivek, S. and Chidambaram, M. (2005) 'Identification using single symmetrical relay feedback test', *Computers and Chemical Engineering*, 29(7), pp. 1625–1630.

Wakefield, B. J. (2018) *Applying Dynamic Bayesian Networks to Processes*. Stellenbosch University.

Wakefield, B. J. *et al.* (2018) 'Monitoring of a simulated milling circuit: Fault diagnosis and economic impact', *Minerals Engineering*, 120, pp. 132–151.

Wang, Q. G. *et al.* (1997) 'Auto-tuning of multivariable PID controllers from decentralized relay feedback', *Automatica*, 33(3), pp. 319–330.

Wei, D. and Craig, I. K. (2009a) 'Economic performance assessment of two ROM ore milling circuit controllers', *Minerals Engineering*. Elsevier Ltd, 22(9–10), pp. 826–839.

Wei, D. and Craig, I. K. (2009b) 'Grinding mill circuits - A survey of control and economic concerns', *International Journal of Mineral Processing*. Elsevier B.V., 90(1–4), pp. 56–66.

Wei, D., Craig, I. K. and Bauer, M. (2007) 'Multivariate economic performance assessment of an MPC controlled electric arc furnace', *ISA transactions*. Elsevier, 46(3), pp. 429–436.

Williams, A. K. and Rameshni, M. (1998) 'Real-time economic control', *Hydrocarbon processing*. Gulf Publishing Co., Houston, 77(9), pp. 99–106.

Wills, B. A. and Napier-Munn, T. (2005) *Mineral Processing Technology: an Introduction to the Practical Aspects of Ore Treatment and Mineral Recovery*. 7th edn, *Wills' Mineral Processing Technology*. 7th edn. Butterworth-Heinemann, Oxford.

Wills, B. a and Napier-munn, T. (2006) *Mineral Processing Technology:An Introduction to the Practical Aspects of Ore Treatment and Mineral Recovery*, *October*.

Yu, C. C. (2006) *Autotuning of PID controllers: A relay feedback approach*. 2(ed), *Autotuning of PID Controllers: A Relay Feedback Approach*. 2(ed).

Zhao, C. *et al.* (2009) 'Economic performance assessment of advanced process control with LQG benchmarking', *Journal of Process Control*, 19(4), pp. 557–569.

Zhou, Y. and Forbes, J. F. (2003) 'Determining controller benefits via probabilistic optimization', *International Journal of Adaptive Control and Signal Processing*, 17(7–9), pp. 553–568.

Appendix A: Milling circuit model

The following section is a guide to understanding the milling circuit simulation model. Key variables and units are discussed to formulate the model. Inherently, the model is complex and requires simplification of abbreviations. Therefore, table A-1 below shows the notation used when naming the volume (X) and the volumetric flow rate (V) for the five components used in the milling circuit simulation model. The components can be divided into water, rocks, solids, fines and steel balls. Rocks are defined as material too large to pass through the mill. In contrast, solids pass through the mill and are composed of fines and coarse particles. The fines are defined as particles that are smaller than 75µm. lastly, the steel balls are used as grinding media. In addition to the notations, all equations and theory for the milling circuit model have been obtained from Le Roux *et al* (2013).

Table A-1: Milling circuit model subscript notation

Subscript	Description
$X_{\Delta-}$	f-feeder, m-mill, s-sump, c-cyclone
$X_{-\Delta}$	w-water, s-solids, c-coarse, f-fines, r-rocks, b-balls, t-total
$V_{--\Delta}$	i-inflow, o-outflow, u-underflow

The feeder unit

The first system in the milling circuit simulation model is the feeder unit. The feeder unit is designed to divide the stream into components, with each component representing 1 of the 5 states fed into the milling unit. From a mass balance the following equations are applicable:

$$V_{fwo}(\text{water}) = MIW \qquad \textbf{Equation A-1}$$

$$V_{fso}(\text{solids}) = \frac{MFS}{DS}(1 - a_r) \qquad \textbf{Equation A-2}$$

$$V_{ffo}(\text{fines}) = \frac{MFS}{DS}(a_f) \qquad \textbf{Equation A-3}$$

$$V_{fro}(\text{rocks}) = \frac{MFS}{DS}(a_r) \qquad \textbf{Equation A-4}$$

$$V_{fbo}(\text{balls}) = \frac{MFB}{DB} \qquad \textbf{Equation A-5}$$

The terms a_r and a_f are the mass fraction of rocks and fines within the solids stream. MIW, MFS, and MFB refer to the mill feed water, solids fed to the mill and steel balls fed to the mill respectively. Lastly DS and DB are the solids and steel ball densities.

Mill

The following equations describe the differential equations for the five components entering the mill module from the feeder unit:

$$\frac{dX_{mw}}{dt} = V_{mwi} - V_{mwo} \qquad \textbf{Equation A-6}$$

$$\frac{dX_{ms}}{dt} = V_{msi} - V_{mso} + RC \qquad \textbf{Equation A-7}$$

$$\frac{dX_{mf}}{dt} = V_{mfi} - V_{mfo} + FP \qquad \textbf{Equation A-8}$$

$$\frac{dX_{mr}}{dt} = V_{mri} - RC \qquad \textbf{Equation A-9}$$

$$\frac{dX_{mb}}{dt} = V_{mbi} - BC \qquad \textbf{Equation A-10}$$

RC refers to the rock consumption, BC refers to the ball consumption and FP refers to the fines produced from the milling process unit. Determining the breakage functions, RC and BC, requires mill slurry and power draw characteristics to be known. Although it is a complex procedure, modelling the breakage function can be simplified with the rheology factor (φ). The rheology factor is an empirically derived parameter used to integrate the density and fluidity effects of the slurry to the grinding performance of the mill. The rheology factor is determined using the principles of packing solids. From experiments, randomly close packed hard spheres are limited to 64% by volumetric fraction. In relation to the mill, the slurry has to contain a

minimum volumetric fraction of 36% water. However, the slurry within a mill does not contain perfectly spherical solids. As a result, the adjusted volumetric fraction of water for the mill is 40% as a minimum. Therefore, ε_{sv} is defined as the maximum solids fraction of 60% within the mill. Using ε_{sv} and the volume of solids and water (X_{ms} and X_{mw} respectively), equation A-11 is derived:

$$\varphi = \left\{\max\left[0{,}1 - \left(\left(\frac{1}{\varepsilon_{sv}}\right) - 1\right)\frac{X_{ms}}{X_{mw}}\right]\right\}^{0.5} \qquad \textbf{Equation A-11}$$

As mentioned previously, the mill power draw (P_{mill}) is required to determine the breakage functions. However, P_{mill} is dependent on the slurry characteristics within the mill. Therefore, P_{mill} can be modelled using φ. For the current milling circuit model, P_{mill} is evaluated with equation A-12. Although several models are presented from literature, the model used has the fewest dependent variables to produce an accurate P_{mill}.

$$P_{mill} = P_{max}\{1 - \delta_{Pv}{Z_x}^2 - 2\chi_P\delta_{Pv}\delta_{Ps}Z_xZ_r - \delta_{Ps}{Z_r}^2\}(\alpha_{speed})^{\alpha_P} \qquad \textbf{Equation A-12}$$

From the mill power draw model, P_{max} is the maximum mill power draw, δ_{Pv} is the power-change parameter associated with the volume, δ_{Ps} is the power-change parameter associated with the solids fraction, χ_P is the cross term associated with P_{max}, α_{speed} is the fraction of critical mill speed and α_P is the fractional change in kW/fines produced per fractional filling of the mill. In addition, Z_x and Z_r incorporate the effects of the total mill charge and slurry rheology on the mill power respectively. Z_x and Z_r are described by equation A-13 and A-15 respectively, whereby v_{Pmax} and φ_{Pmax} are the volume fraction of the mill filled and φ for maximum power draw.

$$Z_x = \frac{LOAD}{v_{mill}v_{Pmax}} - 1 \qquad \textbf{Equation A-13}$$

$$LOAD = X_{mw} + X_{mr} + X_{ms} + X_{mb} \qquad \textbf{Equation A-14}$$

$$Z_r = \frac{\varphi}{\varphi_{Pmax}} - 1 \qquad \textbf{Equation A-15}$$

From a design perspective, the maximum power draw is obtained if Z_x and Z_r are zero. This is achievable if the LOAD fraction within the mill is equal to v_{Pmax} as well as if φ is equal to φ_{Pmax}. Utilising the mill power draw model as well as the rheology factor, the breakage functions RC, BC and FP are defined with equation A-16, A-17 and A-18 respectively. From the equations, additional terms are implemented such as the abrasion rates of rocks and balls (ϕ_r and ϕ_b respectively).

$$RC = \frac{P_{mill}\varphi}{Ds\phi_r}\left(\frac{X_{mr}}{X_{mr}+X_{ms}}\right) \qquad \textbf{Equation A-16}$$

$$BC = \frac{P_{mill}\varphi}{\phi_b}\left(\frac{X_{mb}}{D_S(X_{mr}+X_{ms})+D_BX_{mb}}\right) \qquad \textbf{Equation A-17}$$

$$FP = \frac{P_{mill}}{Ds\phi_f\left(1+\alpha_{\phi f}\left(\frac{LOAD}{v_{mill}}-v_{Pmax}\right)\right)} \qquad \textbf{Equation A-18}$$

Following the determination of each components volume within the mill, their respective flow rates are determined using the subsequent equations. Notably, the rocks and balls are defined as not leaving the mill, therefore, their flow rates are assumed to be 0.

$$V_{mwo} = V_V\varphi X_{mw}\left(\frac{X_{mw}}{X_{ms}+X_{mw}}\right) \qquad \textbf{Equation A-19}$$

$$V_{mso} = V_V\varphi X_{mw}\left(\frac{X_{ms}}{X_{ms}+X_{mw}}\right) \qquad \textbf{Equation A-20}$$

$$V_{mfo} = V_V\varphi X_{mw}\left(\frac{X_{mf}}{X_{ms}+X_{mw}}\right) \qquad \textbf{Equation A-21}$$

$$V_{mro} = V_{mbo} = 0 \qquad \textbf{Equation A-22}$$

Sump

The sump unit is used as a buffer medium for the hydrocyclone. The sump has been modelled with the assumption that the contents are perfectly mixed. Furthermore, the sump only contains water and solids composed of fines are coarse particles. Therefore, the change in the volumes of each component within the sump are defined as follows:

$$\frac{dX_{sw}}{dt} = V_{swi} - V_{swo} + SFW \qquad \textbf{Equation A-23}$$

$$\frac{dX_{ss}}{dt} = V_{ssi} - V_{sso} \qquad \textbf{Equation A-24}$$

$$\frac{dX_{sf}}{dt} = V_{sfi} - V_{sfo} \qquad \textbf{Equation A-25}$$

Incorporated into the water component is the addition of sump feed water (SFW) which is importantly used to manipulate the density of the feed to the hydrocyclone (CFD). Manipulation of CFD plays an important role in the separation efficiency of the hydrocyclone, as will be shown with the hydrocyclone module. Utilising the cyclone feed flow rate (CFF), defined as the sum of the water and solids leaving the sump, the volumetric flow rates of each component leaving the sump are determined using the following equations:

$$V_{swo} = CFF\left(\frac{X_{sw}}{SVOL}\right) \qquad \textbf{Equation A-26}$$

$$V_{sso} = CFF\left(\frac{X_{ss}}{SVOL}\right) \qquad \textbf{Equation A-27}$$

$$V_{sfo} = CFF\left(\frac{X_{sf}}{SVOL}\right) \qquad \textbf{Equation A-28}$$

Whereby, the respective cyclone feed flow rate and sump volume are determined using the subsequent equations.

$$CFF = V_{swo} + V_{sso} \qquad \textbf{Equation A-29}$$

$$SVOL = X_{sw} + X_{ss} \qquad \textbf{Equation A-30}$$

Hydrocyclone

The milling circuit is described by fast dynamics in comparison to the other process units within the system. Therefore, with negligible hold up assumed within the hydrocyclone, the separation process can be evaluated using a series of algebraic equations. To describe the quality of separation, the corrected classification size (d_{50c}) is required. Defined as the particle size whereby 50% of the specific particle size entering the hydrocyclone would report to the overflow and underflow, d_{50c} can be evaluated with the Plitt equation. From equation A-31, F_i is defined as the solids fraction in the inflow to the hydrocyclone and CFF is the cyclone feed flow rate. Fundamentally, an increase in d_{50c} would indicate a larger portion of coarse particles in the stream into the hydrocyclone would report to the overflow (product stream) and, potentially, a smaller PSE would be obtained.

$$d_{50c} = \frac{e^{6.3F_i}}{CFF^{0.45}} \qquad \textbf{Equation A-31}$$

$$F_i = \frac{V_{csi}}{CFF} \qquad \textbf{Equation A-32}$$

The coarse particles in the underflow and overflow restrict the values of the fines and water in those streams respectively. As a result, the coarse particle split is an important factor to determine within the hydrocyclone. The flow rate of coarse particles reporting to the underflow (V_{ccu}) is dependent on the coarse particle inflow (V_{cci}), CFF and the fraction of fines within the solids (P_i). Using these variables, the coarse ore split can be determined.

The cyclone feed flow rate determines the centrifugal forces with respect to the inlet velocity of the hydrocyclone. From the Plitt equation, an increase in CFF would result in a decrease in d_{50c}. Fundamentally, the underflow coarse particle flow rate (V_{ccu}) should increase asymptotically as CFF increases. Therefore, the relationship between the coarse particle split and CFF is described by equation A-33. From the relationship, the parameter C_1 correlates to the coarse particle split at smaller flow rates within the hydrocyclone. In addition, the parameter ε_c indicates the speed to which the coarse particle flow rate reduces to 0 in the overflow as CFF increases.

$$\left(\frac{V_{ccu}}{V_{cci}}\right)_1 = 1 - C_1 e^{\frac{-CFF}{\varepsilon_c}} \qquad \textbf{Equation A-33}$$

In addition to CFF, the fraction of solids within the inflow to the hydrocyclone is a factor in determining the coarse particle split. From the Plitt equation, as F_i increases the number of coarse particles that report to the overflow increases. Therefore, d_{50c} would increase as the fraction of solids within the inlet flow rate increases. This further illustrates the importance of CFD and the SFW for the hydrocyclone system. Using F_i, the coarse particle split fraction can be evaluated using equation A-34. Defined from the relationship is the parameter C_2 which normalises F_i with respect to the upper limit of the packing fraction of solids (ε_{sv}).

Furthermore, the parameter C_3 is used as a functional shape factor for the rate at which the coarse particle split tends towards the solids packing limit.

$$\left(\frac{V_{ccu}}{V_{cci}}\right)_2 = 1 - \left(\frac{F_i}{C_2}\right)^{C_3} \qquad \textbf{Equation A-34}$$

The final variable to be considered, in relation to the coarse particle split, is the fraction of fines in the inlet flow rate (P_i) defined by equation A-35. Intuitively a small value for P_i indicates the inlet material is very coarse whereas a large value indicates a finer slurry entering the hydrocyclone. Resultantly, the coarse particle split can be described by equation A-36, whereby C_4 is a constant which determines how fast the coarse particle split reduces to 0.

$$P_i = \frac{V_{cfi}}{V_{csi}} \qquad \textbf{Equation A-35}$$

$$\left(\frac{V_{ccu}}{V_{cci}}\right)_3 = 1 - {P_i}^{C_4} \qquad \textbf{Equation A-36}$$

Despite the individual relationship between the coarse particle split with CFF, F_i and P_i respectively, an overall relationship is required. The overall relationship can be evaluated as the product of the individual relationships, as is shown in equation A-37:

$$\frac{V_{ccu}}{V_{cci}} = \left(1 - C_1 e^{\frac{-CFF}{\varepsilon_c}}\right)\left(1 - \left(\frac{F_i}{C_2}\right)^{C_3}\right)\left(1 - {P_i}^{C_4}\right) \qquad \textbf{Equation A-37}$$

Defining the coarse particle split is an important parameter for determining the separation within the hydrocyclone. Nonetheless, the water and fines present in the underflow and overflow is required. To determine these variables, the volumetric fraction of solids in the underflow (F_u) is utilised. From equation A-38, F_u is dependent on the solids fraction in the inlet flow rate, the fraction of solids in the underflow (α_{su}) as well as the coarse particle underflow (V_{ccu}). In addition, the equation bounds F_u to ε_{sv}. Alternatively, F_u can be determined from equation A-39. The two equations are, therefore, auxiliary equations required to evaluate the water and fine flow rates in the overflow and underflow respectively.

$$F_u = 0.6 - (0.6 - F_i)e^{\frac{-V_{ccu}}{\alpha_{su}\varepsilon_c}} \qquad \textbf{Equation A-38}$$

$$F_u = \frac{V_{cfu} + V_{ccu}}{V_{cwu} + V_{cfu} + V_{ccu}} \qquad \textbf{Equation A-39}$$

An important assumption within the milling circuit model is the ratio of fines to water in the overflow and underflow is the same as is shown in equation A-40. The assumption is acceptable on the basis that fines are small enough that centrifugal forces are negligible. Using this relationship as well as equation A-39, V_{cwu} and V_{cfu} can be determined, as is shown in A-41 and A-42.

$$\frac{V_{cwu}}{V_{cwi}} = \frac{V_{cfu}}{V_{cfi}} \qquad \textbf{Equation A-40}$$

$$V_{cwu} = \frac{V_{cwi}(V_{ccu} - F_u V_{ccu})}{F_u V_{cwi} + F_u V_{cfi} - V_{cfi}} \qquad \textbf{Equation A-41}$$

$$V_{cfu} = \frac{V_{cfi}(V_{ccu} - F_u V_{ccu})}{F_u V_{cwi} + F_u V_{cfi} - V_{cfi}} \qquad \textbf{Equation A-42}$$

Lastly, with the underflow as well as overflow particles defined, the product particle size (PSE) for the cyclone overflow is described as the volume fraction of the fines leaving the overflow. Importantly, the PSE defines the quality of separation for the hydrocyclone.

$$PSE = \frac{V_{cfo}}{V_{cco} + V_{cfo}} = \frac{V_{cfi} - V_{cfu}}{V_{cci} - V_{ccu} + V_{cfo}} \qquad \textbf{Equation A-43}$$

Parameter values

Table A-2: Parameter values for milling circuit model

Parameter	Description	Value
Feed unit and mill		
α_f	Fraction of fines in the ore	0.055
α_r	Fraction of rocks in the ore	0.465
α_P	Fractional power reduction per fractional reduction from maximum mill speed	1
$\alpha_{\phi f}$	Fractional change in kW/fines produced per change in fractional filling of mill	0.01
α_{speed}	Fraction of critical mill speed	0.712
δ_{Ps}	Power-change parameter for fraction solids in the mill	0.5
δ_{Pv}	Power-change parameter for volume of mill filled	0.5
DB	Density of steel balls $\left(\frac{ton}{m^3}\right)$	7.85
DS	Density of feed ore $\left(\frac{ton}{m^3}\right)$	3.2
ε_{sv}	Maximum fraction of solids by volume of slurry at zero slurry flow	0.6
ϕ_b	Steel abrasion factor $\left(\frac{kWh}{ton}\right)$	90.0
ϕ_f	Power needed per tonne of fines produced $\left(\frac{kWh}{ton}\right)$	29.6
ϕ_r	Rock abrasion factor $\left(\frac{kWh}{ton}\right)$	6.03
φ_{Pmax}	Rheology factor for maximum mill power draw	0.57
P_{max}	Maximum mill motor power draw (kW)	1662
v_{mill}	Mill volume (m^3)	59.12
v_{Pmax}	Fraction of mill volume filled for maximum power draw	0.34
V_V	Volumetric flow per 'flowing volume' driving force h^{-1}	84.0
χ_P	Cross-term for maximum power draw	0

Parameter	Description	Value
Cyclone		
α_{su}	Parameter related to fraction solids in underflow	0.87
C_1	Constant	0.6
C_2	Constant	0.7
C_3	Constant	4
C_4	Constant	4
ε_C	Parameter related to coarse particle split $\left(\frac{m^3}{h}\right)$	129

Appendix B

Normal operating conditions

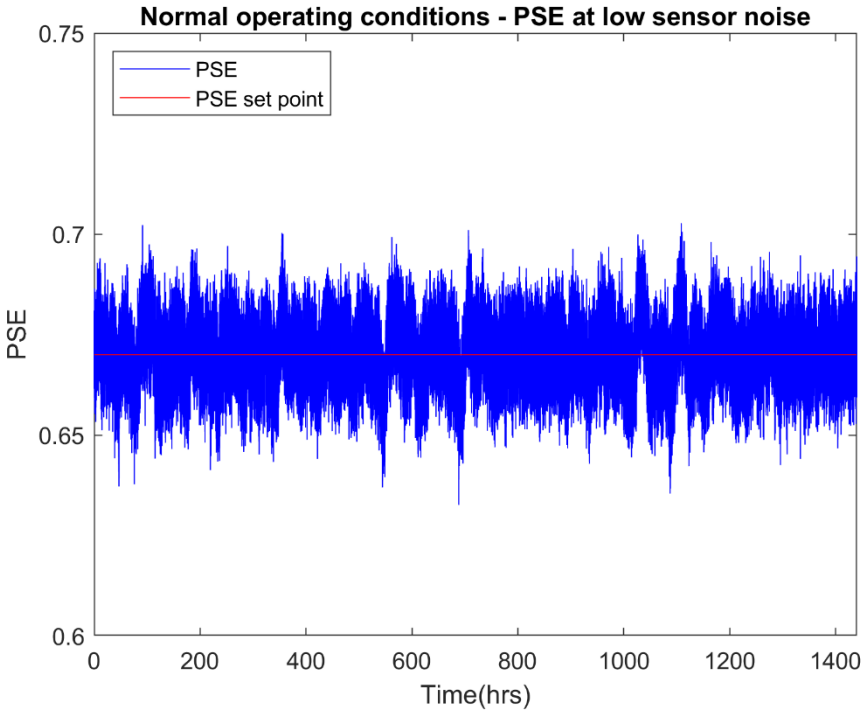

Figure B-1: Normal operating conditions for PSE at $n_L = 0.0075$

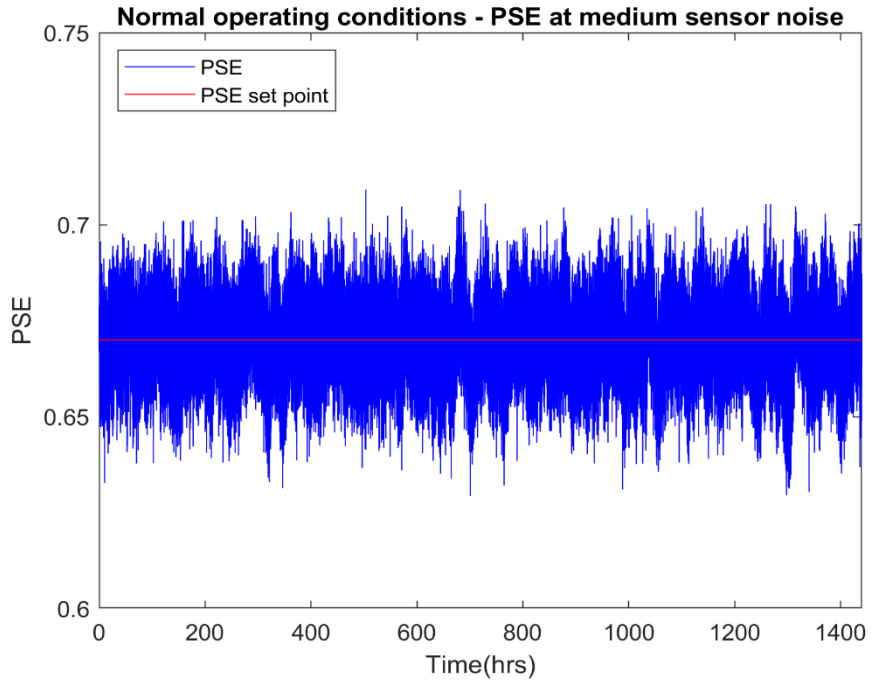

Figure B-2: Normal operating conditions for PSE at $n_L = 0.01$

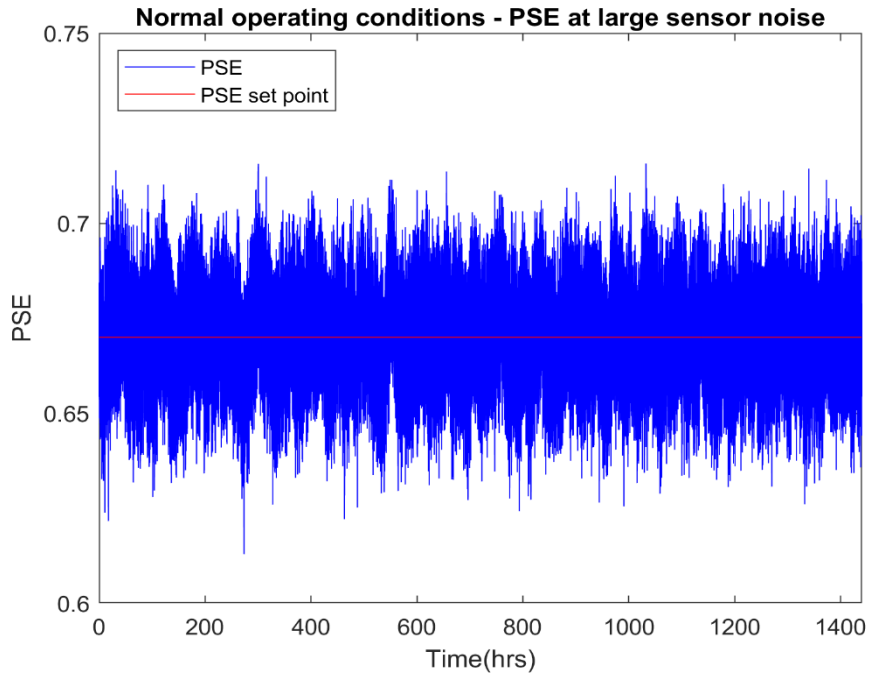

Figure B-3: Normal operating conditions for PSE at $n_L = 0.0125$

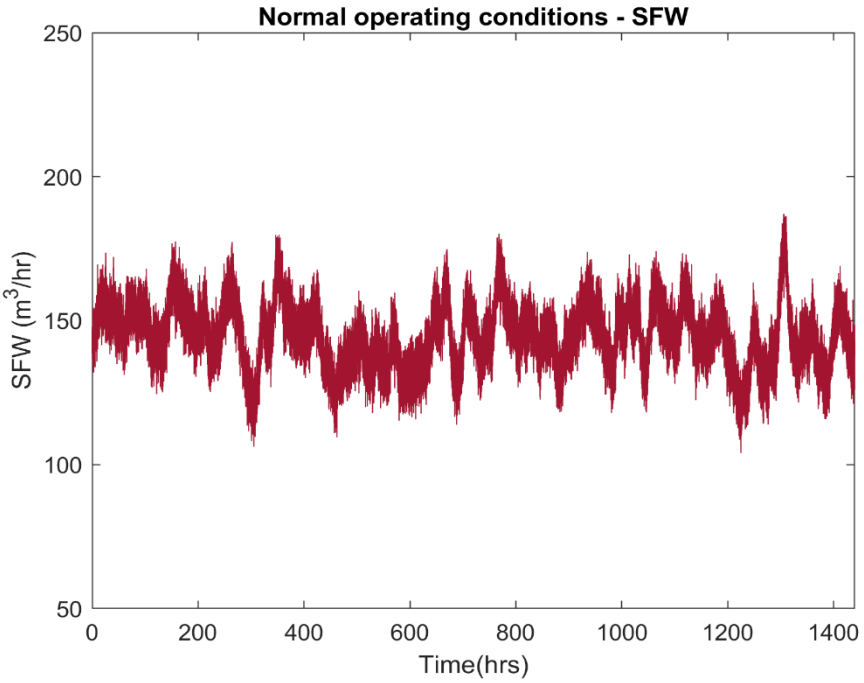

Figure B-4: Normal operating conditions for SFW at $n_L = 0.01$

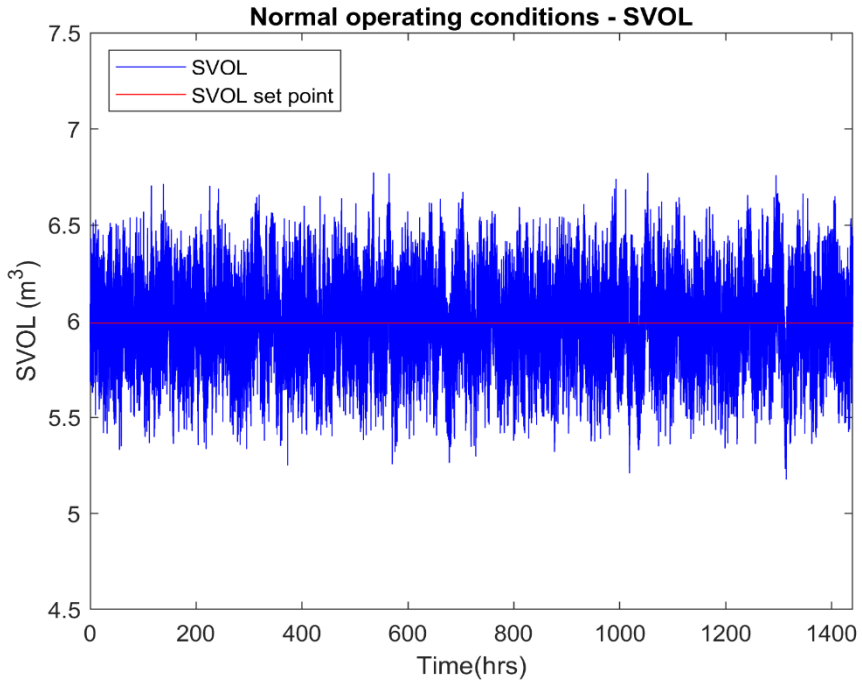

Figure B-5: Normal operating conditions for SVOL at $n_L = 0.01$

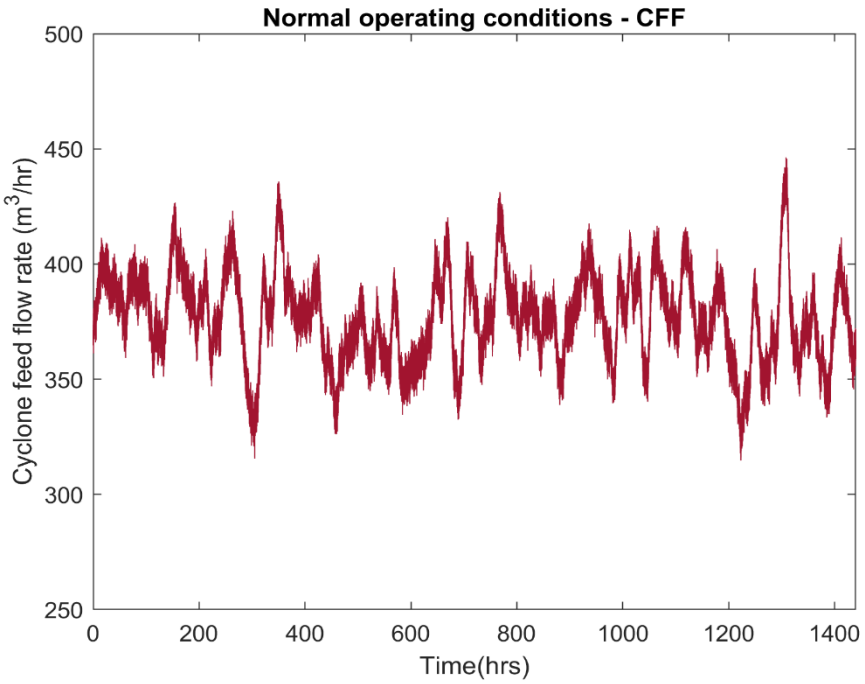

Figure B-6: Normal operating conditions for CFF at $n_L = 0.01$

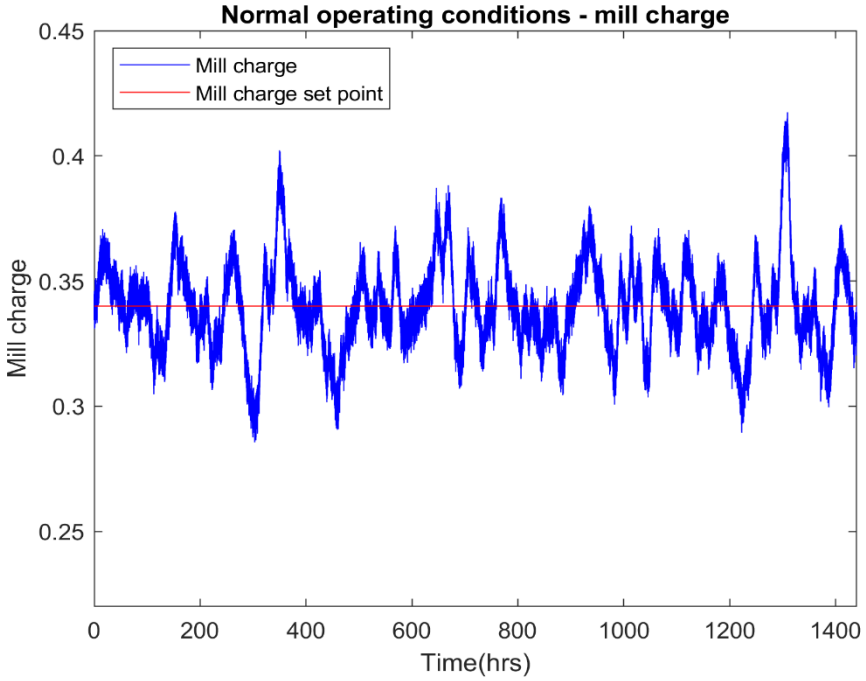

Figure B-7: Normal operating conditions for mill charge at $n_L = 0.01$

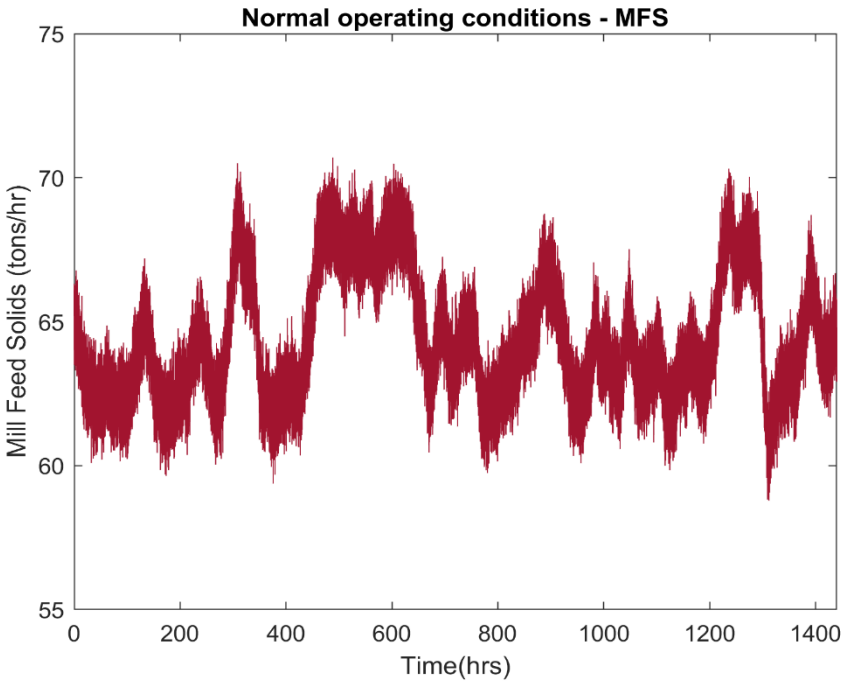

Figure B-8: Normal operating conditions for MFS at $n_L = 0.01$

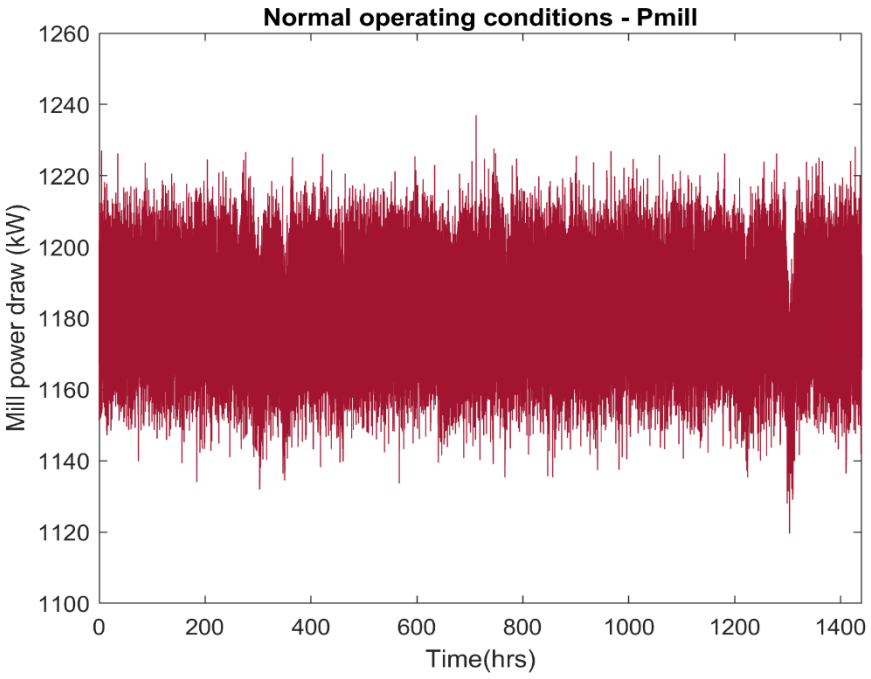

Figure B-9: Normal operating conditions for P_{mill} at $n_L = 0.01$

Product particle size control loop

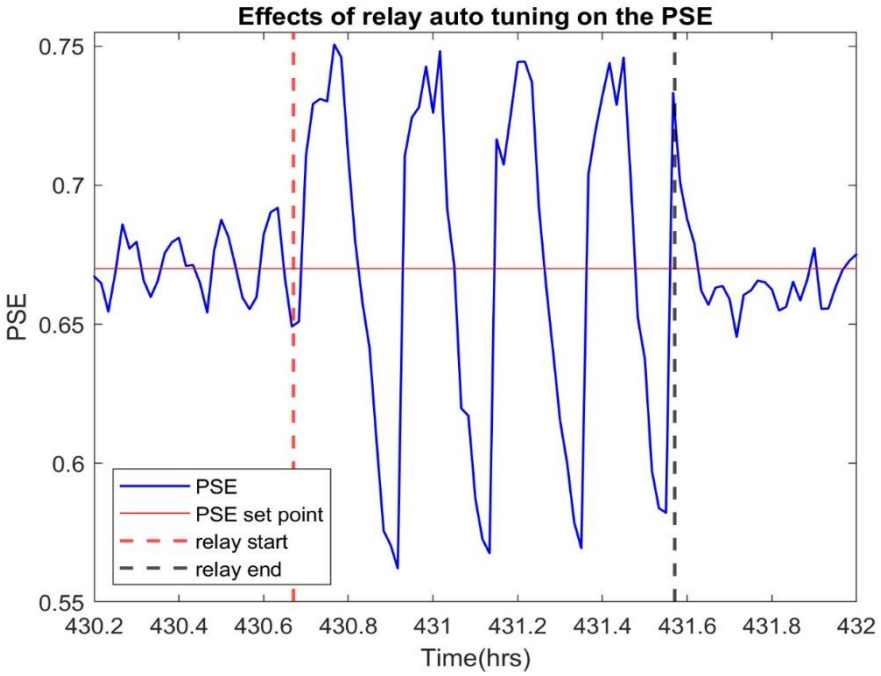

Figure B-10: In-depth illustration of relay procedure on the PSE for $\alpha = 0.45$, $t_{RS} = 4hr$, $f_{RA} = 0.4$ and $n_L = 0.01$

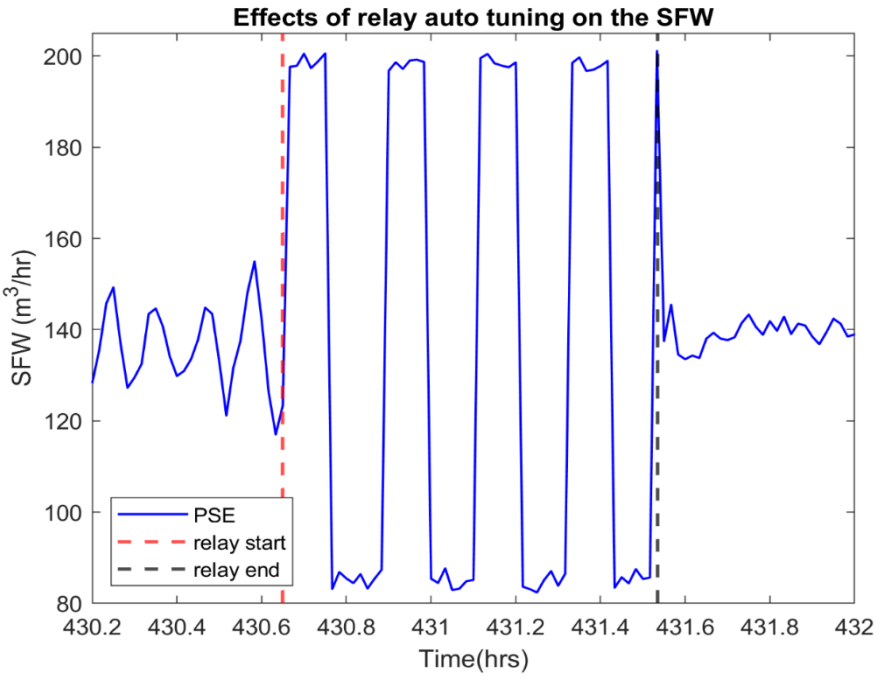

Figure B-11: In-depth illustration of relay procedure on the SFW for $\alpha = 0.45$, $t_{RS} = 4hrs$, $f_{RA} = 0.4$ and $n_L = 0.01$

Sump volume control loop

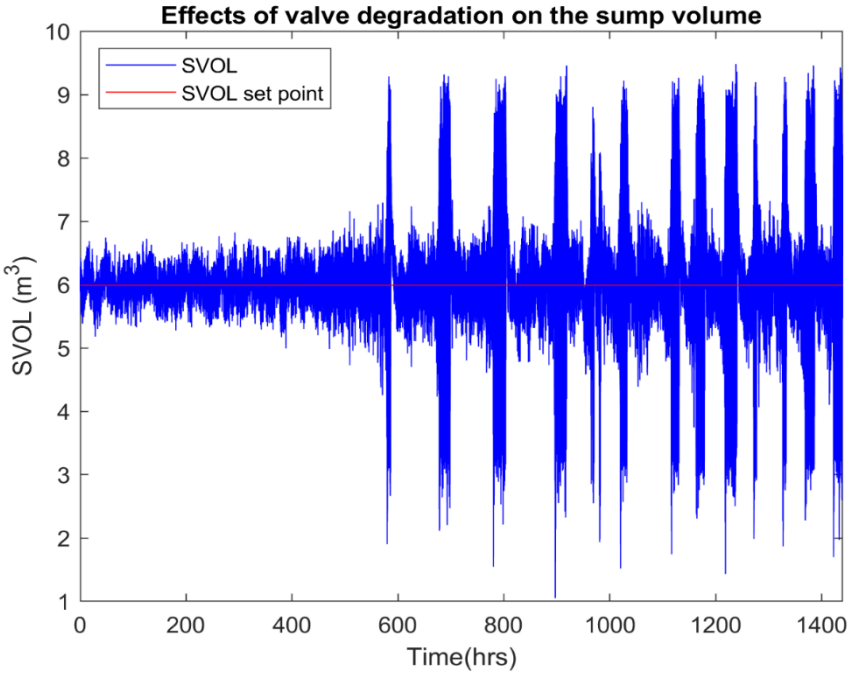

Figure B-12: Effects of valve degradation on the SVOL for $\alpha = 0.45$ and $n_L = 0.01$

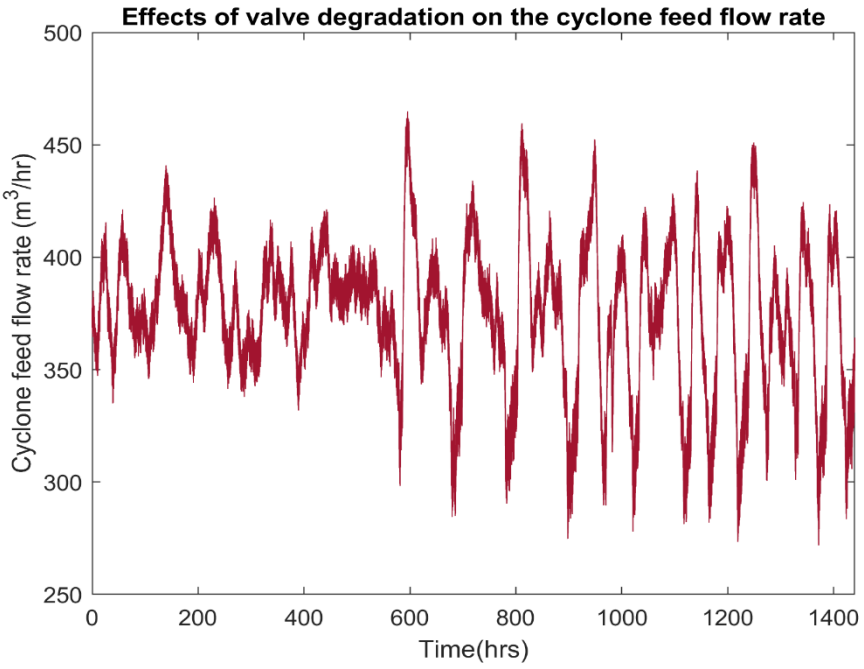

Figure B-13: Effects of valve degradation on the CFF for $\alpha = 0.45$ and $n_L = 0.01$

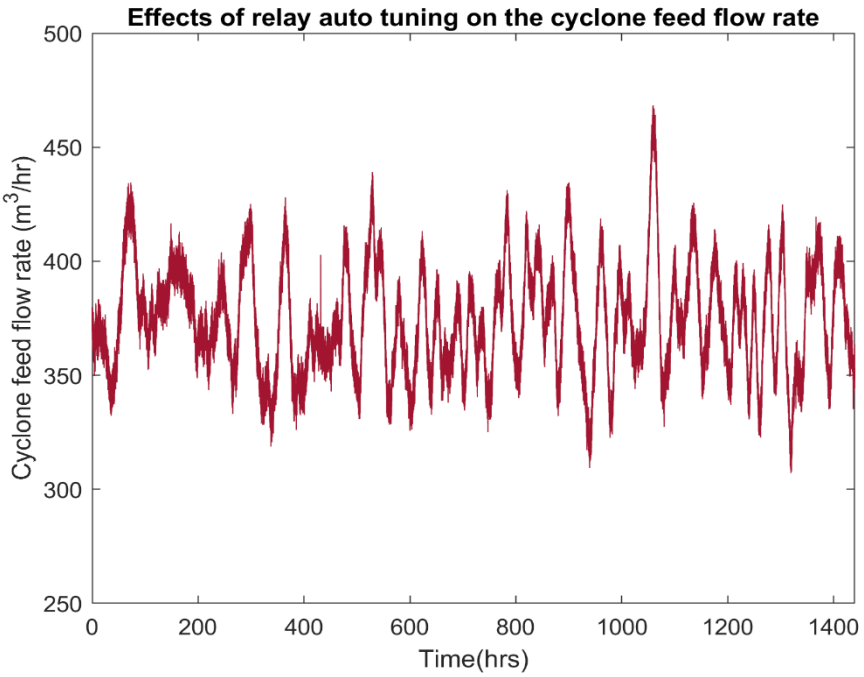

Figure B-14: Effects of relay autotuning on the CFF for $\alpha = 0.45$, $t_{RS} = 4hrs$ and $n_L = 0.01$

Mill charge control loop

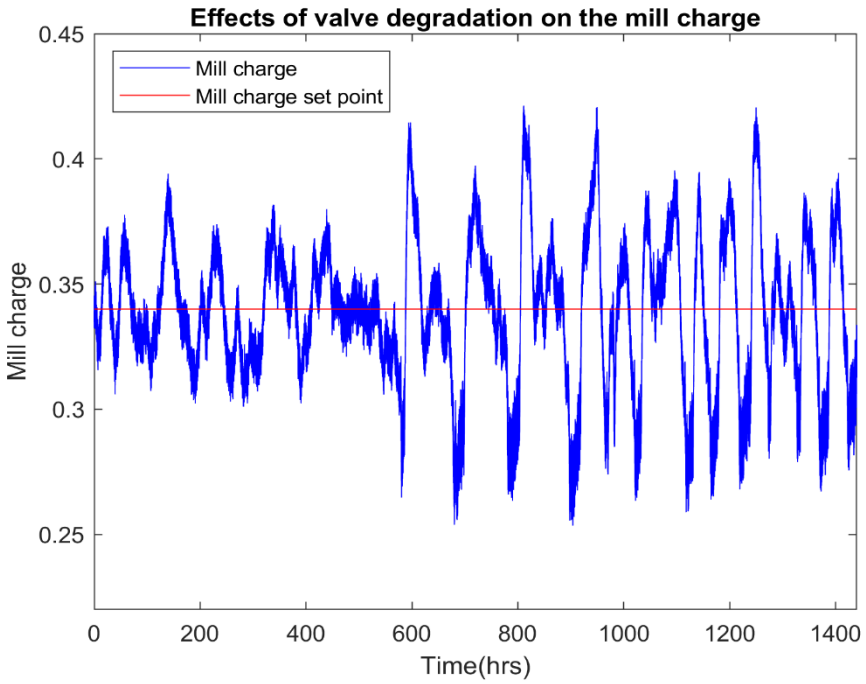

Figure B-15: Effects of valve degradation on the mill charge for $\alpha = 0.45$ and $n_L = 0.01$

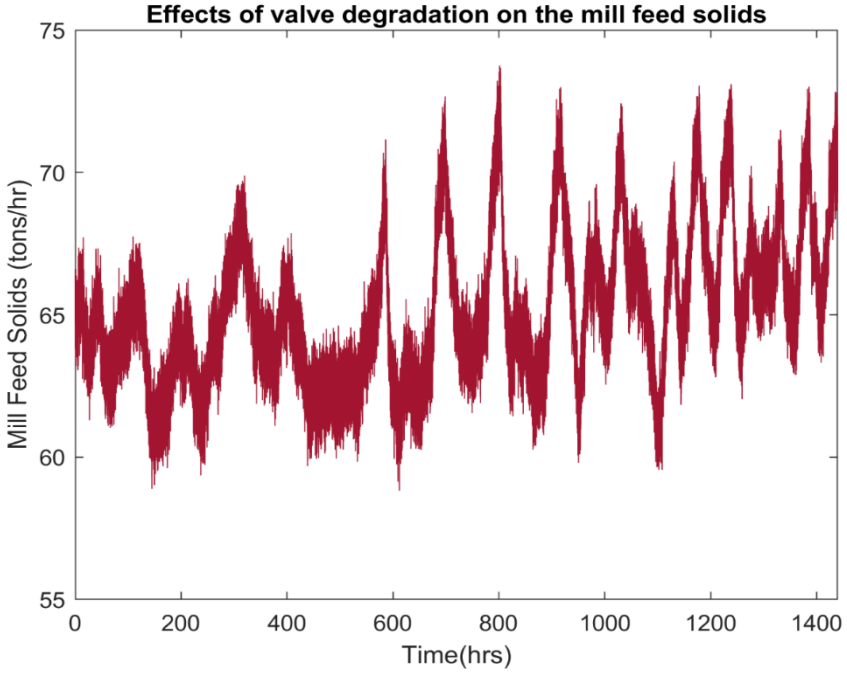

Figure B-16: Effects of valve degradation on the MFS for $\alpha = 0.45$ and $n_L = 0.01$

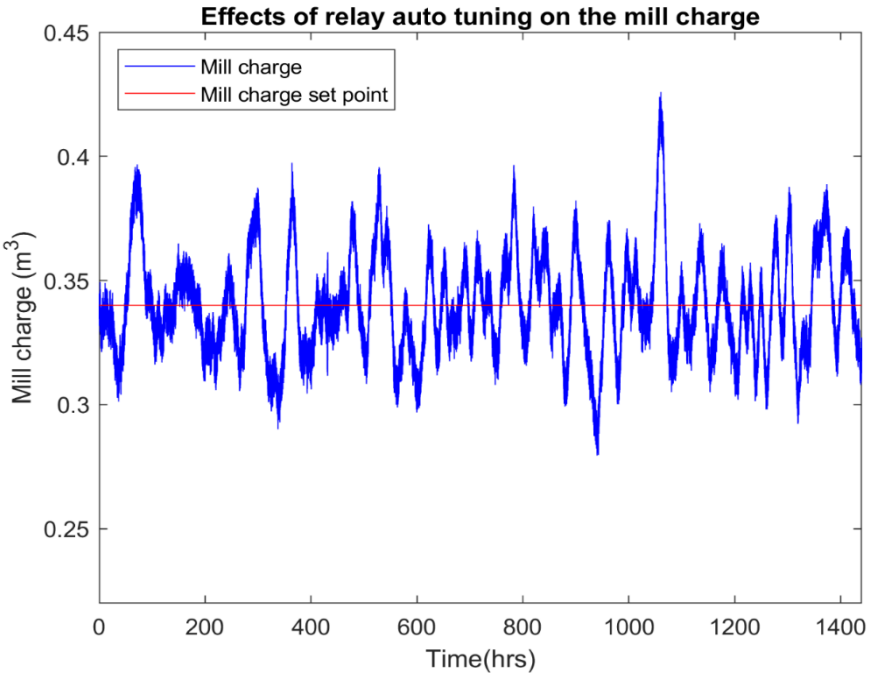

Figure B-17: Effects of relay autotuning on the mill charge for $\alpha = 0.45$ and $n_L = 0.01$

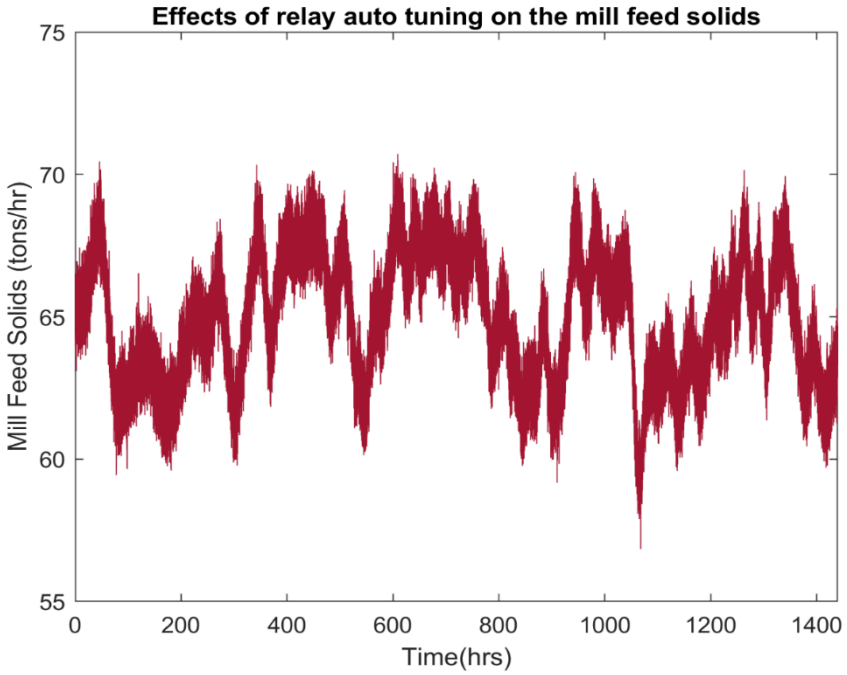

Figure B-18: Effects of relay autotuning on the MFS for $\alpha = 0.45$ and $n_L = 0.01$

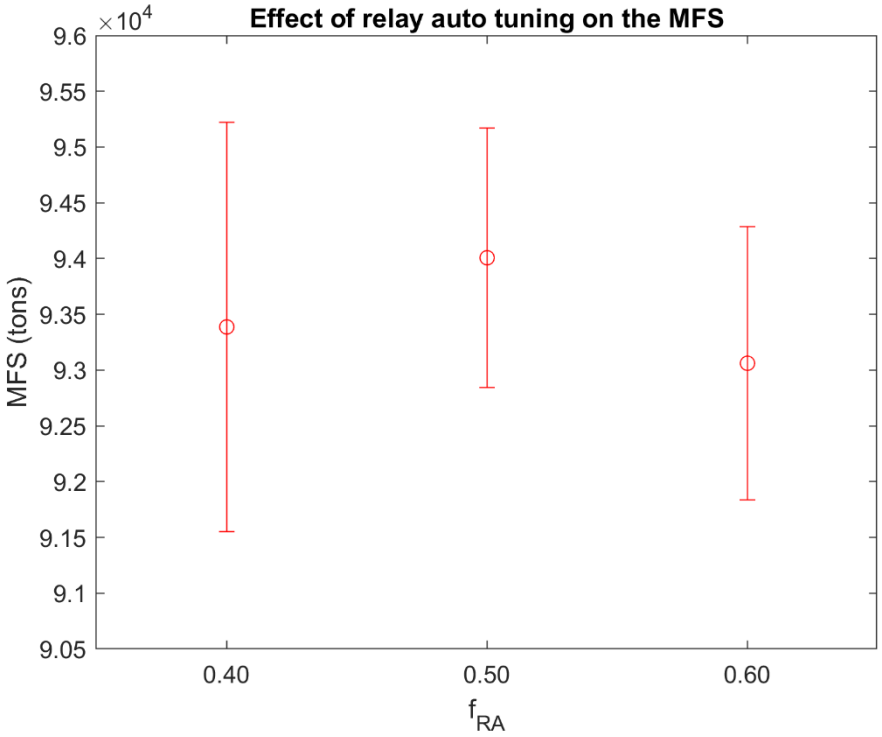

Figure B-19: Effect of relay autotuning on the mean MFS (2σ) for various f_{RA} for $n_L = 0.01$, $t_{RS} = 3hrs$ and $\alpha = 0.45$

Mill power draw

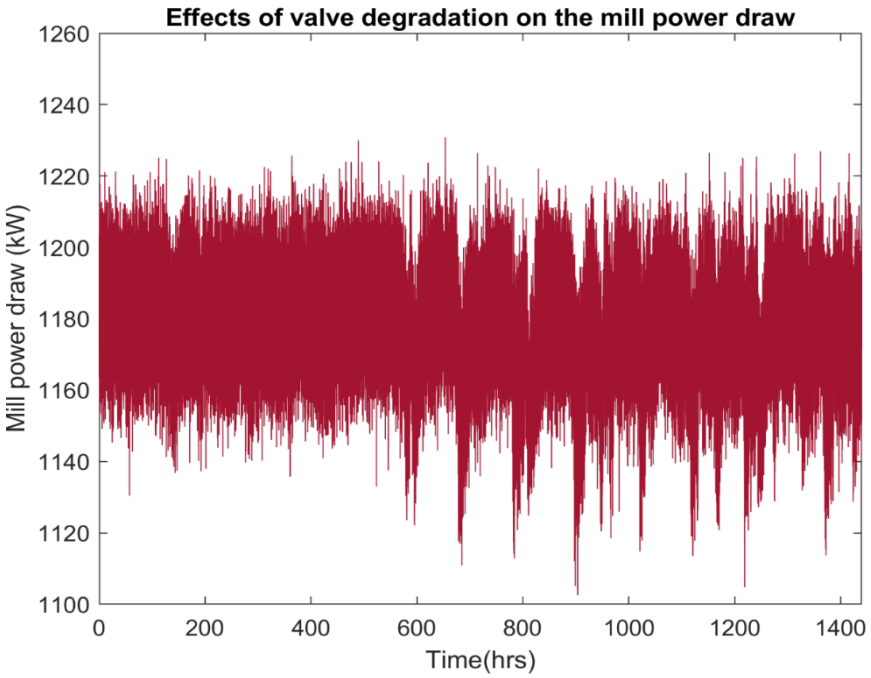

Figure B-20: Effects of valve degradation on P_{mill} for $\alpha = 0.45$ and $n_L = 0.01$

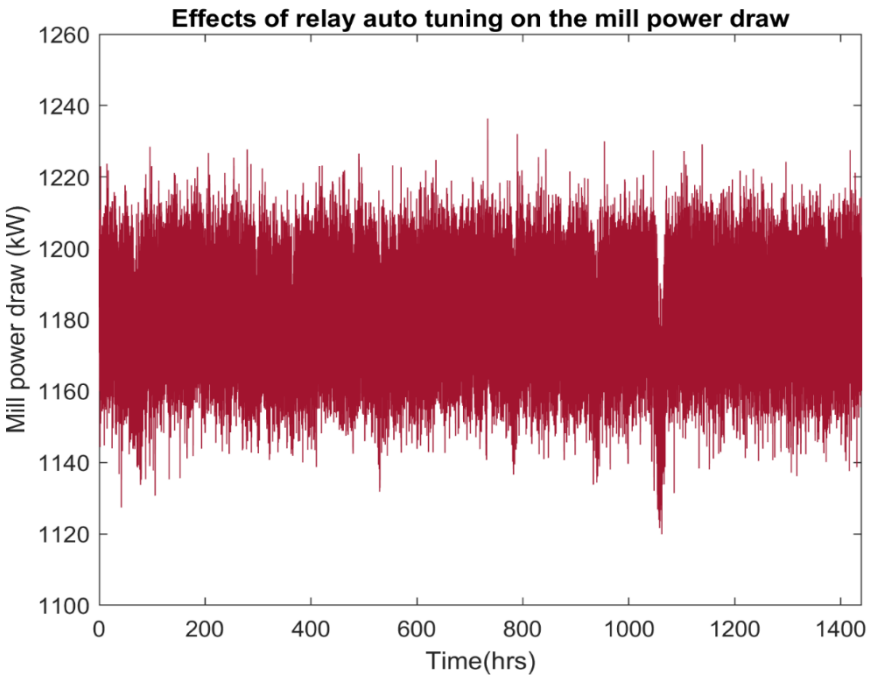

Figure B-21: Effects of relay autotuning on P_{mill} for $\alpha = 0.45$ and $n_L = 0.01$

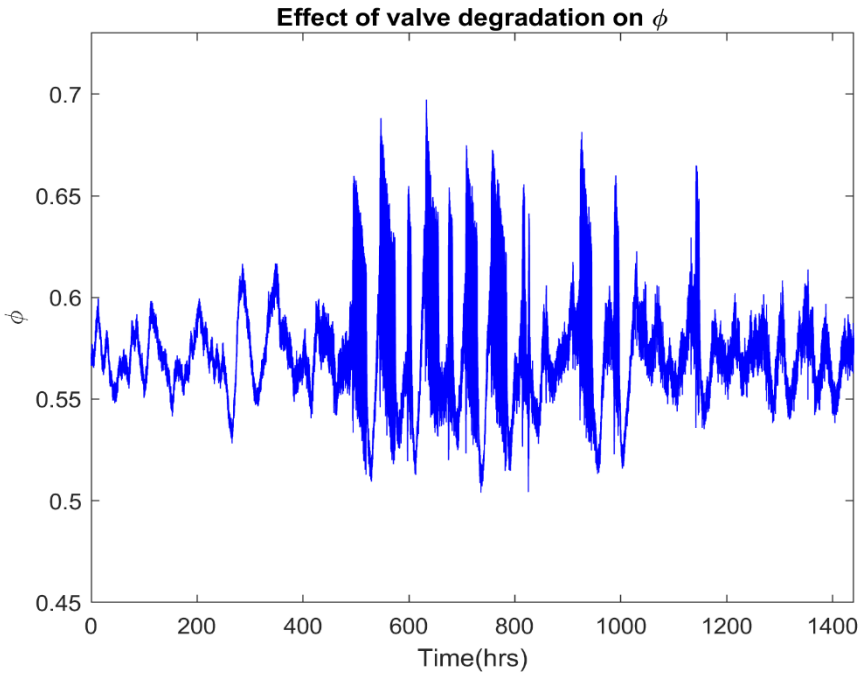

Figure B-22: Effects of valve degradation on φ for $\alpha = 0.45$ and $n_L = 0.01$

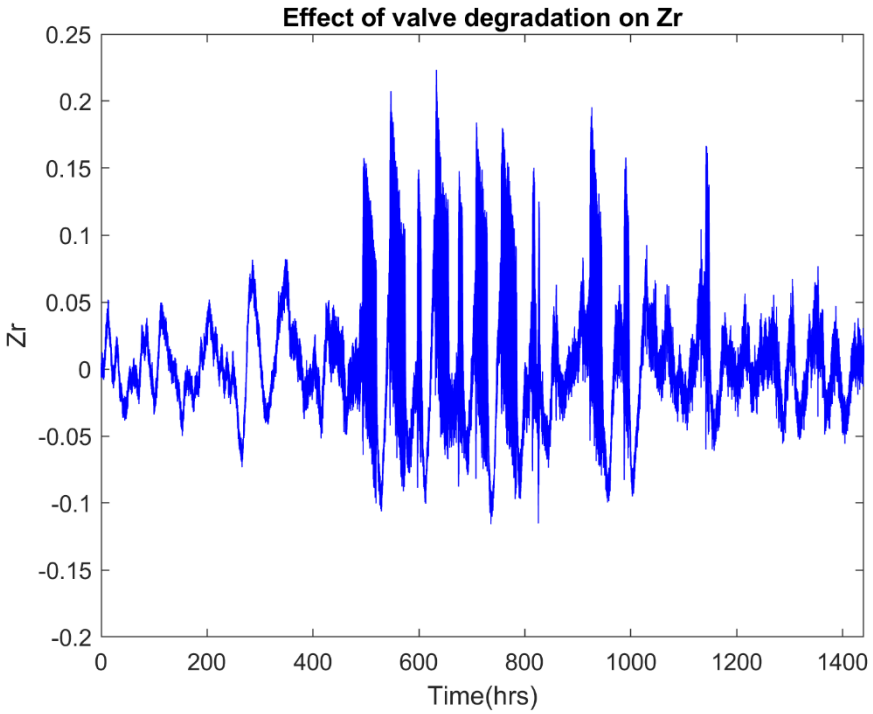

Figure B-23: Effects of valve degradation on Z_R for $\alpha = 0.45$ and $n_L = 0.01$

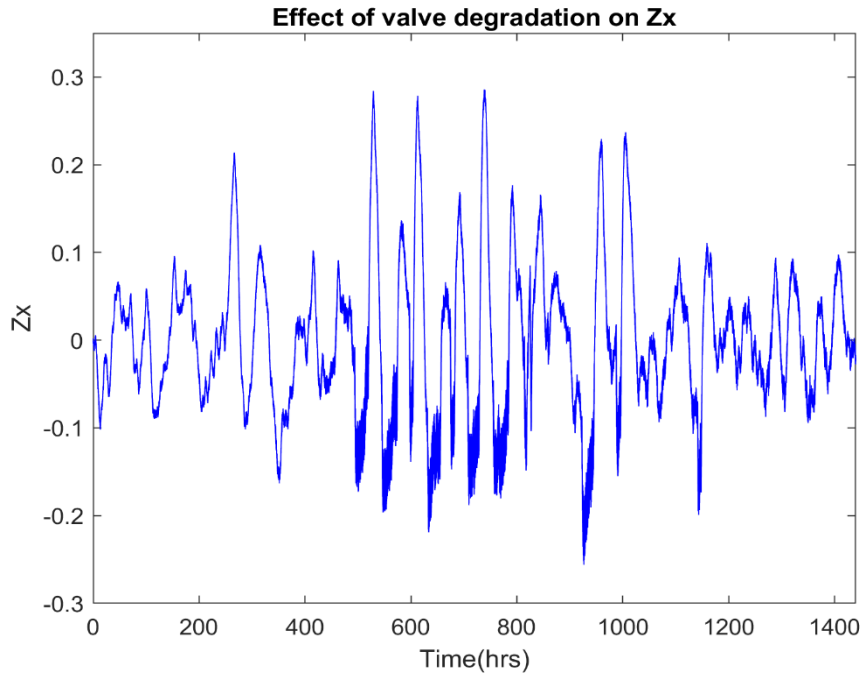

Figure B-24: Effects of valve degradation on Z_x for $\alpha = 0.45$ and $n_L = 0.01$

Extent of valve degradation

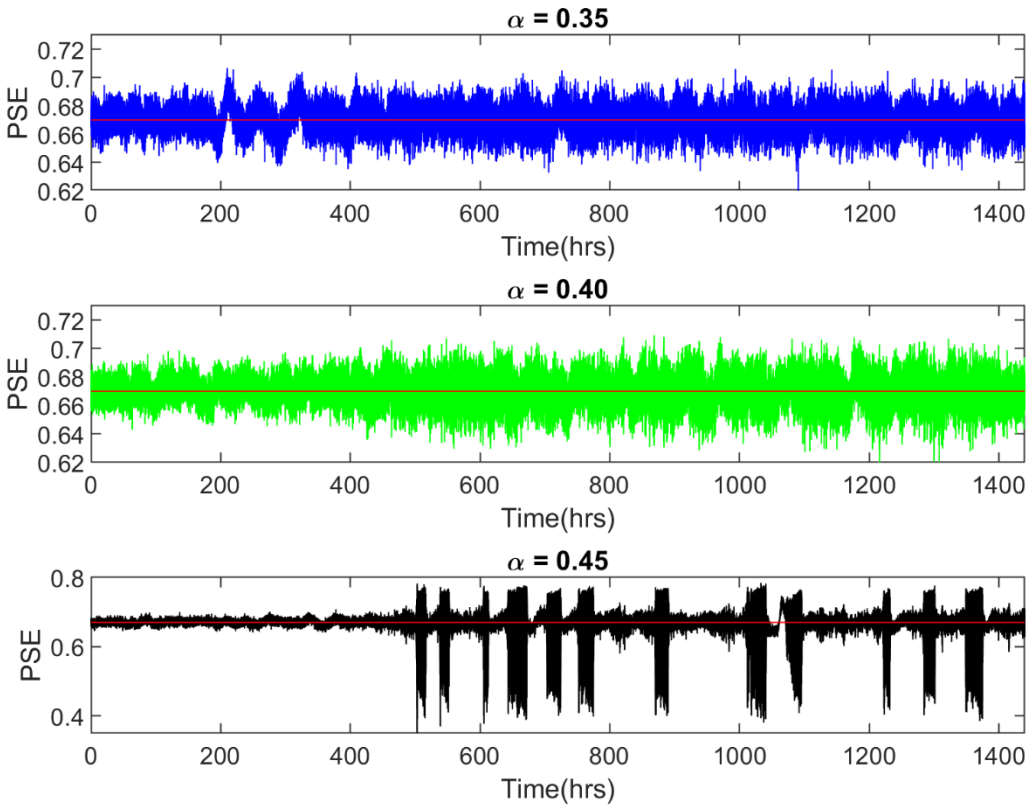

Figure B-25: Effect of the extent of valve degradation on the PSE for $n_L = 0.0075$

Historical benchmark

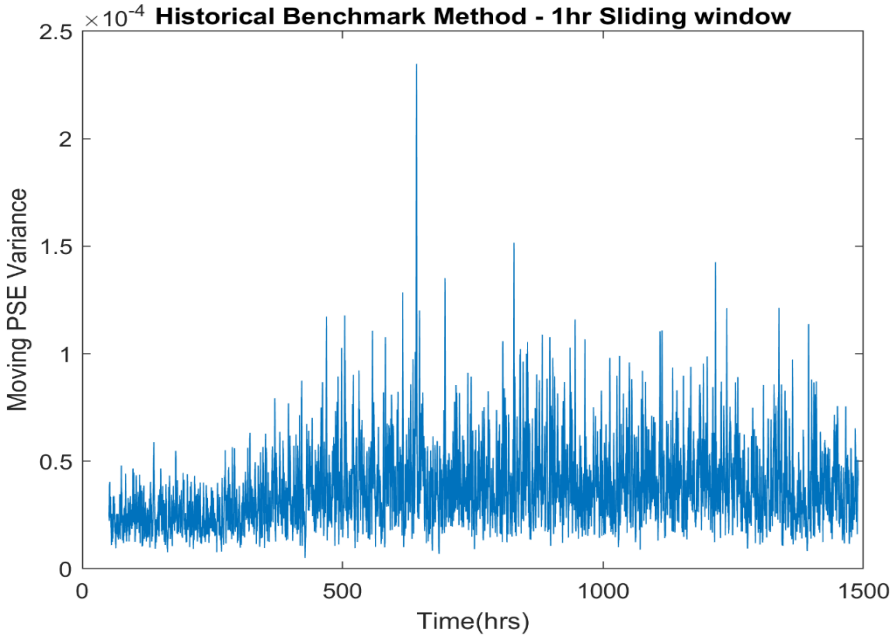

Figure B-26: Historical benchmark method illustrating the shift in the moving variance once $\alpha = 0.35$ for $n_L = 0.01$ and a sliding window of 1hr

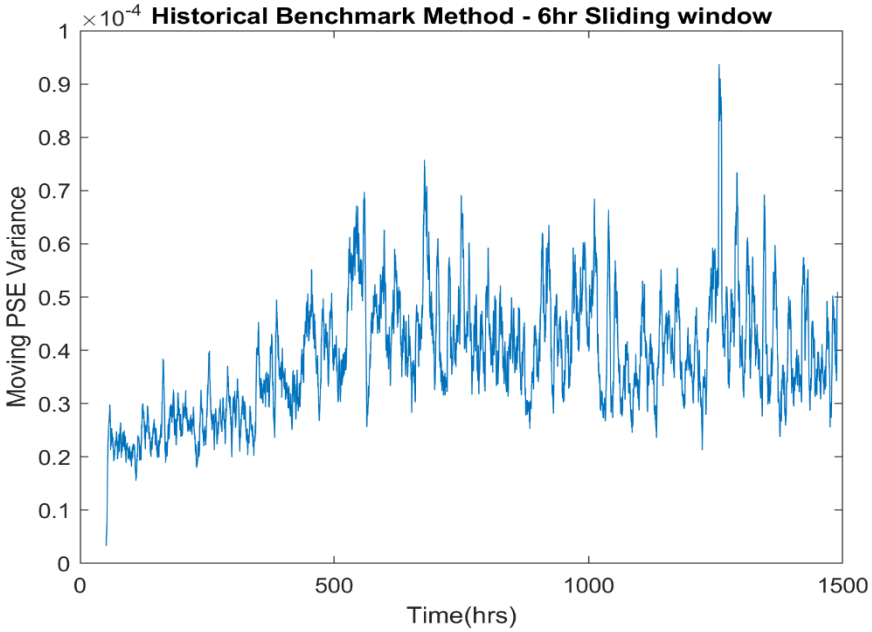

Figure B-27 Historical benchmark method illustrating the shift in the moving variance once $\alpha = 0.35$ for $n_L = 0.01$ and a sliding window of 6hrs

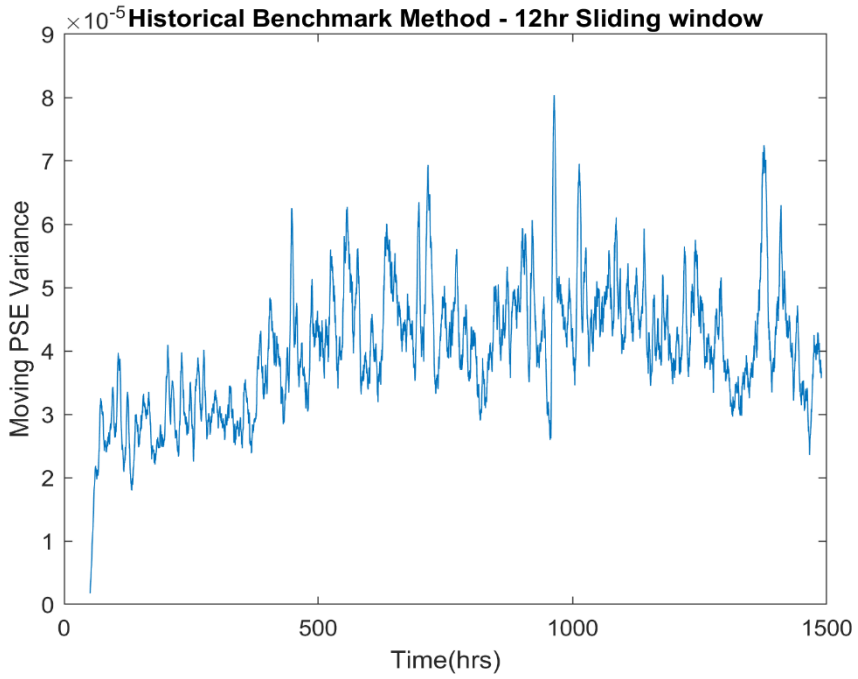

Figure B-28: Historical benchmark method illustrating the shift in the moving variance once $\alpha = 0.35$ for $n_L = 0.01$ and a sliding window of 12hr

Sensor noise & valve degradation

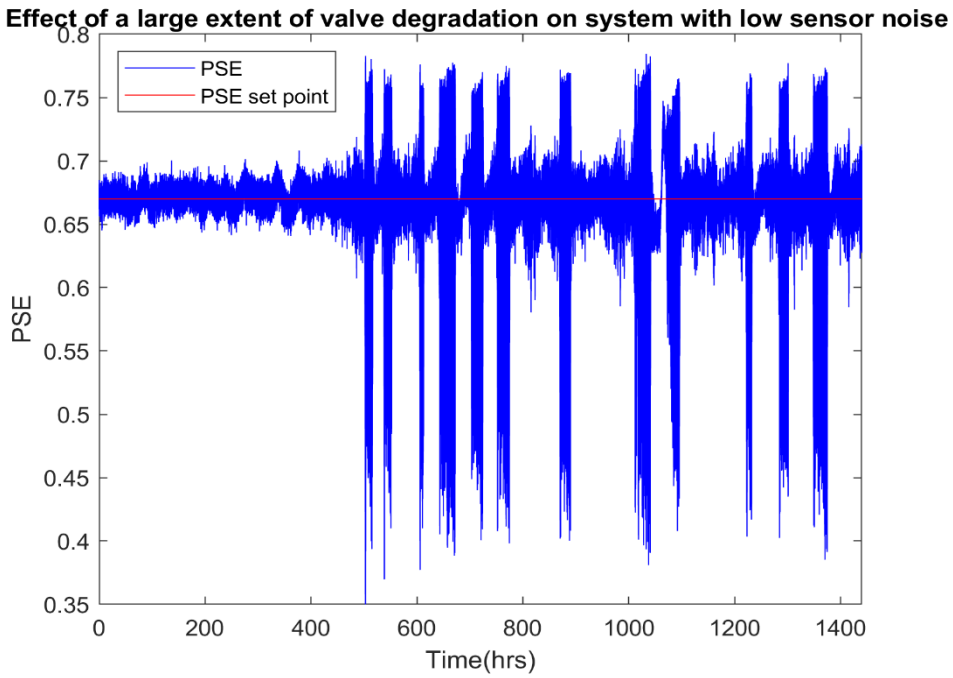

Figure B-29: The PSE for $\alpha = 0.45$ and $n_L = 0.0075$

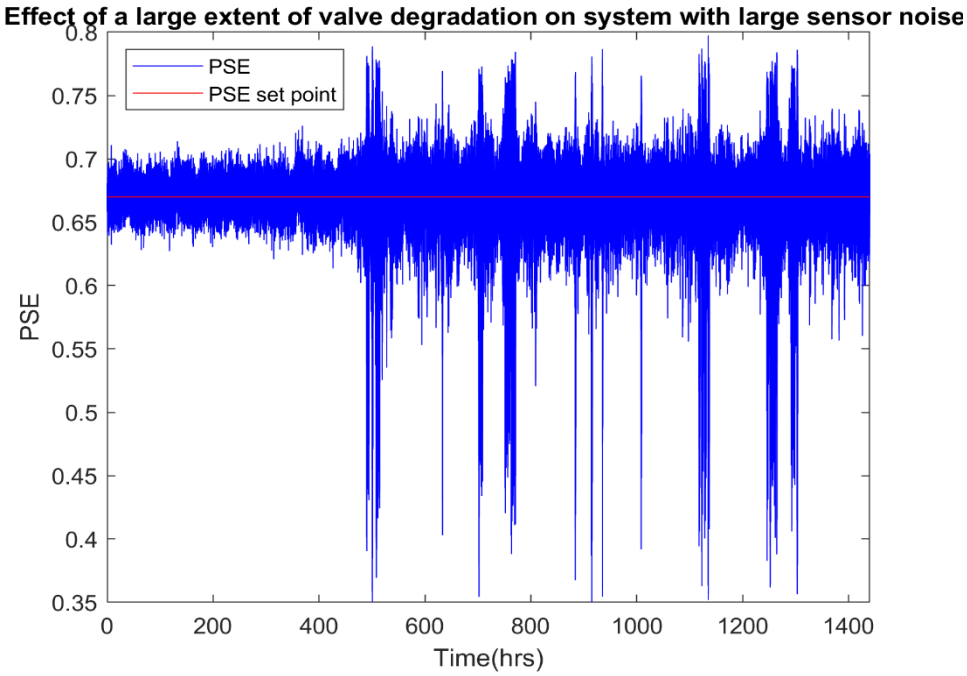

Figure B-30: The PSE for $\alpha = 0.45$ and $n_L = 0.0125$

Hydrocyclone flow rates

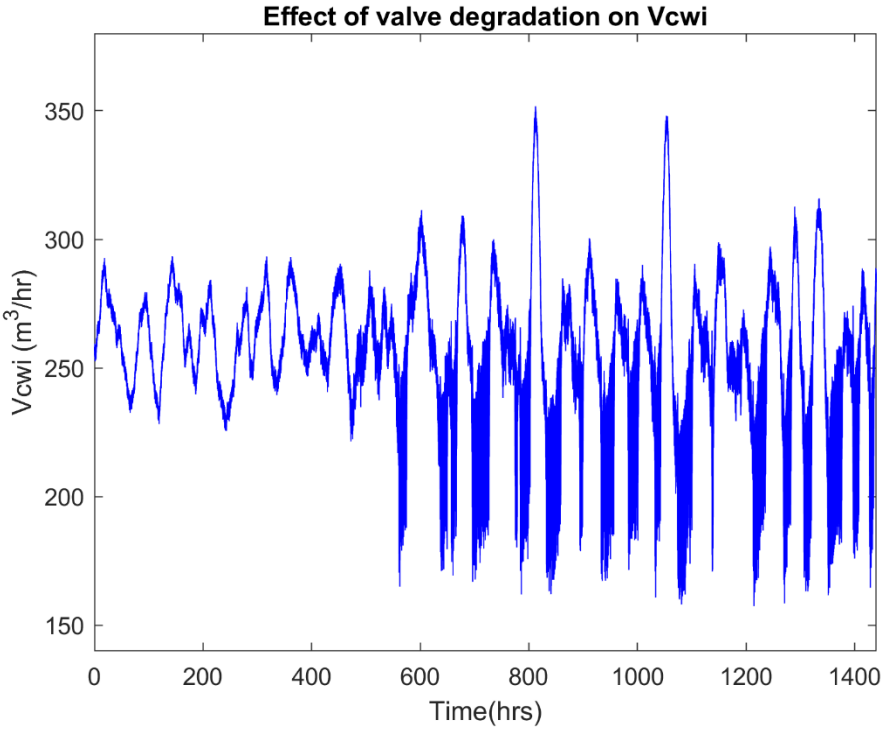

Figure B-31: Effects of valve degradation on V_{cwi} for $n_L = 0.01$ and $\alpha = 0.45$

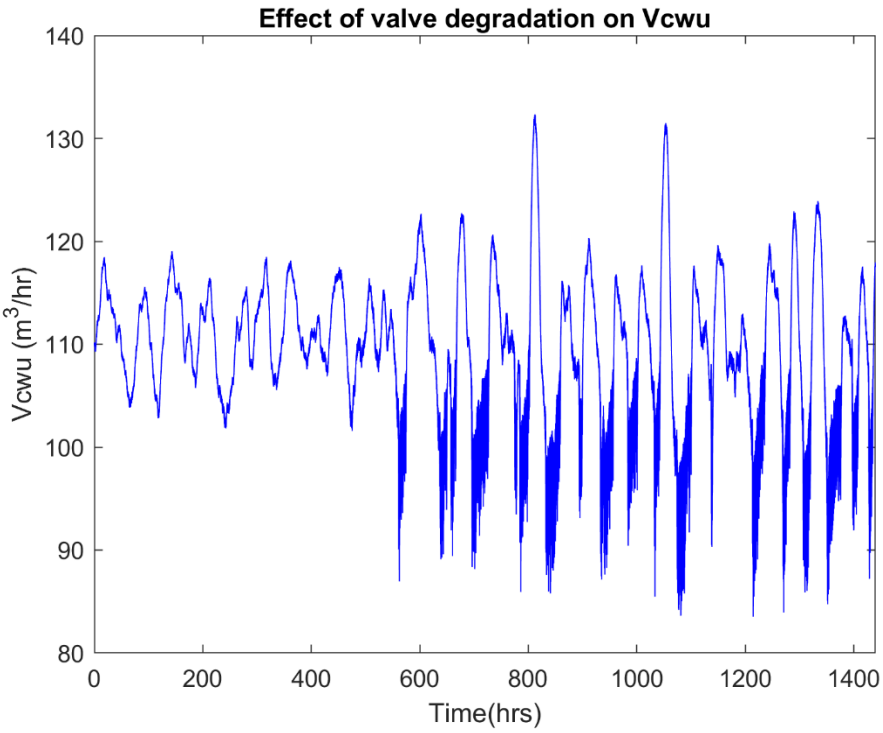

Figure B-32: Effects of valve degradation on V_{cwu} for $n_L = 0.01$ and $\alpha = 0.45$

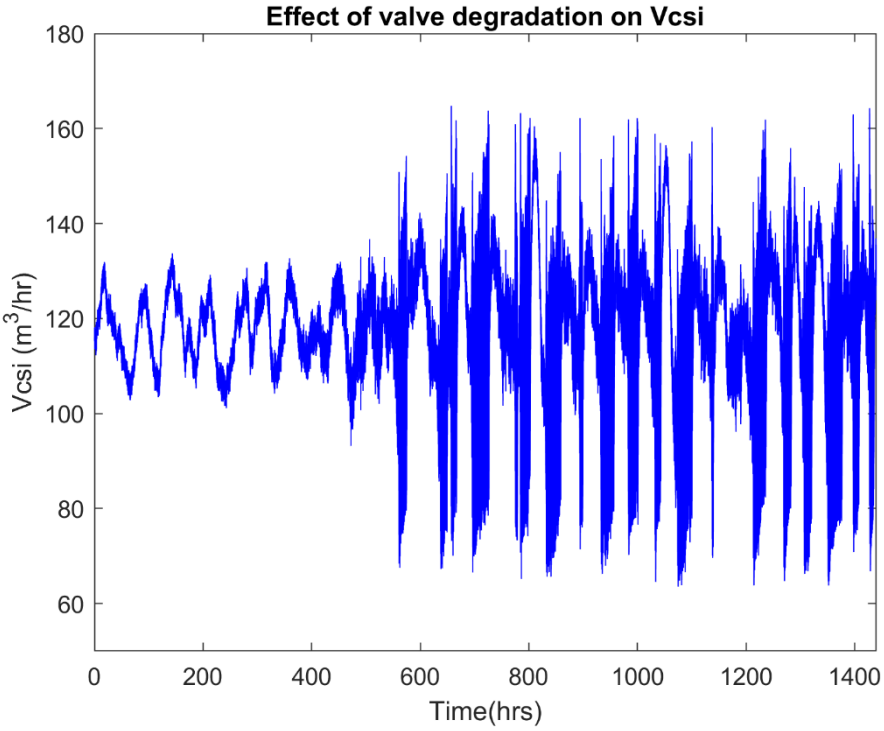

Figure B-33: Effects of valve degradation on V_{csi} for $n_L = 0.01$ and $\alpha = 0.45$

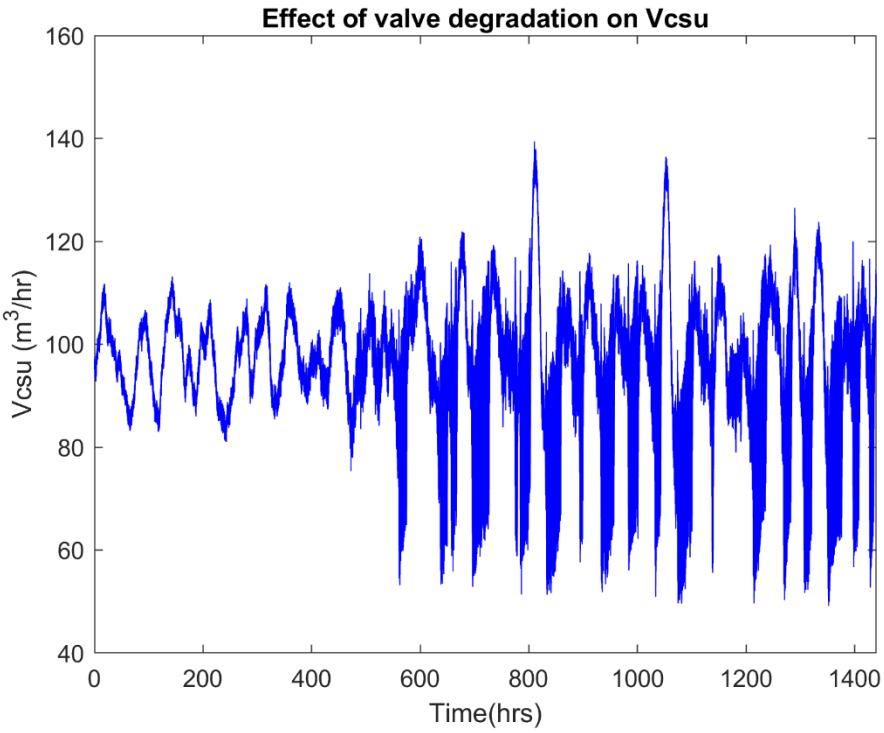

Figure B-34: Effects of valve degradation on V_{csu} for $n_L = 0.01$ and $\alpha = 0.45$

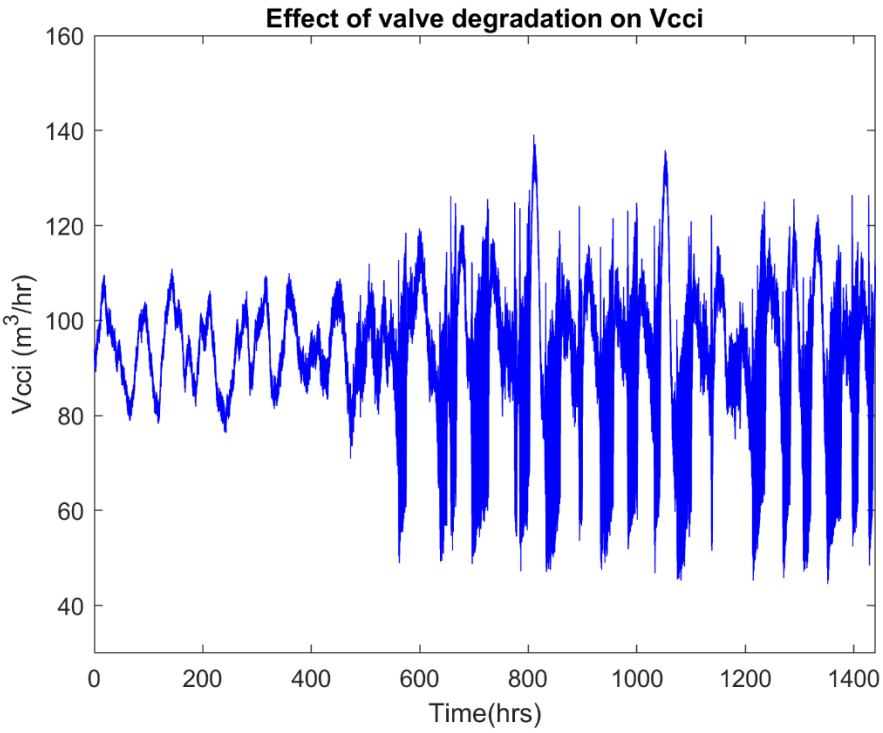

Figure B-35: Effects of valve degradation on V_{cci} for $n_L = 0.01$ and $\alpha = 0.45$

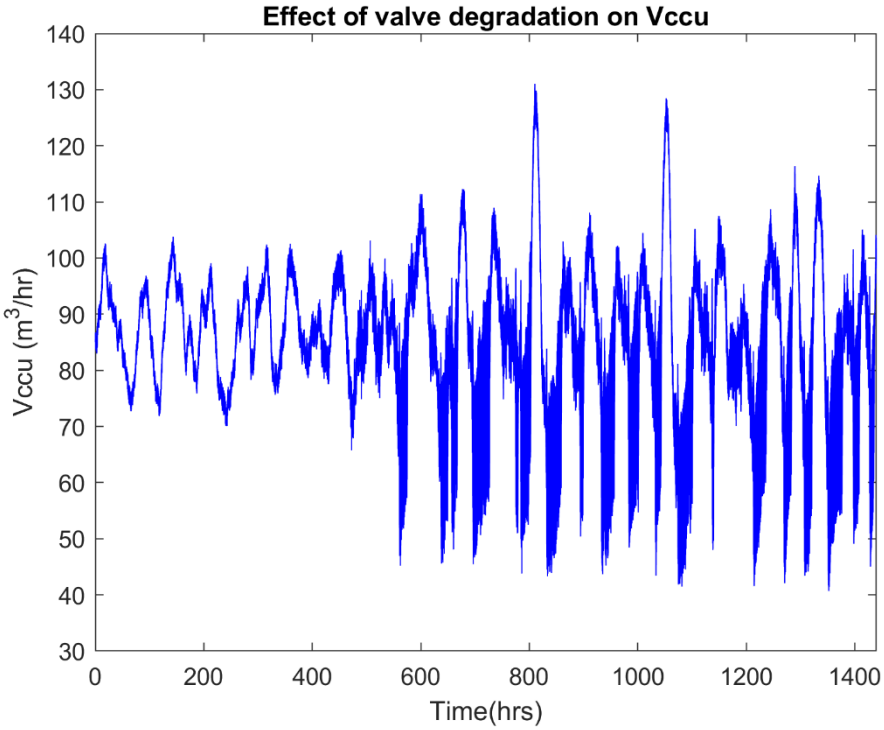

Figure B-36: Effects of valve degradation on V_{ccu} for $n_L = 0.01$ and $\alpha = 0.45$

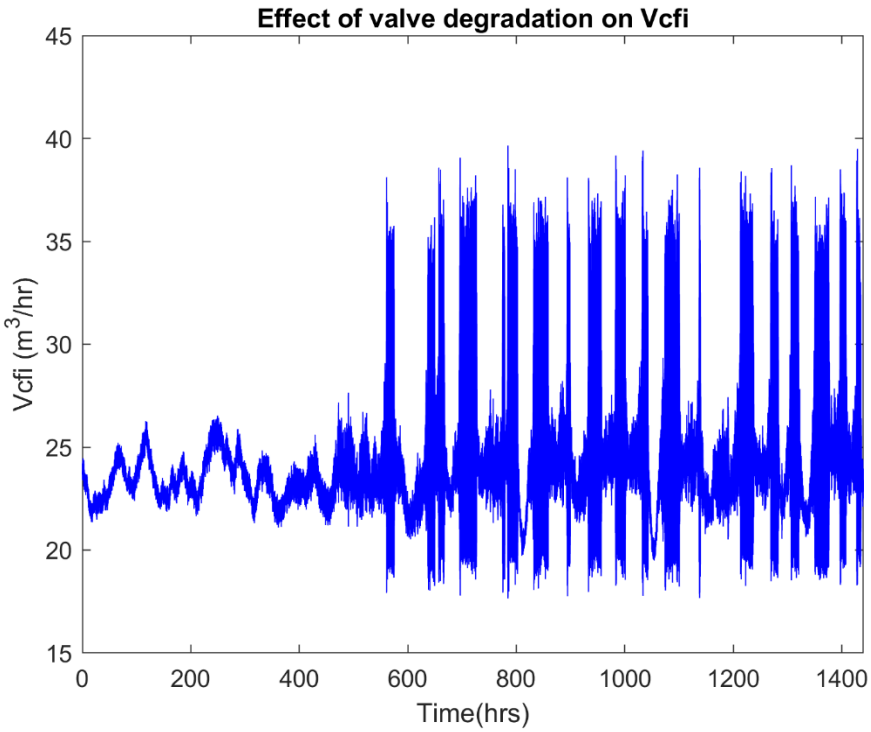

Figure B-37: Effects of valve degradation on V_{cfi} for $n_L = 0.01$ and $\alpha = 0.45$

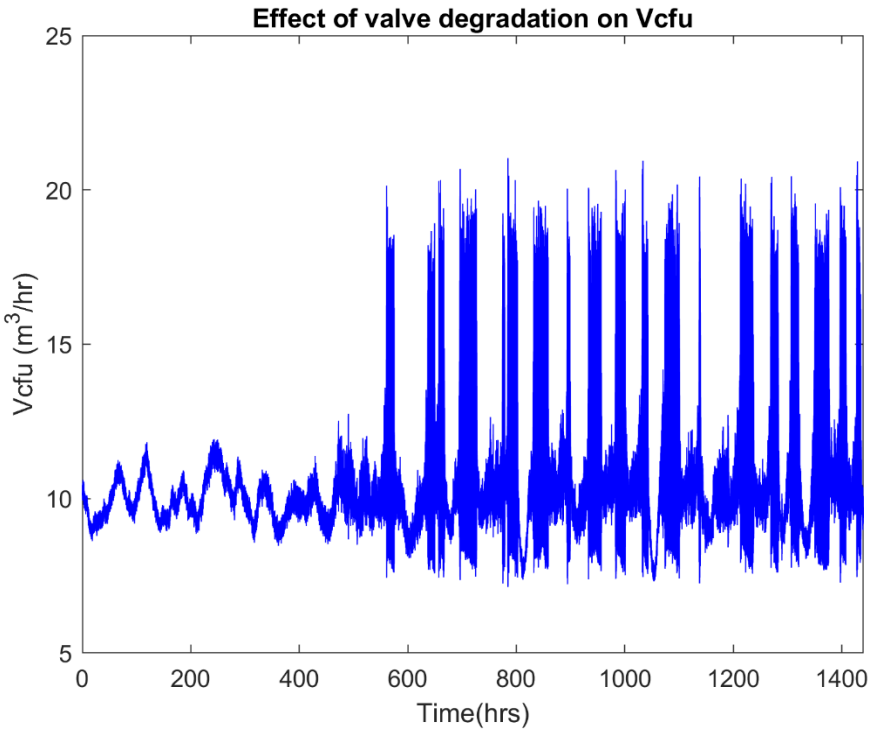

Figure B-38: Effects of valve degradation on V_{cfu} for $n_L = 0.01$ and $\alpha = 0.45$

Sequential relay autotuning

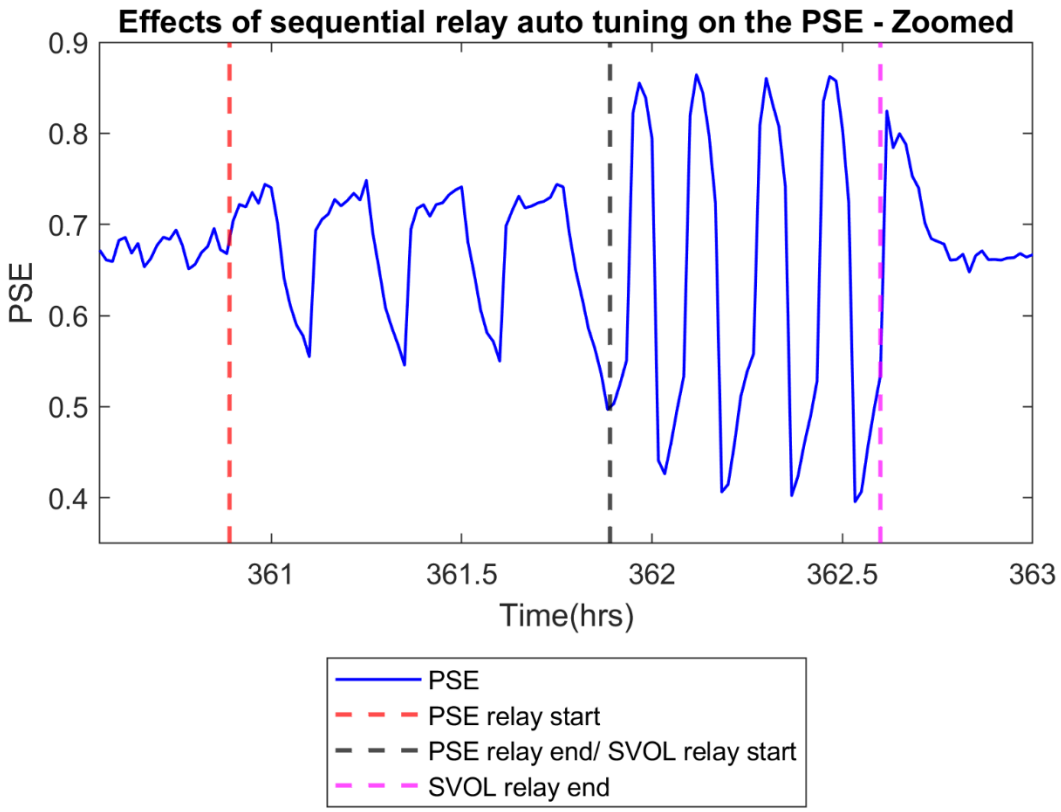

Figure B-39: Sequential relay autotuning of the PSE for $n_L = 0.01, f_{RA} = 0.4, t_{RS} = 3hrs$ and $\alpha = 0.45$

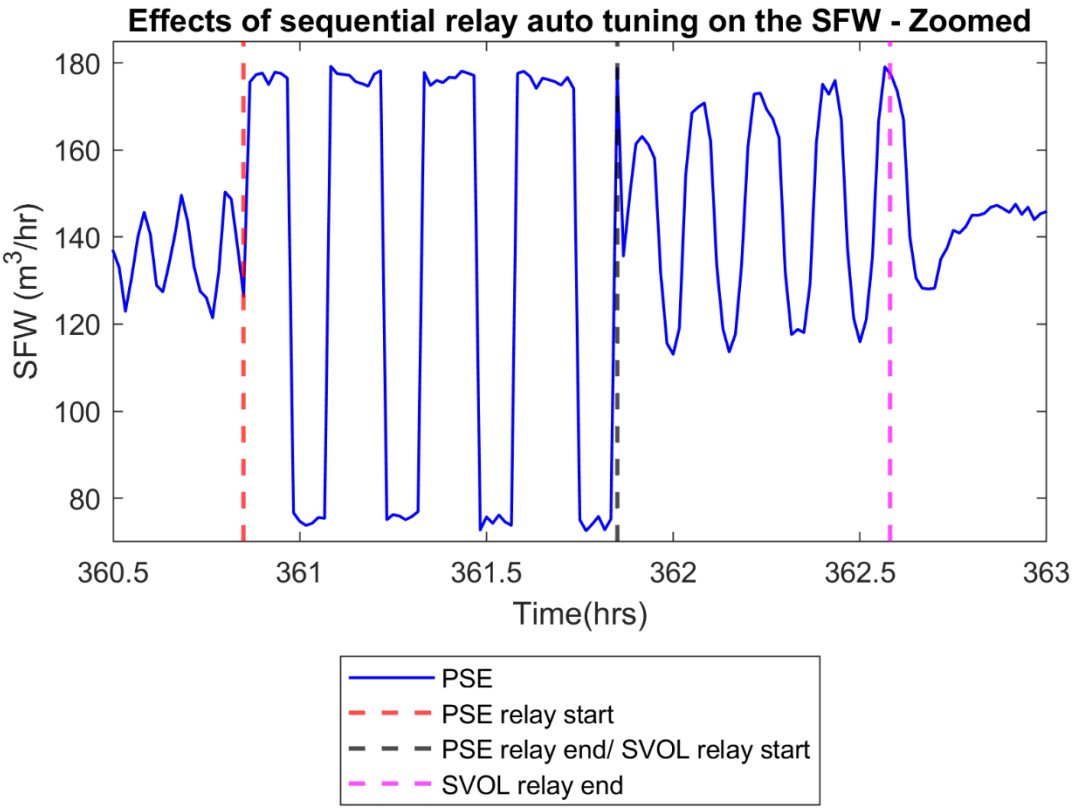

Figure B-40: Sequential relay autotuning of the SFW for $n_L = 0.01, f_{RA} = 0.4, t_{RS} = 3hrs$ and $\alpha = 0.45$

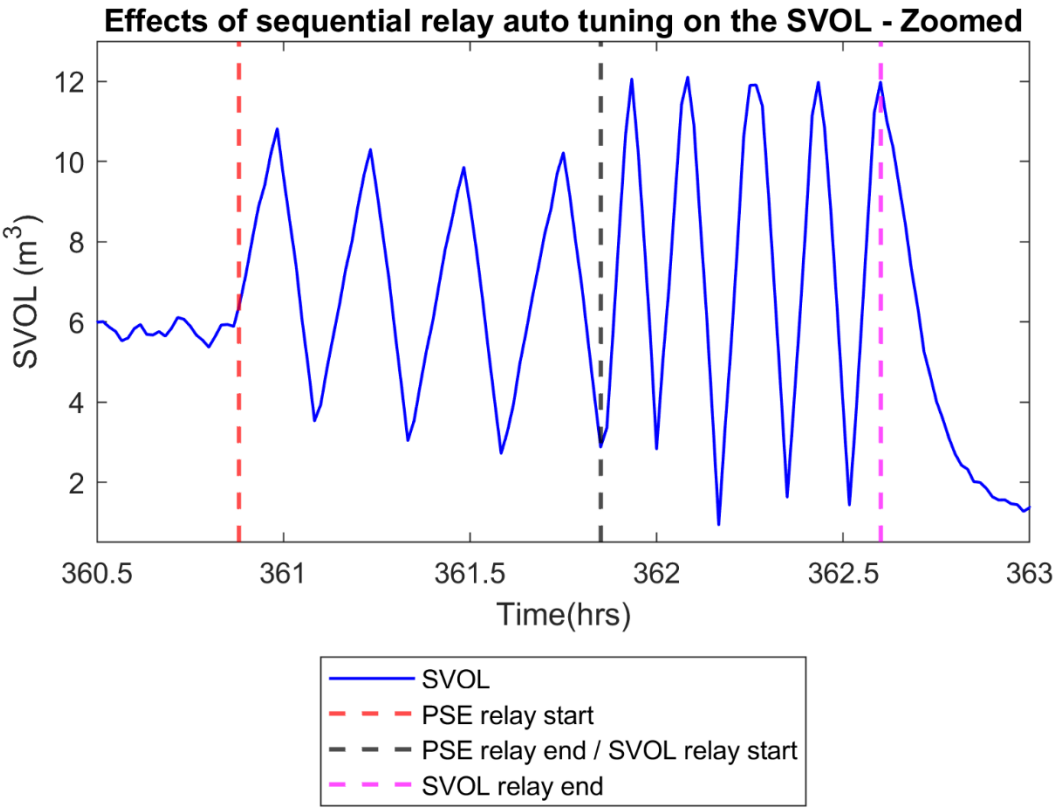

Figure B-41: Sequential relay autotuning of the SVOL for $n_L = 0.01, f_{RA} = 0.4, t_{RS} = 3hrs$ and $\alpha = 0.45$

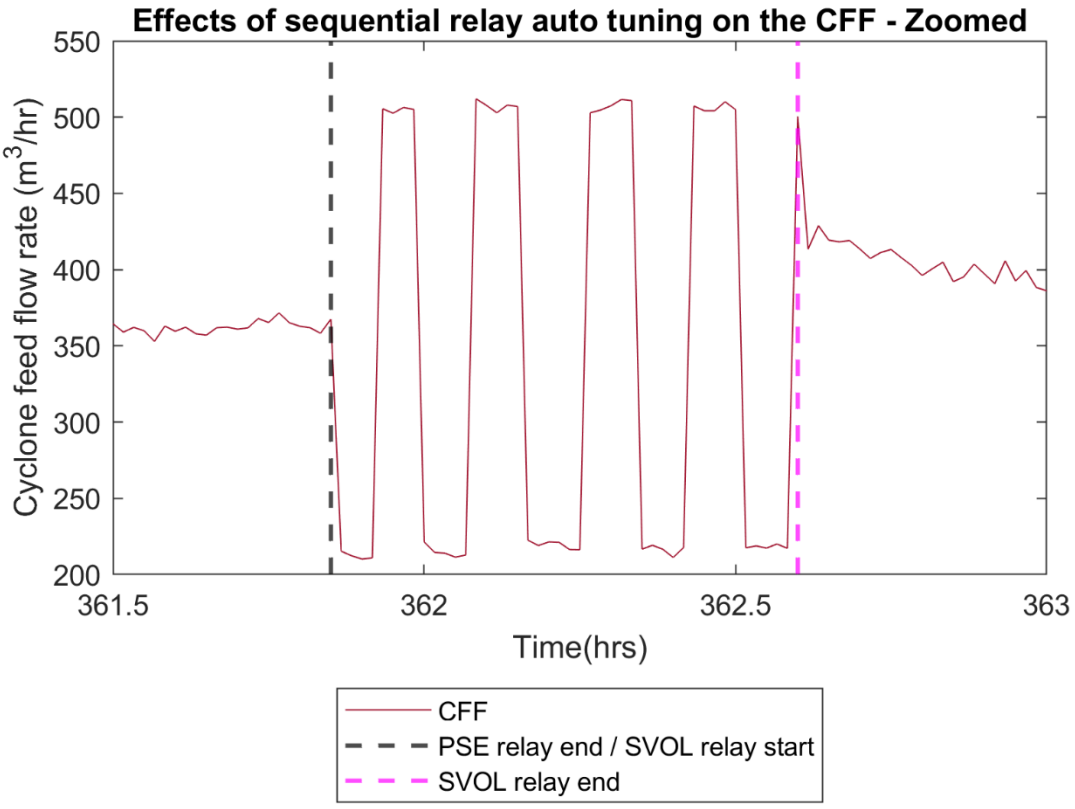

Figure B-42: Sequential relay autotuning of the CFF for $n_L = 0.01, f_{RA} = 0.4, t_{RS} = 3hrs$ and $\alpha = 0.45$

Table B-1: Average CPI as well as controller tuning parameter values obtained from single loop retuning at various f_{RA} for $n_L = 0.01$, $t_{RS} = 3hrs$ and $\alpha = 0.45$

f_{RA}	CPI
0.4	0.55
0.5	0.57
0.6	0.60

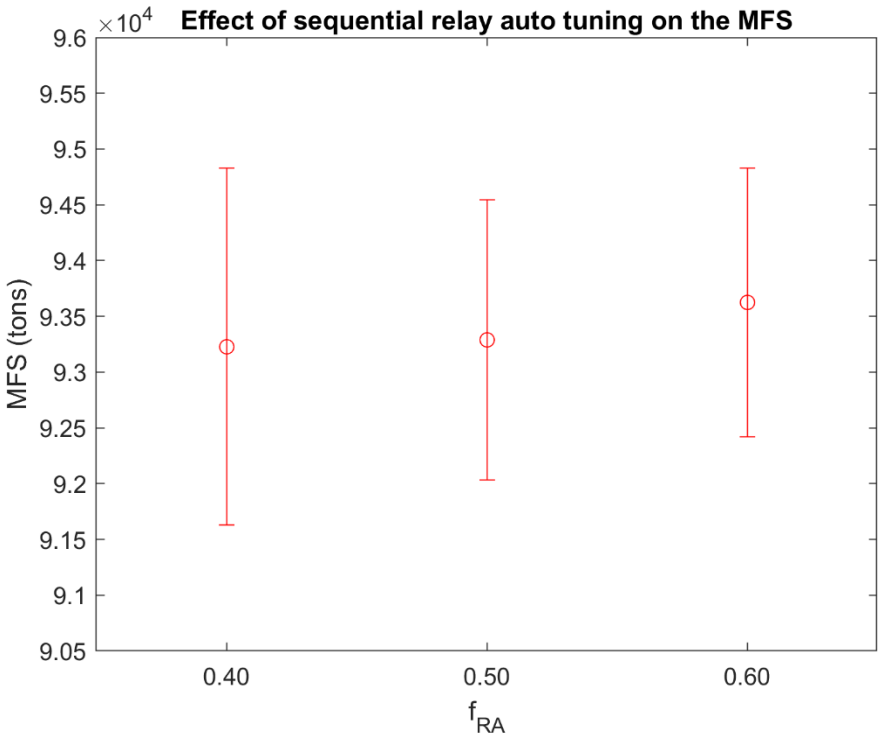

Figure B-43: Effect of sequential relay autotuning on the mean MFS (2σ) for various f_{RA} for $n_L = 0.01$, $t_{RS} = 3hrs$ and $\alpha = 0.45$

Analysis of key parameters data

Table B-2: Mean CPI values and standard error for the key parameters assessed using ANOVA

Factor level	Mean CPI value	Standard error
α		
0.35	0.6191	0.0034
0.40	0.5643	0.0034
0.45	0.5687	0.0034
f_{RA}		
0.40	0.5675	0.0034
0.50	0.5848	0.0034
0.60	0.5997	0.0034
n_L		
0.0075	0.5980	0.0034
0.0100	0.5871	0.0034
0.0125	0.5669	0.0034
t_{RS} (hrs)		
3	0.5532	0.0034
4	0.5767	0.0034
5	0.6221	0.0034